NOTICE

The quality of this microform is heavily dependent upon the quality of the original thesis submitted for microfilming. Every effort has been made to ensure the highest quality of reproduction possible.

If pages are missing, contact the university which granted the degree.

Some pages may have indistinct print especially if the original pages were typed with a poor typewriter ribbon or if the university sent us an inferior photocopy.

Reproduction in full or in part of this microform is governed by the Canadian Copyright Act, R.S.C. 1970, c. C-30, and subsequent amendments.

AVIS

La qualité de cette microforme dépend grandement de la qualité de la thèse soumise au microfilmage. Nous avons tout fait pour assurer une qualité supérieure de reproduction.

S'il manque des pages, veuillez communiquer avec l'université qui a conféré le grade.

La qualité d'impression de certaines pages peut laisser à désirer, surtout si les pages originales ont été dactylographiées à l'aide d'un ruban usé ou si l'université nous a fait parvenir une photocopie de qualité inférieure.

La reproduction, même partielle, de cette microforme est soumise à la Loi canadienne sur le droit d'auteur, SRC 1970, c. C-30, et ses amendements subséquents.

Intestinal Permeability in the Irradiated Ferret

Mia E. Lang

A thesis submitted in partial fulfillment of the requirements for the degree of Master of Science, within the Faculty of Medicine, Department of Physiology, of the
University of Ottawa

ISBN 0-315-75018-9

UNIVERSITÉ D'OTTAWA
UNIVERSITY OF OTTAWA

ABSTRACT

This project had three aims: 1) to develop an animal model to investigate the effects of radiation exposure on intestinal permeability; 2) to investigate the role of altered intestinal permeability as a possible causal mechanism of radiation-induced diarrhea; 3) to test the effect of a 5-hydroxytryptamine type-3 receptor (5-HT_3) antagonist (BRL 43694) on intestinal permeability and radiation-induced diarrhea.

Ferrets received whole-body irradiation (5 Gy, gamma). At different times post-irradiation (PIRR, 2, 24, and 48 hours), measurements of fluid and electrolyte fluxes, and of the blood-to-lumen clearance of ^{51}Cr-EDTA, were compared between *in situ* perfused loops of jejunum and ileum. Intestinal permeation of ^{51}Cr-EDTA was increased (4x control) in both the jejunum and ileum at 2 hours PIRR. At 24 hours PIRR, ^{51}Cr-EDTA permeation was the same as control. At 48 hours PIRR, jejunal permeation of ^{51}Cr-EDTA was not statistically different from control animals, whereas in the ileum, ^{51}Cr-EDTA permeation was increased 10x control. Absorption of luminal fluid was abolished 2 hours PIRR in the ileum. Sodium and chloride fluxes were unaffected by radiation exposure, but at 48 hours PIRR there was a significant secretion of potassium in the ileum. Diarrhea rarely occurred after the first hour post-irradiation suggesting that although radiation exposure did alter intestinal permeability, the changes in intestinal transport that were measured in this protocol were not causal factors of radiation-induced diarrhea.

Serotonin, acting via 5-HT_3 receptors, was investigated as a possible mediator of radiation-induced alterations in intestinal permeability. Pretreatment with the 5-HT_3 antagonist and anti-emetic BRL 43694, significantly reduced the severity of radiation-induced vomiting. Qualitative observations suggested that it offered some therapeutic benefit to radiation-induced diarrhea. However BRL 43694 pre-treatment had no effect on intestinal permeability, suggesting that the regulatory mechanisms that govern intestinal transport were not mediated by 5-HT_3 receptors.

Table of Contents

Table of Contents

List of Tables

Table

Page

List of Figures

Page

Figure

List of Abbreviations

AP	arterial pressure
ATPase	adenosine triphosphatase
BES	balanced electrolyte solution
^{14}C	carbon-14
CI	control injected
Cl-	chloride electrolyte
cm	centimeter
cpm	counts per minute
^{51}Cr	chromium-51
^{137}Cs	cesium-137
DI	drug-injected
DW	dry weight
EDTA	ethylenediaminetetraacetic acid
FE	fractional excretion
g	gram
GI	gastrointestinal
Gy	gray
h	hour
Hb	hemoglobin
HCO_3^-	bicarbonate
5-HIAA	5-hydoxyindoleacetic acid
HR	heart rate
5-HT	5-hydroxytryptamine
K^+	potassium electrolyte
kg	kilogram
L	litre
MAP	mean arterial pressure
MCHC	mean corpuscular hemoglobin concentration
MCV	mean cell volume

List of Abbreviations

μCi	microcurie
μL	microlitre
min	minute
mL	millilitre
mm	millimeters
mmHg	millimeters of mercury
MPV	mean platelet volume
MW	molecular weight
n	number
Na^+	sodium electrolyte
°C	degrees Celcius
p	probability value
P1	first perfusion sample
P7	final perfusion sample
pCO_2	partial pressure of carbon dioxide
PE	polyethylene
PEG	polyethylene glycol
PIRR	post-irradiation
PLT	platelet
PMN	polymorphonucleocyte
s.c.	subcutaneous
SD	standard deviation
SE	standard error
SI	saline-injected
tCO_2	total carbon dioxide
VP	venous pressure
WBC	white blood cell

Acknowledgements

This project, at times challenging and frustrating, was always rewarding thanks to my research supervisor, Dr. Kent Harding. He was always patient and encouraging both on the good days and the bad days. Dr. Harding helped me become a better researcher and a better communicator of scientific ideas, and he encouraged science and education to be fun.

My advisory committee, consisting of Dr. George Biro, Dr. Pavel Hrdina, and Dr. Anthony Krantis, were always available for advice, and thorough and attentive to the several committee reports and meetings. I would also like to thank Dr. Linda Peterson whose input to this project was invaluable.

As equally supportive as my research supervisor and advisory committee were the technicians in the lab: Karen Leach, Louise Prud'homme-Lalonde, and Cathy Ferrarotto. All of them took turns assisting me during the surgical procedures, and offered many helpful suggestions during the protocol development. Cathy Ferrarotto and Louise Prud'homme-Lalonde did the majority of the serotonin and 5-hydroxyindoleacetic acid assays. For this, I am very thankful. Karen Leach and Louise Prud'homme-Lalonde also did the majority of the blood gas analysis. I am also indebted to James Peeke, who performed most of the blood analysis on the LS 9000. But I am even more grateful to all them, for the warm, caring and patient attitude they always showed this at times stubborn and irritating student. They, along with Dr. Harding, always made it fun to come into the lab. Special thanks must go to Karen Leach, who endured working with me for the longest period of time, "yes Karen, there really is a thesis !"

I must also thank the many helpful people who work in the Animal Care Facility of the University of Ottawa, especially Dr. Marilyn Keaney, Dr. Julie Lebeau, Miza Bosc-Davies, and Pierre Bradley. These people were instrumental in the design and functioning of this protocol. They were always ready to help, regardless of the problem, and offered much needed support during the development of the protocol.

I am also grateful to Beecham Pharmaceuticals, for their generous gift of their drug Granisetron. A special thanks to all those who patiently read through drafts of this thesis: Dr. Wallace MacNaughton, Karen Leach, Susan Slater, Gina DiPrimio, and my father, Dr. Donald Lang, who has written more of these than anyone should ever have to in a lifetime.

Lastly, special mention goes to Lac La Peche and Black Bank Beach, where I spent many a mental health day, and to my parents for making me take them, thank-you !

INTRODUCTION

Anatomical and Functional Review of the Gastrointestinal Tract

Organization and Function of the Different Gut Tissue Layers

The gastrointestinal (GI) tract is a modified hollow tube. Anatomically, the major divisions of the GI tract are: mouth, esophagus, stomach, duodenum, jejunum, ileum (the latter three comprise the small intestine), colon (large intestine) and rectum. Common to the esophagus, stomach and intestines are four basic tissue layers: the serosa, the muscularis externa, the submucosa and the mucosa (Figure 1). The manner in which these tissue layers become modified, particularly the mucosa, will determine the functional role of that region (Madara and Trier, 1987).

The mucosa of the small intestine is arranged as folds known as plicae circulares (valves of Kerckring). These folds, which are most prominent in the jejunum, less so in the upper duodenum and distal ileum, increase the surface area of the mucosa by approximately three-fold. Villi are found over the entire mucosal surface of the small intestine. These finger-like projections (0.5 - 1.0 mm in length, 20-40 mm^2 in density, human data) of the mucosa, increase its surface area by approximately 10-fold. Villi are shaped differently between the duodenum (leaf-shaped), the jejunum (rounded), and ileum (club-shaped). These structural differences partially account for functional differences between these organs (Madara and Trier, 1987).

Figure 1.

The general organization of the layers of the gastrointestinal tract. From Berne and Levy, 1988, p. 743.

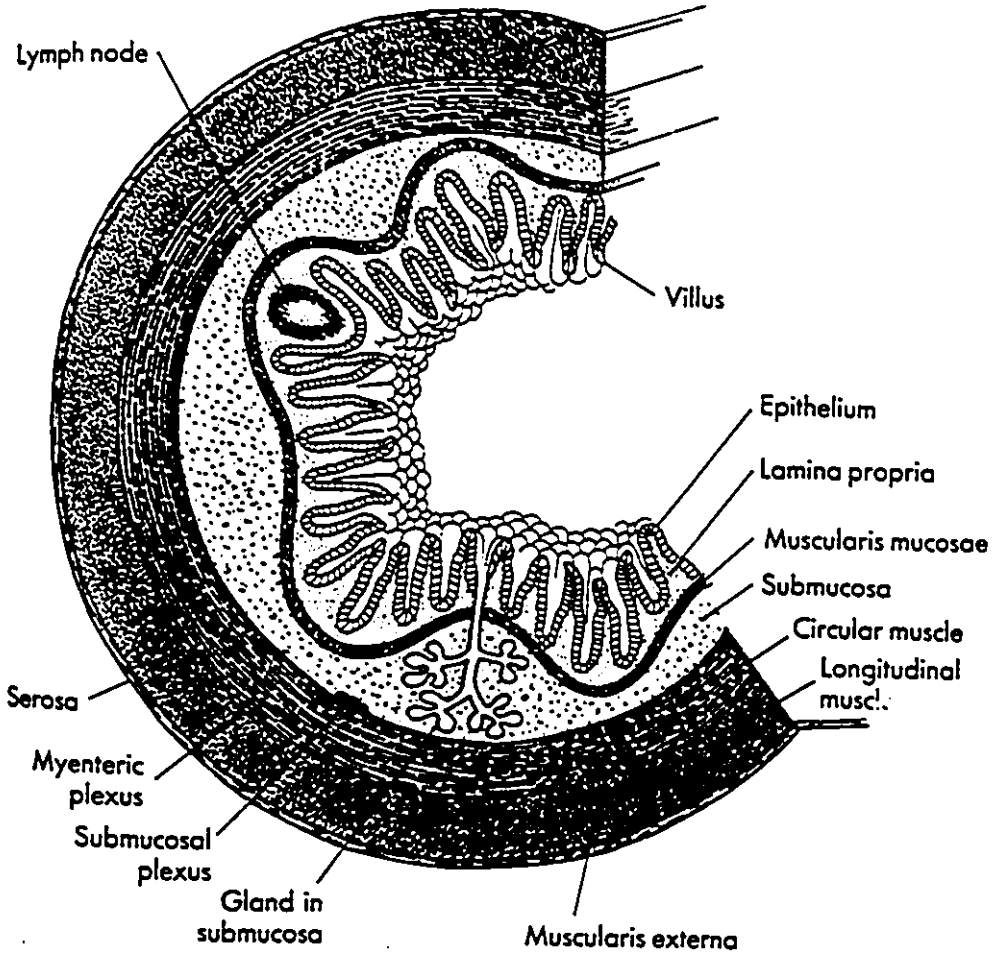
Lymph node
Villus
Epithelium
Lamina propria
Muscularis mucosae
Submucosa
Circular muscle
Longitudinal muscl.
Serosa
Myenteric plexus
Submucosal plexus
Gland in submucosa
Muscularis externa

The intestinal mucosa is divided into three layers. The innermost layer is a continuous thin sheet of smooth muscle (muscularis mucosa) which separates the mucosa from the submucosa. Because of its contractile properties, the muscularis mucosa may be involved in villar movement. These movements may modify the thickness of the unstirred water layer, overlying the villi, which is itself a barrier to intestinal permeation (Csaky, 1984). The middle mucosal layer is the lamina propria which is sandwiched between the surface epithelium and the muscularis mucosa. The lamina propria has important immunological as well as structural functions (Doe, 1989). Within the lamina propria is a central arteriole which travels up the core of the villus. At the villus tip, the arteriole divides, giving rise to the terminal capillary network. This network in turn travels down the villus in close proximity to the basal surface of the epithelium. These capillaries have diaphragm-covered fenestrations, causing them to be very permeable. This middle mucosal layer is thus designed to facilitate efficient removal of absorbed substances by strategic placement of permeable blood vessels along the basolateral membrane of the enterocytes. Also coursing up the villus within the lamina propria is a centrally located lymphatic vessel ("central lacteal"). The third layer of the intestinal mucosa is a continuous epithelial layer surrounding both the villi and the crypts of Lieberkuhn. The epithelial layer is one cell thick, and is in direct contact with the luminal contents. These features of the third mucosal layer greatly facilitate movement of substances between the lumen and the blood (Madara and Trier, 1987).

The major function of the villus epithelium is the absorption of nutrients. The cells that accomplish this task are the absorptive columnar epithelial cells, also called enterocytes. Interposed between the enterocytes are mucus-secreting goblet cells (very abundant in the colon) and a few enteroendocrine cells. Less frequently observed cells in the villar epithelium are the cup cells, and the caveolated, or tuft, cells. The function of these cells is unknown, and it appears that their distribution may be quite species dependent (Madara and Trier, 1987).

The crypt epithelium is composed of a heterogenous population of cells. According to the unitary theory of epithelial cell origin in the small intestine, totipotent stem cells serve as precursors mainly for villar absorptive cells, but probably for a number of other GI surface epithelial cells, in both the villi and the crypts (Becciolini et al., 1985). Stem cells designated as precursors for the villar epithelial cells differentiate and mature as the cells migrate up the villi from the crypts. The movement of the cells up the villi can take anywhere from 2 to 6 days depending on the tissue and on the species (Figure 2) (Gordon, 1989). Part of the maturation process is that cells lose the ability to divide as they migrate up the villi, but at the same time they incorporate new membrane proteins crucial for absorption. Cells die and are sloughed off as they reach the tip of the villi, however they are replaced by new cells which are continually migrating up the villi. This system minimizes the villar area which may become denuded as the older cells are sloughed off. Other cell types found in the crypt epithelium are mucus-secreting goblet cells, Paneth cells, and enteroendocrine cells, in particular the serotonin-containing

Figure 2.

Migration of maturing epithial cells from the crypt to the tip of the villi. From Gordon, 1989.

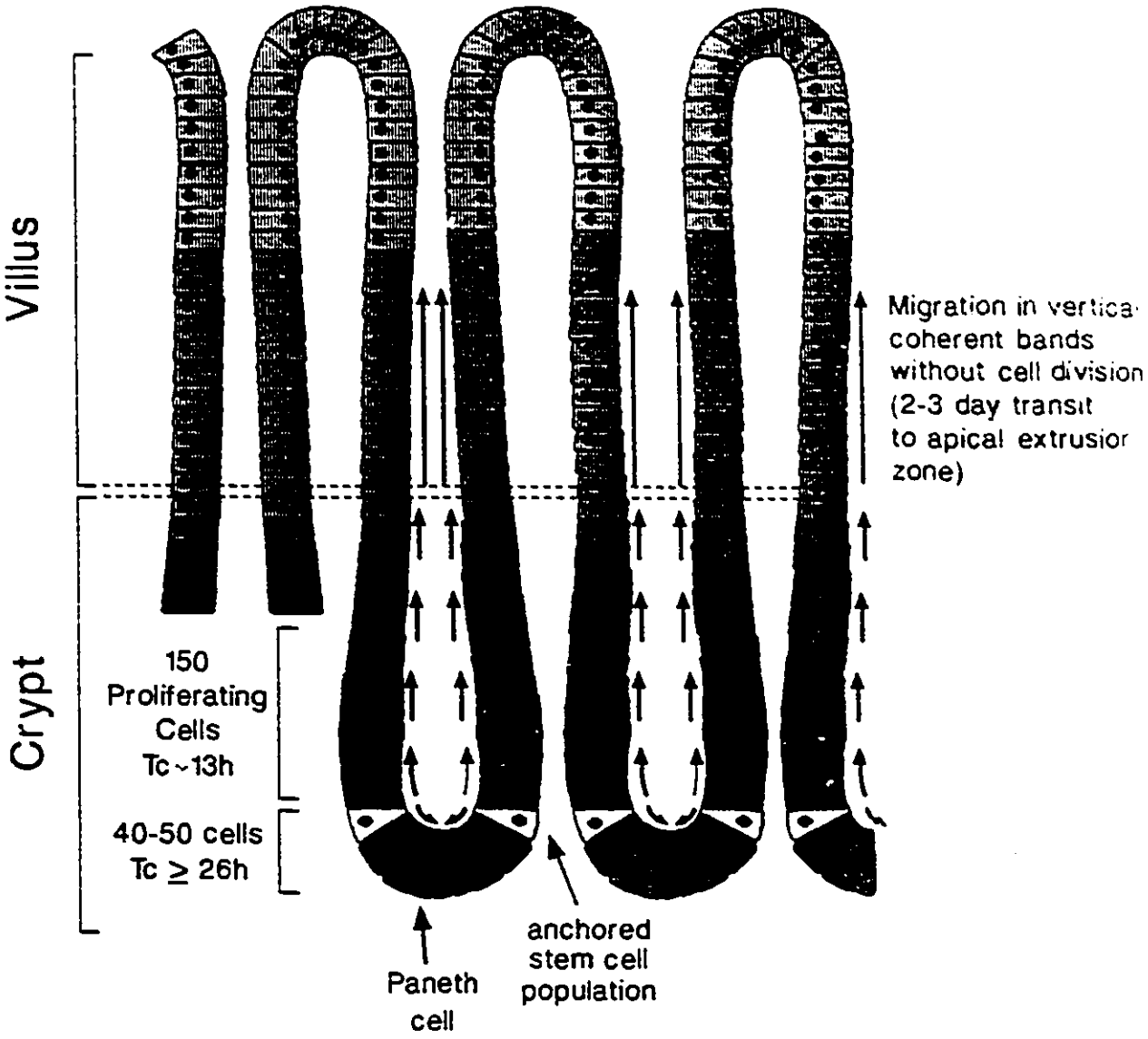
Villus
Crypt
150
Proliferating
Cells
Tc ~ 13h
40-50 cells
Tc ≥ 26h
Paneth
cell
anchored
stem cell
population
Migration in vertica
coherent bands
without cell division
(2-3 day transit
to apical extrusior
zone)

enterochromaffin (EC) cells. With the large variety of cells located in the crypts, many functions are attributed to this area including exocrine secretion into the crypt lumen (via the goblet, Paneth, and undifferentiated cells), electrolyte and water secretion (via the undifferentiated cells), and endocrine secretion both into the lamina propria and into the crypt lumen (via the endocrine epithelial cells), and as previously mentioned the proliferative component of the crypt epithelium is critically involved in epithelial cell renewal (Madara and Trier, 1987).

Structural Organization of Enterocytes

Enterocytes are characterized by a brush border at their apical (luminal) domain, and a junctional complex that anatomically and functionally joins adjacent cells (Figure 3). The brush border membrane is "highly contoured, forming numerous closely packed microvilli which project into the lumen" (Madara and Trier, 1987). The microvilli increase the absorptive surface area approximately 25-fold. Specialized transporters for electrolytes and nutrients are located on and within, this microvillar membrane. The junctional complex consists of three components. The most apically located component is the tight junction (zonula occludens) which consists of a variable number of proteinaceous strands, that completely encircle the apical end of each epithelial cell. The other components of the junctional complex, are the gap junctions (intermediate junction, zonula adherens) located proximal to the tight junction, and the desmosomes (Madara and Trier, 1987).

Figure 3

Schematic diagram of an intestinal absorptive cell. From Madara and Trier, 1987.

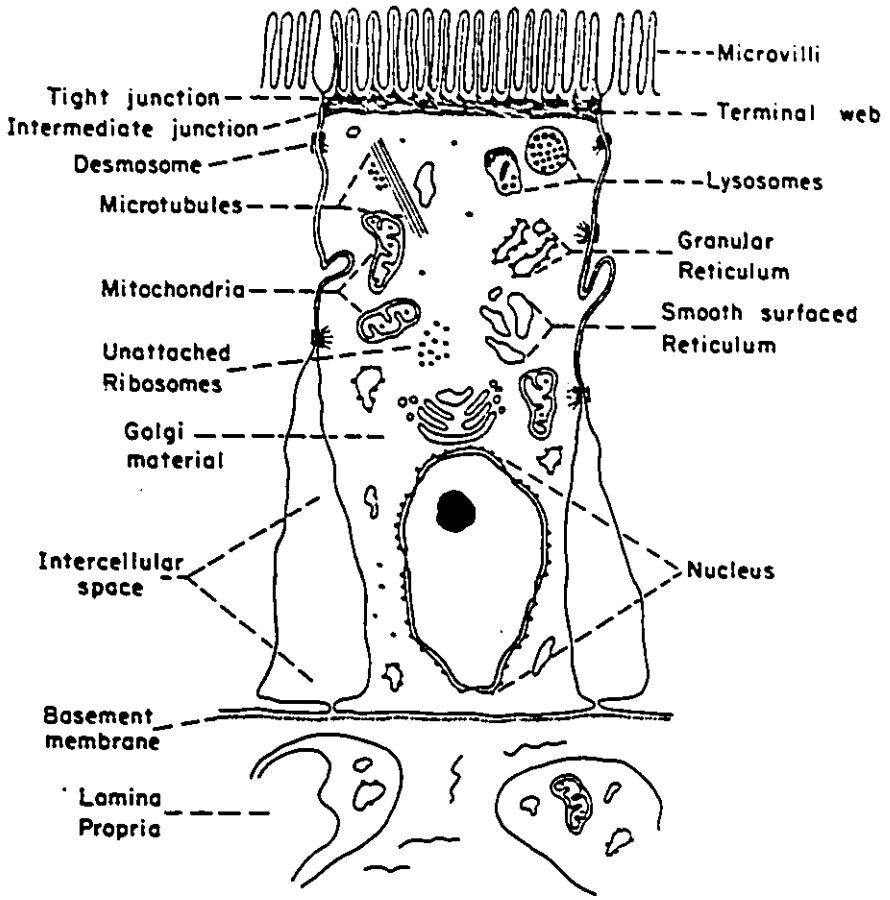
Microvilli
Tight junction
Intermediate junction
Terminal web
Desmosome
Lysosomes
Microtubules
Granular Reticulum
Mitochondria
Smooth surfaced Reticulum
Unattached Ribosomes
Golgi material
Intercellular space
Nucleus
Basement membrane
Lamina Propria

The junctional complex has several functions, which have been described as bridge, gate, and fence (Diamond, 1977). The gap junctions act as the anatomical and functional bridge between adjacent enterocytes, regulating solute movement between cells (Diamond, 1977). The tight junctions have a dual role as both gate and fence. As a gate, the tight junction helps regulate the diffusion of ions and neutral molecules through the paracellular (shunt) pathway (Gumbiner, 1987). Some gates are stronger than others, i.e., some tight junctions are composed of a greater number of structural strands, or have strands that are organized in a more regular fashion. Strand number and organization are believed to be the basis for classification of tight junctions into either "leaky" or "tight" (Diamond, 1977).

Intestinal Permeation

A simple yet sensitive measure of the gate function of tight junctions is the transepithelial electrical resistance (Gumbiner, 1987). The transepithelial resistance is directly proportional to the permeability of the epithelial layer to inorganic ions (Gumbiner, 1987). These ions may permeate this layer via one of two transport pathways: through the cell (transcellular), or between adjacent cells (paracellular) through the junctional complex (Figure 4; Csaky, 1984). Although there are a number of physical and chemical barriers to permeation, the four major barriers to permeation are: the apical membrane, the basolateral membrane, the tight junction, and the intercellular space (ICS). The epithelium may be depicted as a simple electrical circuit (Figure 5), and the major barriers to permeation represented as

Figure 4.

Routes of permeation across the intestinal mucosa. Although a bidirectional process, this schematic illustrates permeation from the blood compartment to the luminal compartment, i.e., secretion. Diagram modified from Csaky, 1984.

Routes of Intestinal Permeation [9]

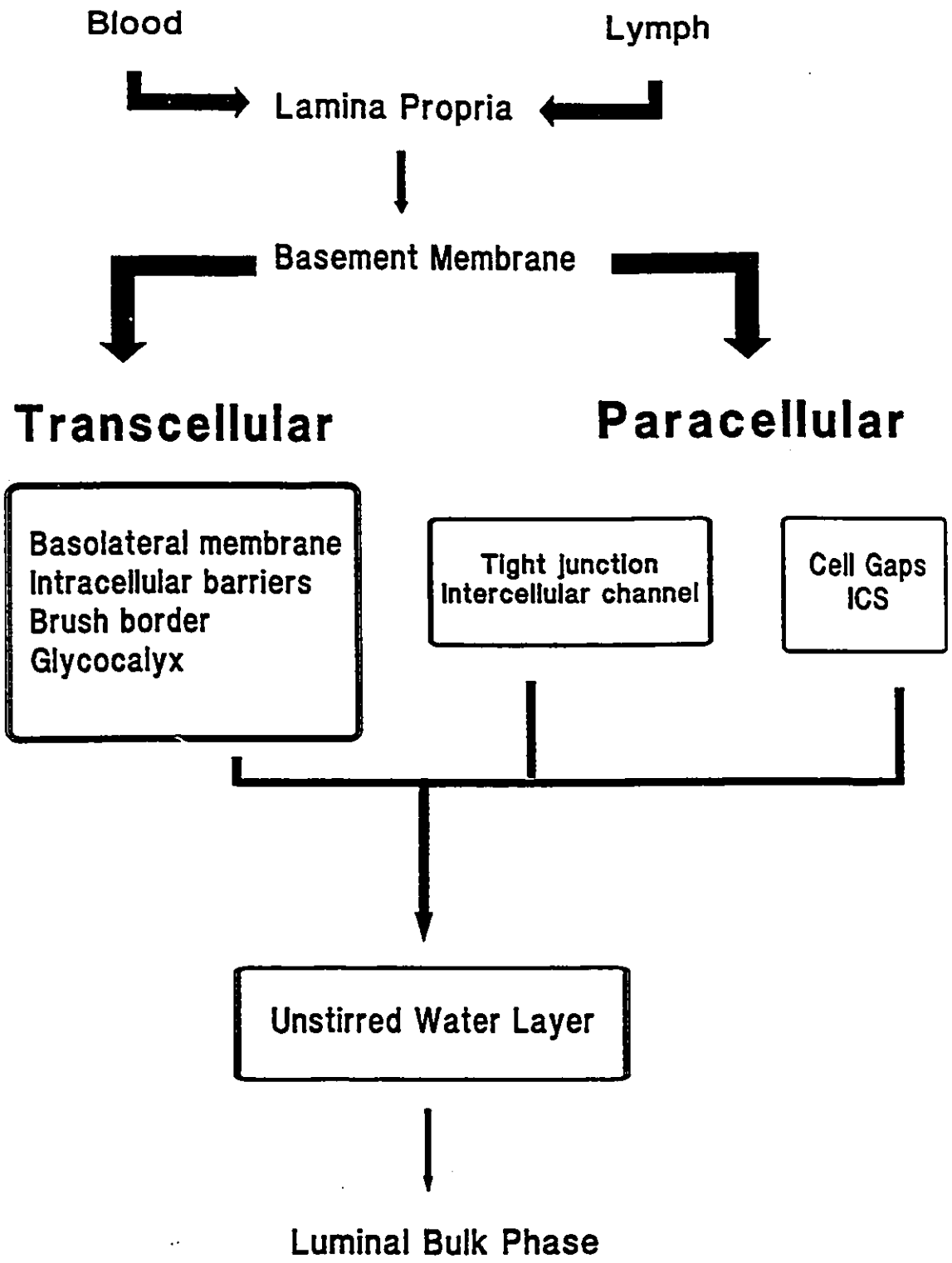

Modified from Csaky, 1984

Figure 5.

Equivalent circuit of enterocyte membranes. See text for details of equations. M refers to mucosal surface, S refers to serosal surface. From Powell, 1981.

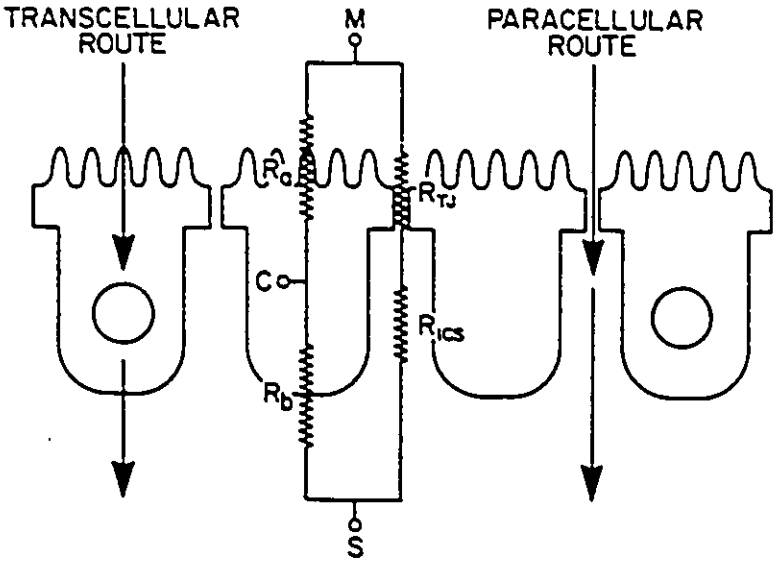

$$R_C = R_a + R_b$$

$$R_S = R_{TJ} + R_{ICS}$$

$$R_T = \frac{(R_C)(R_S)}{R_C + R_S}$$

$$G_T = G_C + G_S$$

$$\frac{G_S}{G_T} = \frac{G_S}{G_C + G_S}$$

resistances (Powell, 1981). The major barriers to substances permeating via the transcellular pathway are the apical and basolateral membranes. Together the sum of the resistances of these barriers (R_a and R_{bl}) equals the cellular resistance (R_c). Likewise, the sum of the major resistances to substances permeating via the paracellular route (barriers = JC and ICS) equals the resistance of the paracellular (shunt) pathway (R_s). Tissues with "leaky" tight junction (leaky epithelia) have a tissue resistance ($R_T = (R_c)(R_s)/[R_c+R_s]$) less than 1000 ohms/cm^2, an R_c greater than R_p, or a shunt conductance ($G_s=1/R_s$) greater than 50 % of the total tissue conductance ($G_T = G_c + G_s$). Using these criteria, the small intestine, along with the choroid plexus and renal proximal tubule, have been characterized as leaky epithelia. In reference to its role as a gate, the tight junction in leaky epithelia is "open" a greater proportion of the time than in tight epithelium (examples of tight epithelia include gastric fundus and esophagus) (Powell, 1981). Progressing down the intestinal tract, permeability decreases from the jejunum ("very leaky") to the ileum ("moderately leaky") to the colon ("moderately tight") (Table 1).

Table 1. Relative permeabilities along the intestinal tract.

Jejunum	**Ileum**	**Colon**
High permeability	---------->	Low permeability
Low mucosal R	---------->	High mucosal R
Low PD	---------->	High PD

R = resistance, PD = potential difference

(Binder, 1989)

Permeability vs Permselectivity

The term *permeability* refers to the magnitude of the barrier and it is this property that is quantified by the transepithelial electrical resistance. The weaker the barrier to substance "X", the greater will be the permeability (to substance "X"), and this will be reflected by a lower transepithelial electrical resistance. The term *permselectivity* is a qualitative measure of the barrier's "ability to discriminate and show preference for either cations or anions, and within a series of cations or anions" (Powell, 1981). Permselectivity arises from both the tight junction's role as a gate, but also as a fence. As a fence, the tight junction forms a physical barrier, segregating the apical domain from the basolateral domain. This segregation prevents intramembranous proteins (such as transporters) from moving in the fluid lipid bilayer from one domain to the other, thus restricting them to their respective compartments. As a result of this "fencing" property, ion transporters have a polarized distribution across the cell membrane resulting in the generation of chemical and electrical gradients, and thus facilitating vectorial transport (Rodriguez-Boulan and Nelson, 1989).

Permselectivities of the apical and basolateral membranes are a reflection of the different transport mechanisms (carriers, pumps, conductance channels) that exist in those domains *(permeability would reflect the number of transporters that would exist)*. Table 2 lists the major transport mechanisms that exist across the apical and basolateral membranes of an enterocyte in the human small intestine (Armstrong, 1987).

Table 2. Major ion transport mechanisms across the apical and basolateral membranes of small intestinal epithelia.

	Apical Membrane		Basolateral Membrane	
	Substance	Mechanism	Substance	Mechanism
Electrogenic	Na^+-glucose	co-transport	Na^+-K^+	ATPase antiport
	Na^+-amino acids	co-transport	K+	conductance channel
Electroneutral	Na^+-H^+	antiport	K^+-Cl^-	symport
	Cl^--HCO_3^-	antiport	Cl^--HCO_3^-	antiport
	Na^+-Cl^-	symport		

(Binder, 1989)

Enterocytes are Na^+ transporting epithelia. The primary active step of transport across all polarized epithelial cells, is the active movement of Na^+ out across the basolateral membrane via the Na^+-K^+-ATPase transporter. This transporter is restricted to the basolateral membrane because of the fencing role of the tight junction (Rodriguez-Boulan and Nelson, 1989). The gradient for Na^+ entry across the apical membrane is created by the action of the Na^+-K^+-ATPase, which by actively extruding Na+ from the cell, generates a favourable electrochemical gradient for the apical entry of Na^+ (Table 2). Although these apical Na^+ transporters do not directly require energy for their activity, their function is dependent upon the electrochemical gradients created by energy-dependent Na^+-K^+-ATPase. Therefore, apical transporters are often considered to be "secondary active"; similarly, solute movement through the paracellular pathway, normally considered to

be passive, can be called "tertiary active" (Moe et al., 1990).

At the apical membrane, permselectivities (PS) are $PS_{Na+} > PS_{Cl-} > PS_{K+}$. This order is reversed at the basolateral membrane, i.e. $PS_{K+} > PS_{Cl-} > PS_{Na+}$. While permselectivities of the barriers to the transcellular pathway are largely dependent on the polarized distribution of transporters, the permselectivity of the paracellular pathway is highly dependent on the negative charges (carboxyl, phosphoric acid, or sulfuric acid radicals) that line the tight junction and intercellular space. Hence permselectivity to the shunt pathway is cation selective, and generally $PS_{K+} >> PS_{Na+} > PS_{Cl-}$ (Madara and Trier, 1987).

Regional Differences in Intestinal Transport

The upper small intestine (duodenum, jejunum, and proximal ileum) accounts for the bulk of fluid absorption, whereas the distal small intestine is more important for conservation (absorption) of sodium (Na^+) (Table 3). As well, some substances are only absorbed in the upper small intestine (fat and water soluble vitamins), while others only in the terminal ileum (bile salts, vitamin B_{12}). Although the colonic surface epithelium is devoid of villi and plicae, it has a tremendous capacity to absorb fluid. This efficiency of colonic fluid absorption is due to the characteristics of the striated columnar cells lining the mucosa (Madara and Trier, 1987).

The combined effect of the permselectivities of the intestinal epithelial cell barriers is to absorb large amounts of luminal Na^+ and to a lesser extent Cl^- and K^+. Another important role of the small intestine is to conserve water. Normally the

Table 3. Regional differences in intestinal transport

Tissue	Transport Mechanisms
Jejunum	1° solvent drag secondary to monosaccharide absorption 2° electrogenic, glucose-stimulated, HCO_3^- stimulated
Ileum	1° electroneutral Na^+-H^+ and Cl^--HCO_3^- exchange 2° electrogenic, solvent-drag very poor due to relatively lower permeability to jejunum
Colon	Glucose and other non-electrolytes do not stimulate Na^+ and H_2O absorption No active nutrient absorptive processes Mineralocorticoid sensitive 1° electrogenic (distal colon) 2° electroneutral Na^+ independent Cl^--HCO_3^- exchange

(Binder, 1989)

small intestine receives 9 L of fluid per day: approximately 1.5 - 2 L from ingested food and liquids, the remainder from salivary, gastric, pancreatic, biliary, and intestinal secretions. Roughly 44 % of this fluid is absorbed in the duodenum and jejunum, 39 % by the ileum, and a further 11 % by the colon. The actual cellular route of fluid absorption is unknown but studies measuring the cell membrane water permeability indicate that fluid moves primarily, but not exclusively, through the epithelial cell (Binds 1989). Fluid permeates across an epithelium in response to two major forces: hydrostatic pressures ("P") and osmotic pressures ("π") (Naftalin and Tripathi, 1985). The proposed mechanism of fluid absorption is described below, under the *"Three compartment model of intestinal permeation."*

Three Compartment Model of Intestinal Permeation

Curran and MacIntosh (1962) developed a three compartment-double membrane model to explain the mechanism of intestinal permeation (Figure 6). Compartments A, B, and C, respectively correspond to the epithelial cell, the lateral intercellular space, and the capillary. The two membranes, alpha and beta, respectively represent the basolateral membrane, and the more permeable capillary membrane. This compartment model is very useful to explain the current theory of fluid absorption from the intestinal lumen. Secondary active transporters on the apical membrane of enterocytes transport salts into the cell from the lumen. This creates a localized osmotic gradient inside the cell, causing luminal fluid to passively enter the cell. Some of the intracellular salts (Na^+ and Cl^-) are then actively

Figure 6

Three-compartment model of intestinal permeation. The top portion of the figure depicts a double-membrane model that can permit fluid to move from compartment A to compartment C, against a concentration gradient. The bottom portion of the figure depicts the proposed anatomical sites of the double-membrane model in epithelia. From Binder, 1989.

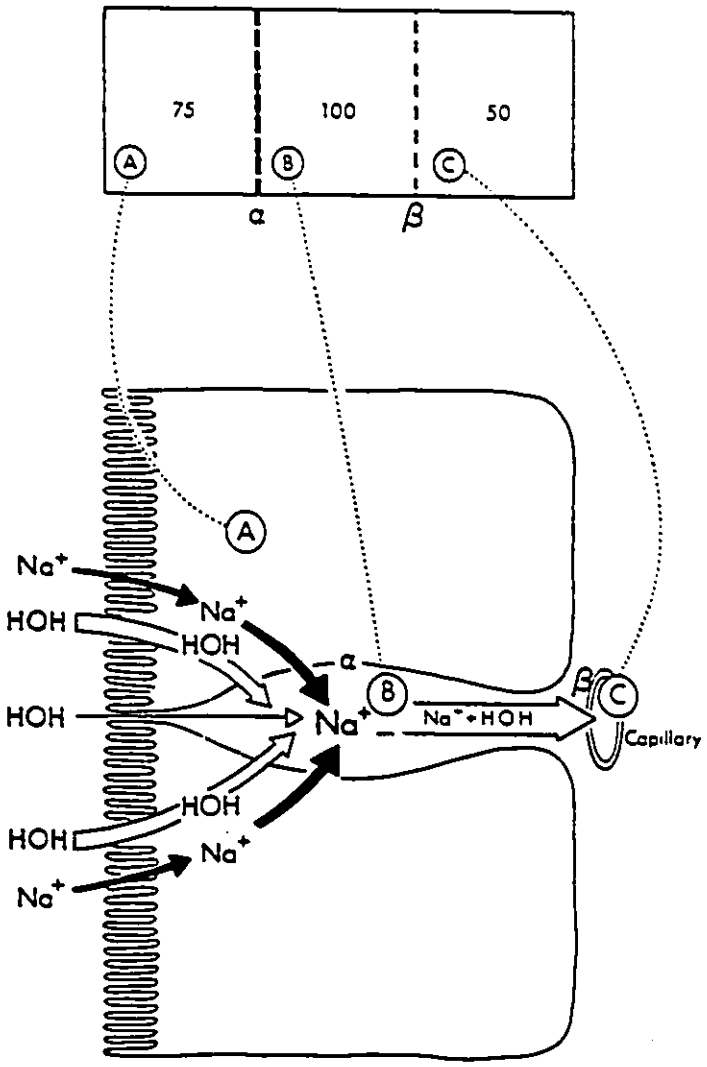
75
100
50
A
B
C
α
β
Na+
HOH
Na+
HOH
α
HOH
Na+
B
Na+ + HOH
β
C
Capillary
HOH
HOH
Na+
Na+

extruded across the lateral cell membrane into the lateral intercellular spaces (LICS), again creating a localized osmotic gradient. Fluid will then flow out of the cell, following the salt into the LICS. In response to the osmotic pressure in the LICS (π_{LICS}), some luminal fluid will also enter the LICS via the paracellular pathway. Although the entry of fluid into the LICS dissipates (or at least minimizes) the osmotic pressure, it also increases the hydrostatic pressure inside this compartment (P_{LICS}). Starling's equation of transcapillary fluid flux[1] may be used to show that the combination of a high P_{LICS} and a low π_{LICS} relative to the values of these pressure forces inside the capillary lumen (low P_c, high π_c), results in net absorption of fluid from the LICS across the highly permeable capillary endothelium into the third compartment, the capillary lumen (blood) (Curran and MacIntosh, 1962).

Methods of Investigation of Intestinal Permeation

Several methods exist for investigating intestinal permeability (Table 4). There are a number of *in vitro* preparations derived from isolated loops of intestine. One of the most commonly used *in vitro* methods is the intestinal sheet method developed by Ussing and his colleagues (1951). In the Ussing chamber method, the gut is excised and opened, the muscle layer is stripped away and the resultant

---

[1]Starling flux equation: $J_v = K_{FC}[(P_c - P_{LICS}) - \sigma_d(\pi_c - \pi_{LICS})]$
where J_v is the net volume flow occurring across the microvascular wall, P_c and P_{LICS} are the capillary and lateral intercellular space hydrostatic fluid pressures, π_c and π_{LICS} are the capillary and lateral intercellular space oncotic pressures. K_{FC} is the capillary filtration coefficient and σ_d is the osmotic reflection coefficient (Taylor and Townsley, 1987).

Table 4. Methods of investigation of intestinal permeability.

I. *In vitro Techniques*:

- A) Isolated Loops:
  - i) Uneverted loops
  - ii) Everted loops
  - iii) Loops with mainly mucosa
  - iv) Intestinal rings
  - v) Intestinal sheets (Ussing Chambers)
  - vi) Intestinal villi
  - vii) Isolated enterocytes
  - viii) Isolated epithelial membranes

II. *In vivo Techniques*:

- A) Conscious Animals:
  - i) Thiry-Vella fistula
  - i) Method of Cori
  - iii) Blood/urine level after oral load of substrate
- B) Anesthetized Animals:
  - i) Closed system (tied loops)
  - ii) Open system (luminal perfusion)

(Csaky, 1984)

mucosal tissue is mounted as a sheet between two sides of a chamber, such that the mucosal and serosal surfaces are bathed with fluids of known composition. A very useful modification of this technique is the application of the short-circuit current to the system. Measurement of this current is an estimate of the net active ion transport across the tissue. Isolated enterocyte preparations, although technically difficult, are another practical *in vitro* method, as only the cells that are involved in transport are investigated. *In vitro* techniques allow the investigator to limit the number of biological variables. The drawback of these techniques is that the results are obtained from an artificial preparation, i.e. controlling or eliminating biological variables that may participate in normal function. It was therefore decided to use an *in vivo* model to investigate intestinal permeation in this thesis.

Currently there are three established models of intestinal permeation in conscious animals (Table 4). (i) The Thiry-Vella fistula was developed in the mid 1800's as a preparation for larger animals (usually dogs). Under anesthesia, an intestinal segment with its blood, lymphatic and nerve supply intact, is isolated and exteriorized. End-to-end anastomosis connects the rest of the intestine. Substrates are injected into the exteriorized segment and their rate of disappearance is quantitated as absorption. (ii) The Method of Cori is a similar application. In this technique, a known volume and concentration of a substrate is gavaged. After a period of time, the animal is killed and the entire gastrointestinal tract is removed and washed. Again, the disappearance of the substrate is quantitated as absorption. (iii) The third application in conscious animals is one used routinely in clinical

practice. An oral load containing a permeability probe is given to the patient. After a defined time interval, a blood or urine sample is taken, and the rate of appearance of the probe in the sample is quantitated as absorption. Generally, a urine sample is taken, as it is less invasive than a blood sample.

A common disadvantage with the Cori Method and the oral loading method is that information cannot be obtained about permeability defects in a specific region of the intestinal tract. Experiments on anesthetized animals though allow regional comparisons to be made in the intestinal tract. One option is a closed system designed such that loops or "sausages" of intestine of varying length, can be tied off and filled with known volumes and substrates. The disadvantage with this system is that the luminal fluid is static, and an increasing unstirred water layer may affect the permeability of the segment. This method has been used experimentally to characterize a neonatal disorder known as necrotizing enterocolitis (Miller et al., 1990). The other method for investigating intestinal permeability in anesthetized animals is the luminal perfusion of cannulated intestinal segments. This was the method chosen for the present project and thesis. It is essentially identical to the closed system preparation, except that the loops are perfused at a known rate, minimizing the unstirred water layer and stabilizing the gradient.

Markers of Intestinal Permeability

There are a number of criteria for a substance to be considered a probe or marker of permeability. The probe must be non-toxic, metabolically inert, absorbed by passive diffusion, distributed in the extra-cellular compartment, water soluble, lipid insoluble, rapidly excreted in the urine, and accurate and simple to assay (Jenkins et al., 1986; Hollander et al., 1988). Table 5 lists some of the commonly used permeability probes which meet these criteria.

Table 5. Molecular characteristics of permeability probes.

Probe	Weight (daltons)	Surface Area (angstroms^2)	Diameter (angstrom)
Rhamnose	164	166	8.3
Mannitol	182	186	6.7
Cr-EDTA	341	268	10.5
Cellobiose	342	313	10.3
Lactulose	342	313	9.5

(Hollander et al., 1988)

Routes of Intestinal Permeation of Permeability Probes

Much of the permeability literature falsely correlates the molecular weight of the tested permeability probe with intestinal permeation. Computer-generated 3-D models of the probes listed in Table 5, indicate that intestinal permeability is inversely related to the cross-sectional diameter of the probe (Hollander et al., 1988). The smallest of the two listed probes, rhamnose and mannitol, are presumed to pass

through small aqueous "pores" of high frequency located in the enterocyte membrane. These pores are assumed to comprise the transcellular permeation pathway. Lactulose (a disaccharide composed of galactose and fructose) and ^{51}Cr-EDTA are presumed to pass through larger aqueous "channels" of low frequency situated within tight junctions and/or cell extrusion zones (Maxton et al., 1986). This dual transport pathway hypothesis gained support by comparing the permeation of the probes in response to different luminal stresses. Ingestion of a hyperosmolar or cetrimide-containing solution increased the permeation of ^{51}Cr-EDTA and lactulose but had no effect on the permeation of rhamnose or mannitol. These stresses are known to affect permeation of the paracellular pathway. As well, villous atrophy produced an increase in permeation of the larger probes but a coincident decrease in the smaller ones (rhamnose, mannitol) (Maxton et al., 1986).

Functional Significance of ^{51}Cr-EDTA Intestinal Permeation

Alterations in the permeation of ^{51}Cr-EDTA are believed to reflect irregularities in mucosal morphology before they are revealed by histological examination (Bjarnason et al., 1983; Elia et al., 1987). As a radiolabelled probe, ^{51}Cr-EDTA is one of the easiest probes to accurately assay. For these reasons ^{51}Cr-EDTA has become the probe most commonly used for gastrointestinal permeability studies, in particular for models of ulcerative colitis and Crohn's disease (Bjarnason et al., 1983). This probe however has yet to be used to detect intestinal permeability changes in response to radiation exposure.

Radiotherapy

It has been almost a century since ionizing radiation was introduced as an effective form of cancer therapy. Up until the mid 1950's, the radiation was delivered using orthovoltage equipment, approximately 200 - 300 kilovolt X-Rays. This equipment often resulted in burning of the skin, thereby limiting the effectiveness of the treatment. Since the introduction in the mid 1950's of supervoltage (one megavolt or greater), radiotherapy has become increasingly prominent and effective in the role of curative and palliative management of cancer patients (Kinsella and Bloomer, 1980). The supervoltage equipment produces short-wavelength, high frequency X-rays or gamma rays that are of sufficient energy to produce ionization in body tissues that absorb the energy.

The rad and the Gray (Gy) are the units of measure for ionizing radiation. One Gray equals 100 rads, and is the international unit for radiation energy. The intensity of delivered or absorbed energy is expressed as a dose rate, i.e., so many rads (or Gy) per unit time. One Gray equals the energy deposition of one joule per kilogram (Earnest and Trier, 1989).

Approximately 50 % of cancer patients will receive radiation therapy at some time during the course of the disease (Kinsella and Bloomer, 1980). Radiotherapy can be very effective in the primary treatment of cancers such as squamous cell carcinoma of the cervix, carcinoma of the intrinsic larynx, and certain testicular malignancies. Radiotherapy is also a component of the treatment regimen of other curable tumors such as squamous cell carcinoma of the oral cavity, endometrial

adenocarcinomas, carcinoma of the breast, and certain forms of lymphoma and pediatric tumors (Smith and DeCosse, 1986). Irradiation of gastrointestinal tissues is often unavoidable in many of these procedures.

For radiation therapy to be effective in the treatment of neoplastic disease, it is necessary to deliver high doses of radiation. While the benefit of radiotherapy is high, so too is the cost that normal tissues pay as a consequence of radiation exposure. All cells that are exposed to ionizing radiation will sustain some damage or effect. However some cells are more radiosensitive than others. As interference (or even inhibition) of DNA synthesis is perhaps the primary lethal effect of ionizing radiation, those cells that are rapidly dividing will be the most vulnerable to radiation damage. This is the basis of radiotherapy; malignant cells have a very high mitotic activity and are thus relatively susceptible to radiation injury. However, some normal (non-malignant) cells are also rapidly dividing, including: lymphocytes, reproductive germ cells, immature hematopoietic cells and cells of the intestinal epithelium (Earnest and Trier, 1989). Unfortunately because of the high proportion of cancers located in the abdominal and pelvic areas, the intestine can be frequently exposed to ionizing radiation. For a typical radiotherapy regimen, total dose delivered to the abdomen (i.e. partial body radiation) can be within the range of 50 to 60 Gy, delivered over a number of radiotherapy sessions spanning several days or weeks (Berthrong, 1986). Clinical complications subsequent to radiation exposure of the intestinal tract are referred to as radiation enteritis. Symptoms of this condition can be classified into acute and chronic (long-term) side effects (Table 6).

Table 6. Clinical manifestations of radiation injury to the small bowel.

Acute	Chronic
Nausea	Obstruction
Vomiting	Perforation
Cramps	Bleeding
Diarrhea	Malabsorption
Tenesmus (straining)	Tenesmus
Abdominal pain	Abdominal pain
	Fistulas

(Smith and DeCosse, 1986)

The long-term complications, and mortality rate can be substantial for radiation enteritis. However there are several factors which can influence the risk of complications of radiation therapy (Table 7) and these should be considered when considering the cost/benefit of radiotherapy, and in interpreting the data from radiation experiments on biological systems.

Table 7. Factors which influence the risk of radiation therapy.

Technical	Clinical
Dose	Tumor type and grade
Overall time	Stage of disease
# of fractions	Anatomic factors
Individual dose	Age and sex of patient
Treatment volume	Nutritional status
Beam quality	Hematopoietic factors
Integral dose	Previous surgery
Quality of technique	

(Churnratanakul et al., 1990)

Effects of Radiation on Intestinal Structure and Function

Cellular Responses to Irradiation:

The severity of cellular damage depends to a large extent on what stage of the cell cycle (Figure 7) the cells are in when they are irradiated (Earnest and Trier, 1989).

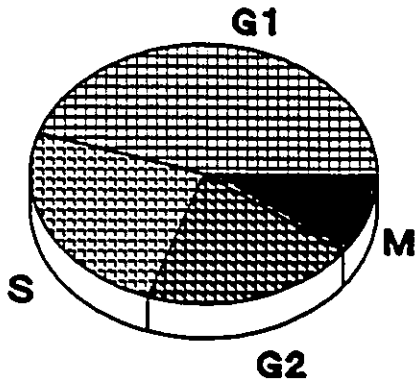

Figure 7. The Cell Cycle

Cells are most sensitive to radiation injury during mitosis, the phase of active cell division. Resistance to radiation injury increases during the first rest interval (G1) after mitosis (M), reaches a peak during the DNA synthesis (S) phase, and then rapidly declines during the second rest phase (G2). Cycling cells receiving a lethal dose outside of M, can function apparently normally, until they enter M and die (Earnest and Trier, 1989).

The actual mechanism(s) of cellular death from radiation exposure has never been confirmed, however one likely mechanism involves the production of free radicals. The energy absorbed by the cell from the ionizing radiation can react with intracellular water, producing free radicals (peroxyl radical ($HO_2\cdot$), hydroxy ($OH\cdot$), hydrogen radical ($H\cdot$), and superoxide anion ($O_2^{-}\cdot$)), which are substances with a reactive unpaired electron. The free radicals can then interact with DNA to interfere with replication, transcription, and ultimately protein synthesis (Smith and DeCosse, 1986).

Intestinal Changes to Radiation Exposure:

Acute pathological changes induced in the intestine by radiation include abnormal epithelial cell proliferation and maturation associated with decreased crypt cell mitosis (Trier and Browning, 1966; Vigneulle et al., 1990). Consequences of these changes include villus shortening and decreased mucosal thickness. Hyperemia, edema formation, and extensive inflammatory cell infiltration of the mucosa can also occur (Quastler, 1956; Buell and Harding, 1989). Depletion and impaired maturation of villus absorptive cells leads to reduced brush border enzyme and ion transporter activity (Thomson et al., 1989). As well, ionizing radiation can directly affect the cell membrane, resulting in alterations in intestinal transporters (Quastler and Hampton, 1962; Curran et al., 1960). Also associated with the early phase of radiation exposure is a predominant swelling of capillary endothelial cells, and an increase in capillary luminal diameter (Abbas et al., 1990). Capillary and lymphatic walls may have an

altered permeability as suggested by the presence of interstitial edema. These vascular changes may be severe enough to cause mucosal ischemia, potentiating the deleterious side effects of radiation on the intestinal epithelium (Earnest and Trier, 1989). All of these histopathological factors can disrupt the barrier function of the surface epithelium, leading to an altered permeation of various substances (Earnest and Trier, 1989). However, it is possible that radiation exposure may also alter intestinal permeability via physiological mechanisms. These could include direct or indirect stimulation of enteroendocrine cells causing release of secretagogue substances (Matsuoka et al., 1962; Penttila et al., 1975), altered motility (Summers et al., 1987; Otterson et al., 1988), and alterations in intestinal blood flow (Kabal et al., 1973; Timmermans and Gerber, 1980).

Prodromal Effects of Radiation

Prodromal effects simply refer to those symptoms which indicate the onset of any disease. The prodromata following radiation exposure in humans and certain other animals include nausea, retching, vomiting, diarrhea, and malaise (Harding, 1988). Nausea is the disagreeable sensation that frequently precedes vomiting. Symptoms of nausea, which include pallor, sweating, excessive salivation, tachycardia, and hyperventilation, are caused by changes in autonomic activity (Borison, 1989). Several retches frequently precede the act of vomiting, hence retching has been described as a "priming mechanism" for vomiting (McCarthy and Borison, 1974). Retching is characterized by contraction of the respiratory muscles and the rectus

abdominus against a closed glottis. This action forces the gastro-esophageal contents and some of the upper proximal intestinal contents (which enter the stomach by retrograde peristalsis) into the relaxed esophagus. The respiratory and abdominal muscles then relax, allowing return from the esophagus to the stomach. Vomiting is identical to retching except that there is a sudden upward movement of the diaphragm, which transfers the abdominal pressure to the thorax. This generates sufficient force to propel the gastric contents into the mouth via a relaxed pharyngo-esophageal sphincter. Although nausea, retching, and vomiting can occur independently of each other, they generally occur together and all are considered to be components of the vomiting sequence (Barnes, 1984).

The area postrema is a circumventricular organ located on the floor of the fourth cerebral ventricle. The pioneering work of Borison and Wang (1953) first suggested that this is the site of a "chemoreceptor trigger zone" (CTZ) for emetic stimuli borne in blood or in cerebral spinal fluid. Vagal afferents from the mucosa and muscle layers of the gut wall can also relay information about irritating gut stimuli, either chemical (eg. hypertonic NaCl) or mechanical (distension of gastrointestinal organs), to the area postrema, to the nucleus tractus solitarius, and to the dorsal motor nucleus of the vagus. The vomiting center was originally conceived as a discrete neural area that received vagal afferent or chemosensory information, and coordinated and controlled the emetic process (Borison and Wang, 1953). Since then, however, there have been numerous studies (Miller and Wilson, 1983) which suggest that there is no discrete vomiting center. Davis et al. (1986)

have proposed an alternate organizational model, suggesting that vagal afferent fibers and projections from the area postrema and other central sites, communicate with separate effector nuclei (respiratory and cardiovascular centres as examples), which in turn elicit the emetic appropriate response via vagal efferent fibers.

Vomiting most likely evolved as a quick way to expel upper gut contents that were potentially toxic. In an analagous manner, diarrhea may be considered as a method to rapidly expel toxins sensed further down the gut. It is interesting that many of the emetic stimuli also induce diarrhea (Andrews et al., 1988). There are several types of diarrhea: osmotic diarrhea, caused by impermeant agents (such as mannitol) in the intestinal lumen, diarrhea as a consequence of altered motility, diarrhea due to malabsorption of water and electrolytes (as in some conditions of intestinal inflammation), and, secretory diarrhea, caused by intestinal secretagogues (examples include serotonin, and vasoactive intestinal peptide) (Binder, 1989).

The Role of Serotonin in Intestinal Function

Synthesis of Serotonin

Serotonin (5-Hydroxytryptamine, 5-HT) is a monoamine synthesized from the essential amino acid L-tryptophan. Tryptophan 5-hydroxylase is the rate limiting enzyme in 5-HT synthesis (Thompson, 1971). The primary metabolic pathway of serotonin is oxidative deamination by monoamine oxidase, forming 5-hydroxyindoleacetic acid (5-HIAA) (Figure 8). Humans have approximately 10 mg

Figure 8.

Metabolic pathway of the synthesis of serotonin (5-hydroxytryptamine, 5-HT).

Biosynthesis and Metabolism of Serotonin

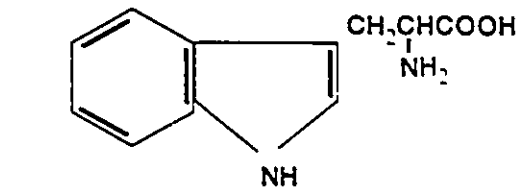

Tryptophan

tryptophan hydroxylase

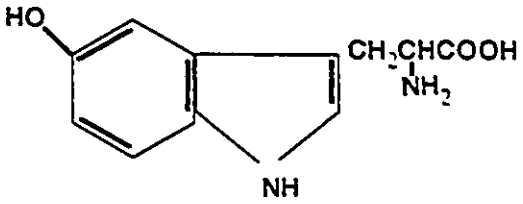

5-Hydroxytryptophan

l-aromatic amino acid decarboxylase

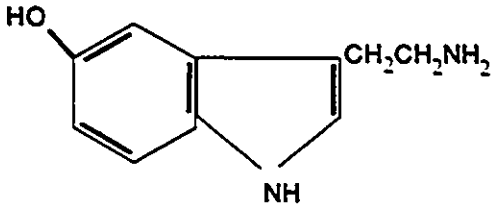

5-Hydroxytryptamine

monoamine oxidase

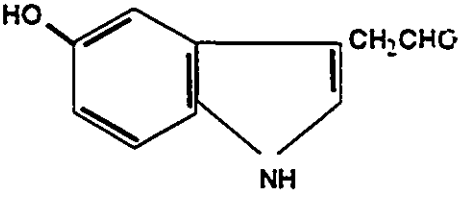

5-Hydroxyindoleacetaldehyde

aldehydedehydrogenase

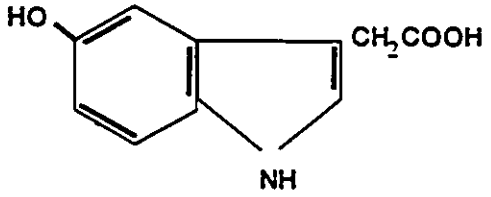

5-Hydroxyindoleacetic acid

of serotonin, stored mainly in intracellular granules in various regions of the body: platelets, mast cells, enteric neurons, and gut enterochromaffin (EC) cells (the primary source of serotonin in some species) (Thompson, 1971). 5-HT is synthesized in the cytoplasm of the EC cell and is actively accumulated, stored and released from specific granules (Penttila and Kormano, 1971).

Serotonin Receptor Classification

Serotonin receptors were originally classified into two groups called M and D (Gaddum and Picarelli, 1957). The "M" receptors were so-named because they were considered to be blocked by morphine. The "D" receptors were unaffected by morphine, and were named based on the antagonistic action of dibenzyline. However, subsequent to Gaddum and Picarelli's work (1957), it has been established that neither morphine nor dibenzyline act directly on the 5-HT_3 receptors (their inhibitory effect may be on interneurons receiving synaptic inputs of serotonergic neurons) (Gershon et al., 1990). Nevertheless, it is still possible to classify serotonin receptors *functionally* into two main families: G-protein coupled receptors which include 5-HT_1, 5-HT_2, and the putative 5-HT_4, and ligand-gated ion channels for the 5-HT_3 receptor class. It has also been proposed that the 5-HT_2 receptor is the equivalent of Gaddum and Picarelli's "D" receptor, while the 5-HT_3 receptor corresponds to the "M" receptor (Hoyer, 1990).

Both 5-HT_1 and 5-HT_2 receptors have well characterized subtypes: 5-HT_{1A}, 5-HT_{1B}, 5-HT_{1C}, 5-HT_{1D}, and 5-HT_{2A}, 5-HT_{2B}. The 5-HT_{1C} subreceptor has several

features (amino acid sequence, pharmacological and electrophysiological profiles) in common with the 5-HT_2, and is now considered a subreceptor of the 5-HT_2 family (Schmidt and Peroutka, 1989). Further confusion in the literature involves the classification of the 5-HT_{1D} subreceptor type, which is also referred to as the 5-HT_{1P} subreceptor. This subreceptor has a similar pharmacological profile to the recently described non-classical serotonin receptor, 5-HT_4 (Dumuis et al., 1989). Currently there is a debate as to whether the 5-HT_{1P} and the 5-HT_4 receptors represent distinct entities. Both of these receptors, along with the 5-HT_{1A} and 5-HT_3, are located on enteric neurons (Dumuis et al, 1989; Gershon et al., 1990). Resolution of the 5-HT_{1P} and 5-HT_4 debate would be of great interest to gastrointestinal physiologists, as these receptors have been shown pharmacologically to be involved in control of intestinal motility.

5-HT_3 Receptors

While the 5-HT_{1A}, 5-HT_{1C} and 5-HT_2 receptors have been cloned, sequenced, and expressed, relatively little is known about the molecular structure of the 5-HT_3 receptor (Hoyer, 1990). It has been estimated that in rat cortical membranes, the molecular weight (MW) of the 5-HT_3 receptor is approximately 35 kDa, considerably smaller than the MW of the G-protein coupled receptors 5-HT_1 and 5-HT_2 (Gozlan et al., 1989). Like the nicotine, $GABA_A$, and glycine receptors, the 5-HT_3 receptors are an intrinsic part of an ion channel, possibly a calcium channel (Schmidt and Peroutka, 1989) formed of multiple subunits (Hoyer, 1990). The receptor-activated

channels are permeable to potassium and sodium, but not to chloride, and as expected produce fast responses (fast excitatory post-synaptic potentials (EPSP)) that desensitize very rapidly (Hoyer, 1990). These receptors have been found on sensory neurons, sympathetic and parasympathetic neurons, and on neurons within both the myenteric and submucous plexus of the enteric nervous system (Hoyer, 1990). Just as with the other classical 5-HT receptors (5-HT_1 and 5-HT_2), pharmacological studies have suggested that the 5-HT_3 receptor has several subtypes (Richardson et al., 1985), which have yet to be fully characterized.

Development of 5-HT_3 Receptor Antagonists

Initial classification of the 5-HT_3 receptor arose from the work of Fozard and colleagues on the effects of 5-HT on the rabbit heart (Fozard and Mobarok Ali, 1978). One of the most potent antagonists to 5-HT blockade of sympathetic neurones to the rabbit heart was (-)cocaine, while agonists and antagonists to the 5-HT_1 and 5-HT_2 receptors were without effect. Fozard and his colleagues carried out further studies to verify that local anesthesia was not responsible for the 5-HT_3 antagonistic action of (-)cocaine. They discovered that procainamide, an antiarrhythmic agent, was an effective 5-HT_3 blocker (in the heart) at concentrations well below those causing local anesthesia (Fozard et al., 1979).

Substitution of the benzene ring of procainamide produces metoclopramide, a substituted benzamide with little analgesic activity or cardiac antiarrhythmic activity. Metoclopramide is a substituted benzamide with dopamine D_2 receptor

blocking activity. In Europe, metoclopramide has been prescribed as an anti-emetic since the 1950's, and it received federal approval in North America in the late 1970's. Metoclopramide is still clinically indicated for emesis associated with post-operative care, gastritis, migraine, dysmenorrhoea, and for patients receiving chemo- and radiotherapy. Metoclopramide is also a prokinetic agent, i.e., it can increase gut motility. It was believed that both the anti-emetic and prokinetic properties of metoclopramide were associated with its D_2 receptor antagonism. However domperidone, a potent D_2 receptor antagonist with some anti-emetic activity, failed to stimulate gut motility. Subsequently, attention turned towards investigating alternative mechanisms (to D_2 antagonism) to explain the mechanisms of action of metoclopramide (Sanger and King, 1988).

Fozard and his colleagues demonstrated that metoclopramide, was also a potent antagonist of the sympathetic neuronal 5-HT_3 receptor of the rabbit heart (Fozard and Mobarok Ali, 1978). Further studies demonstrated that this drug could block certain neuronally-mediated actions of 5-HT_3 in isolated guinea pig ileum and colon, events probably mediated by the 5-HT_1 or 5-HT_4 receptors and which probably account for the prokinetic action (Sanger and King, 1988). From Fozard's cardiac studies with (-)cocaine, substituted benzoic acid esters of tropine (a crystalline alkaloid) were synthesized and tested, producing the first selective 5-HT_3 receptor antagonist, MDL 72222. Other 5-HT_3 receptor antagonists were being synthesized as indole esters of tropine, producing structures more similar to 5-HT than to metoclopramide. The von Bezold-Jarisch reflex is caused by stimulation of 5-HT_3

receptors located on coronary vagal afferents and it typically produces apnea, hypotension, and bradycardia. Inhibition of this reflex in rats was used as a simple and reproducible model to test the potency of newly developed 5-HT_3 receptor antagonists. One of the most potent inhibitors of this reflex is an indole ester of tropine, BRL 43694 (Granisetron; Beecham Pharmaceuticals). BRL 43694 incorporates a highly electronegative 2-N, and the amide link of metoclopramide, which together promote stability of the compound (Figure 9) (Sanger and King, 1988). Although there are a variety of 5-HT_3 receptor antagonists, which appear different chemically (Figure 9), many contain some common salient features: a 6,5-aromatic nucleus connected, via a carbonyl group and a 4-atom unit, to a basic nitrogen atom. These functions may be relevant to the 5-HT_3 binding site (Sanger and King, 1988).

Pathophysiological Effects Mediated by 5-HT_3 Receptors

Serotonin is a pain-producing substance, and experiments have established that 5-HT_3 receptors mediate both the pain-producing and the pain-enhancing effects of serotonin (Richardson et al., 1985). The 5-HT_3 receptor antagonist, MDL 72222, proved effective in clinical trials of migraine headaches (Fozard et al., 1985). Separate studies by Miner et al. (1987) and Costall et al. (1987) demonstrated that 5-HT_3 antagonists, acting on vagal afferents, were effective anti-emetics in models of cytotoxic drug and radiation-induced emesis. This finding was clinically important because the standard anti-emetic, metoclopramide, while very effective, can

Figure 9.

Chemical structures of some 5-HT_3 antagonists. BRL 43694 (Granisetron) is illustrated in the bottom left, GR38032 (Ondansetron) is illustrated in the bottom right. From Fozard, 1989.

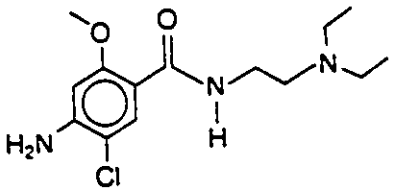

Metoclopramide

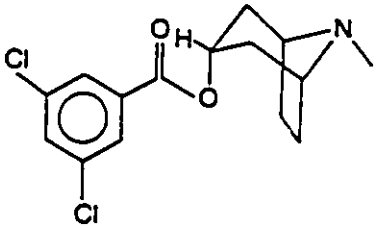

MDL 72222

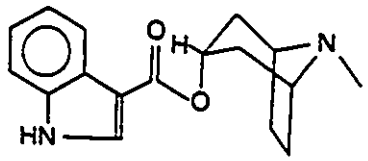

ICS 205–930

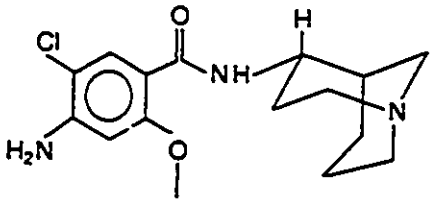

BRL 24924

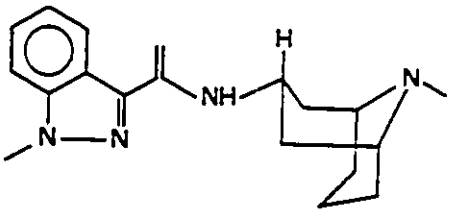

BRL 43694

Granisetron

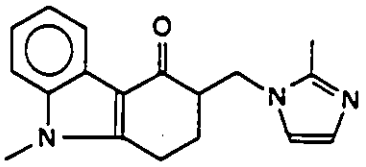

GR38032

Ondansetron

sometimes have undesired extra-pyramidal side-effects related to its dopamine D_2 receptor antagonism (Sanger and King, 1988). As the 5-HT_3 antagonistic property of metoclopramide was exploited in its derivative compounds, the anti-emetic activity was increased (Sanger and King, 1988). One of the 5-HT_3 antagonists, GR38032 (Ondansetron, Glaxo Pharmaceuticals), has just received federal approval in North America as an anti-emetic in both radio- and chemotherapy patients, under the trade name Zofran®. BRL 43694 has federal approval in some European countries, and is expected to receive federal approval in Canada shortly. While the anti-emetic efficacy of these 5-HT_3 antagonists has been well characterized, their potential beneficial role in other gastrointestinal pathologies, such as diarrhea, has yet to be fully studied.

Gastrointestinal Functions of Serotonin

Serotonin has been classified as a putative neurotransmitter (Gershon and Erde, 1981) in the gastrointestinal tract. 5-HT-like neurons have been localized (by immunohistochemistry) to both the myenteric and submucous plexus of the enteric nervous system. Furness and Costa (1982) proposed that the 5-HT neurons could play a role as interneurons in descending neuronal pathways within the intestinal wall. As early as 1958 it was recognized that serotonin had a modulatory action on intestinal motility of guinea pigs and rabbits (Bulbring and Crema, 1958), and that this action was indeed a physiological response was confirmed recently by Hopkinson et al., (1989). Serotonin's action as a modifier of GI motility is interesting from the

clinical perspective, as its levels are found to increase in the mucosa and circular muscle of the sigmoid colon in patients with severe idiopathic constipation (Lincoln et al., 1990). Serotonin has also been reported to exert an inhibitory action on vagally stimulated gastric acid secretion and motility in the rat (Stephens et al., 1989).

Serotonin can also elicit a prominent secretory response. Ussing chamber studies have demonstrated that serotonin (2.6×10^{-6} M) added to the serosal surface of rabbit ileum, caused a net reduction in NaCl absorption (Donowitz et al., 1980). This group suggested that serotonin's actions were confined to the electroneutral Na^+/Cl^- co-transporter. Cholera toxin also mediates its secretory effect (at least partly) by causing release of intestinal 5-HT (Nilsson et al., 1983). The combination of 5-HT_2 and 5-HT_3 receptor antagonists has been demonstrated to completely abolish cholera toxin induced intestinal secretion (Beubler and Horina, 1990). Such data suggest that serotonin antagonists may be effective in controlling the secretory diarrhea seen in cholera. The 5-HT_3 antagonist, Ondansetron, has also been reported to be effective in controlling the diarrhea in irritable bowel syndrome (Steadman et al., 1990).

While the secretory action of serotonin may deleteriously alter intestinal permeability, pretreatment with a large dose of serotonin (20 mg/kg i.p.) a few minutes prior to whole-body X-irradiation has been shown to dramatically increase the survival time in rats (Gray et al., 1952) and mice (Bacq, 1954). It is believed that this protective effect is related to the vasoconstrictor properties of 5-HT, producing a transient tissue anoxia. The decreased oxygen tension in the tissues is believed to

minimize the production of free radicals (Gray et al., 1952) which are proposed mediators of radiation-induced cellular death (Bacq, 1954).

Stimulators of Serotonin Release

There are several known stimuli for degranulation of EC cells and release of 5-HT. Luminal stimuli include hypertonic glucose (Drapanas et al., 1962), acid pH (Fujita and Kobayashi, 1973), and increased luminal pressure (Bulbring and Crema, 1959). Vagal (Tansy et al., 1971, Ahlman et al., 1976) and splanchnic (Burks and Long, 1966) nerve stimulation are also known stimulators of 5-HT release from EC cells. Vagal stimulation is mediated by both adrenergic and cholinergic mechanisms. Ultrastructural studies of Pettersson et al., (1980) suggest the presence of adrenergic nerve terminals at the base of EC cells. Pharmacological studies by Pettersson et al., (1980) and Gronstad et al., (1987) suggest that vagally-stimulated basal release of 5-HT from EC cells is mediated by beta-adrenoceptors. Further work by Gronstad et al., (1987) suggests that the luminal release of 5-HT (from EC cells), is under vagal cholinergic control, and that this luminal release is qualitatively small in comparison with the adrenoceptor-mediated basal release of 5-HT. The ratio of intraluminally to intraportally released 5-HT has been estimated to be less than 1:100. However, the majority (roughly 90 %) of the serotonin released into the portal circulation is rapidly bound to platelets, hence inactivated, while the 5-HT released into the intestinal lumen remains bioavailable. The half-life of intestinal serotonin is between 6 and 12 hours, while that in the portal circulation is only a couple of minutes

(Thompson, 1971). Therefore luminally-released serotonin may be of greater biological significance than 5-HT released into the portal circulation (Gronstad et al., 1987).

Intestinal inflammation is a symptom of many intestinal pathologies, including ileitis and colitis, as well as in radiation enteritis. Areas of inflamed bowel often exhibit changes in mast cell number (Perdue et al., 1989). Degranulation of the mast cells will result in release of a number of mediators of intestinal inflammation and damage, including serotonin. Release of serotonin is also stimulated by whole body exposure to radiation in small rodents (Matsuoka et al., 1962, Kockmierska-Grodzka et al., 1976). The mechanism of radiation-induced serotonin release is still undefined. Whether it represents a direct effect of ionizing radiation on the EC cells, or a secondary reaction due to inflammatory processes, or nerve stimulation remains to be determined. Histochemical and cytofluorescence studies of EC cells from whole-body irradiated (4 Gy) rats (Penttila et al., 1975) and irradiated (10 and 30 Gy) exteriorized mouse jejunal loops (Penttila and Kormano, 1971) have suggested that the EC cells are highly resistant to radiation-induced degranulation. However both these studies confirm that irradiation does cause a decrease in the content of intestinal 5-HT. These authors further suggest that the source of 5-HT may be from cytoplasmic stores in the EC cell, the permeability of which may be altered by radiation exposure.

Rationale for Study

The intestinal mucosa is considered to be a protective layer, or boundary, separating the internal and external environments. Selective movement of fluid and nutrients across the mucosa is regulated by the permeability and permselectivity characteristics of the mucosa. These characteristics include the physical and chemical properties of the mucosa (Jenkins et al., 1986). At present, it is unknown if radiation exposure affects the intestinal permeation of ^{51}Cr-EDTA, a permeability probe considered to reflect irregularities in mucosal morphology before they are revealed by histology. Therefore, an animal model was developed: to examine intestinal permeation, to determine if physiological mechanisms (i.e., release of the secretagogue serotonin) could account for any observed radiation-induced changes in intestinal permeation, and to determine if radiation-induced diarrhea is associated with changes in intestinal permeability.

Animal Model

The ferret (*Mustela putorius furo*) has been used for a variety of research purposes involving neurology, endocrinology, embryology, virology, bacteriology, teratology, and reproduction (Fox, 1988), but it was not until Florczyk et al.'s study in 1982 of cisplatin-induced emesis in the ferret, did the suitability of the ferret for investigating gastrointestinal pathologies become apparent. Experiments using the ferret as an animal model for radiation-induced emesis have been conducted since the mid 1980's. Separate studies by Gylys and Gidda (1986) and Andrews et al.

(1986), suggested that the ferret's initial emetic response following radiation exposure, occurred at a lower threshold and at an earlier latency than any other species. These results (confirmed by King, 1988) indicate that the ferret's emetic response to X-radiation is more sensitive than any other species (Davis, 1988). Davis (1988) characterized the emetic dose-response of whole-body X-irradiated (0.50 - 16 Gy) ferrets. The ED_{100} for vomiting of X-irradiated ferrets was 1.25 Gy. Ferrets were also observed to have diarrhea in response to all of the tested doses (0.5, 0.75, 1.0, 1.25, 1.50, 2.00, 4.00, 6.00, 8.00, 12, and 16 Gy) of X-irradiation. The severity of the diarrhea increased with increasing dose of radiation, becoming a profound mucoid or watery diarrhea by 8 Gy. The intensity of the diarrhea response peaked at approximately 60 minutes post-irradiation, and generally lessened by 5 hours post-irradiation (Davis, 1988). Based on their lower sensitivities to radiation exposure, ferrets became the preferred animal for studies of emesis and testing of anti-emetic compounds (Andrews and Hawthorn, 1987; Miner et al., 1987; Davis, 1988). The recent use of the ferret in intestinal transport studies (Greenwood et al., 1990) also favoured these animals as the animal model of choice for this project.

Research Aims

Utilizing the ferret as a working model for the effects of irradiation in certain radiotherapy patients, the following questions were asked:

1) Does radiation exposure alter intestinal permeation (of the radio-labelled probe ^{51}Cr-EDTA, of fluid, and of electrolytes)?

2) Are there regional differences in radiation-induced permeation changes along the intestinal tract ?

3) How do the radiation-induced permeation changes vary with the time post-irradiation ?

4) Is radiation-induced diarrhea related to the radiation-induced permeation changes ?

5) Would a 5-HT_3 receptor antagonist be therapeutic for radiation-induced diarrhea, and would it effect the parameters of intestinal permeation ?

MATERIALS and METHODS

Animals

Adult male ferrets (1.0 - 1.5 kg, Figure 10), descented and castrated, were purchased from Marshall Farms (New York State). The ferrets were given a minimum of three days to rest and to acclimatize to the new environment before any experimentation was done. Ferrets are very susceptible to viruses (Fox, 1988), therefore a separate room with controlled access was provided for the ferrets. The animals were housed individually in a metal cage (45 cm x 60 cm x 80 cm). The cage had two wooden platforms, allowing the ferrets to climb and play. The housing rooms had controlled lighting (12:12), temperature (23 °C) and ventilation (15 changes/hour, humidity approximately 40-45%). Ferrets had continual access to fresh cool tap water, and were fed daily in the afternoon. Diet consisted of a mix of wet (Miss Mew Chicken Dinner) and dry (Purina cat chow) cat food. Food bowls were placed inside the cage and remained there until the next feeding time. The litter beds were changed three times a week. All procedures involving the ferrets were conducted in accordance with the guidelines established by the Canadian Council on Animal Care.

Experimental Groups

Phase 1:

The objective of phase 1 was to design an animal model which could assess radiation-induced changes in intestinal permeation. A concise methodology for this newly developed protocol is described in this chapter, more detailed information is presented in Appendix I.

Figure 10

An adult male ferret (*Mustela putorius furo*)

Phase 2:

In phase 2, the working protocol was used to establish baseline permeability data in the irradiated ferret. Four groups of animals were investigated:

1) Control (Sham + non-irradiated)
2) 2 hours post-irradiation (PIRR)
3) 24 hours PIRR
4) 48 hours PIRR

Ferrets in the 2 hour PIRR group were anesthetized immediately after irradiation and collection of intestinal perfusates began approximately 2 hours post-irradiation (± 20 min). Ferrets in the 24 and 48 hour PIRR groups were anesthetized either at 24 or 48 hours PIRR. Animals in the control group consisted of 3 non-irradiated and 3 sham-irradiated (one at each post-irradiation time point). Table 8 lists the number of experiments that were performed in each experimental group of phase 2.

Phase 3:

The effects of the 5-HT_3 antagonist Granisetron (*endo*-N-(9-methyl-9-azabicyclo[3.3.1]non-3-yl0-1-methyl-1H-indazole-3-carboxyamidehydrochloride;BRL 43694) on radiation-induced retching, vomiting, and diarrhea, and on intestinal permeation were tested in Phase 3. As the results (permeation, fluid flux, biochemistry) of the control "irradiated" ferrets of Phase 2 were not significantly different from those in the 24 hour PIRR group, the 24 hour PIRR group was not examined in Phase 3. The experimental groups in phase 3 were:

1) Irradiation Control
2) 2 hours PIRR
3) 48 hours PIRR

Table 8. Experimental groups used in phase 2.

Prodromal Effects of Irradiation

Group	n value
Sham-Irradiated	
24 hour PIRR	1
48 hour PIRR	1
Non-Irradiated	
24 hour PIRR	1
48 hour PIRR	1
Control Irradiated =	4
24 hour PIRR	5
48 hour PIRR	5
Total Irradiated =	10

Clearance of ^{51}Cr-EDTA, and Net Fluid Flux (in brackets)

Group	Total #	Complete Experiments	
		Jejunum	Ileum
Sham-Irradiated			
2 hour PIRR	2 (2)	1 (1)	2 (1)
24 hour PIRR	1 (1)	1 (1)	1 (1)
48 hour PIRR	1 (1)	1 (1)	1 (1)
Non-Irradiated			
2 hour PIRR	2 (1)	1 (1)	1 (1)
24 hour PIRR	1 (0)	1 (-)	1 (-)
48 hour PIRR	1 (1)	0 (1)	0 (1)
Control Irradiated =	8 (7)	5 (5)	6 (5)
2 hours PIRR	9 (9)	5 (5)	6 (6)
24 hours PIRR	7 (6)	6 (6)	6 (6)
48 hours PIRR	9 (7)	5 (5)	6 (5)

PIRR = post-irradiation
Total # refers to the number of experiments that were attempted
Complete Experiments refers to the number of attempted experiments in which complete data were obtained for both jejunum and ileum
Bracketed numbers indicate the numbers of jejunal and fluid flux experiments

Only a single dose of Granisetron (0.4 mg/kg) was tested in this project. This dose was selected based on the numerous scientific and clinical studies with Granisetron as an anti-emetic compound. The dose of Granisetron used in animal studies ranges from 0.5 mg/kg to 5 mg/kg, while in clinical studies (which have already completed dose response curves for Granisetron as an anti-emetic) the current recommended dose (as an anti-emetic) is 0.04 mg/kg (Cassidy et al., 1988). Granisetron was injected subcutaneously (s.c., suprascapular) 30 minutes before the start of irradiation. The drug was delivered in 0.5 mL of 0.9 % saline, and was controlled for by sham-injecting (SI) other ferrets with 0.5 mL of 0.9 % saline, 30 minutes before irradiation. Granisetron was injected 30 minutes before irradiation to allow sufficient time for the drug to be absorbed into the circulation. The mean half-life of Granisetron in human plasma is approximately five hours, with plasma clearance being primarily through hepatic metabolism (Upward, 1990). Table 9 lists the number of experiments that were performed in each experimental group of phase 3.

Irradiation Protocol

All irradiations were total body, using a bilateral cesium (^{137}Cs) irradiation unit (Gammacell 40, Atomic Energy of Canada Ltd). A single dose of 5 Gy was delivered at a rate of 1.22 Gy/min. This dose was selected for two reasons. First, it is intermediate to the doses (2 and 8 Gy) used by Davis (1988), who established the emetic responses of ferrets to X-irradiation (ED_{100} = 1.25 Gy). Davis noted that with a dose of 8 Gy all ferrets still vomited (a greater number of times, and with a

Table 9. List of experimental groups in phase 3.

Clearance of ^{51}Cr-EDTA, and Net Fluid Flux (in brackets)

Group	Total #	Complete Experiments	
		Jejunum	Ileum
Sham-Irradiated			
Saline Injected (SI)	5	4 (3)	4 (3)
Drug Injected (DI)	7	5 (5)	4 (3)
2 hour PIRR			
Saline Injected (SI)	5	4 (4)	3 (3)
Drug Injected (DI)	8	4 (3)	6 (6)
48 hour PIRR			
Saline Injected (SI)	3	3 (3)	3 (3)
Drug Injected (DI)	5	4 (4)	4 (5)

PIRR = post-irradiation
Total # refers to the number of experiments that were attempted
Complete Experiments refers to the number of attempted experiments which yielded data at all collection times
Numbers in brackets refer to number of complete fluid flux experiments

reduced latency), and in addition a profound mucoid (occasionally bloody) diarrhea was also present. Second, the radiation protocol was designed to be within the treatment range for some cancers (mainly leukemias).

Irradiation Procedure

The cesium source is contained in two cylindrical sliding drawers located above and below the sample cavity. When the source is activated, the source drawers move by pneumatic piston cylinders from the shielded position to the irradiate position. The dual location of the ^{137}Cs source, above and below the sample cavity, results in a bilateral beam of gamma radiation, a more efficient dispersal pattern compared to unilateral sources, resulting in a more uniform distribution of the gamma energy (throughout the animal). Ferrets were placed in a circular plastic sample tray (30.5 cm diameter by 10.5 cm deep), fitted with ventilation holes. Although the tray was not large enough to allow the ferrets to stand, the animals could freely move about inside the sample tray. As ferrets are natural burrowers, a darkened, relatively confined space was presumed to not present a severe stress. Nevertheless, for the first 10 irradiation experiments, the ferrets were removed from their housing cages, transported downstairs (two levels) to the room containing the Gammacell, and were sham irradiated. This procedure was repeated two or three times before the actual irradiation. As there was no difference in the experimental results between animals that had undergone the sham irradiations prior to irradiation, and those that had not, the practice of habituating the ferrets to the

irradiation protocol was discontinued.

Dosimetry Experiments

A ferret (1.3 kg) that was to have been used in other experiments, died during anesthesia. The ferret had been irradiated 24 hours earlier. In order to assess the exact amount of gamma radiation delivered to the gut tissues, it was decided to use this ferret for a dosimetry experiment. Small thermoluminescence dosimeters (TLD's) were heat sealed within a 2 cm length of PE-(polyethylene) 260 tubing. The TLD's were then glued within the lumina of various gut regions of the cadaver ferret. The ferret was then irradiated as usual with a 5 Gy dose of gamma radiation from the cesium source. Following irradiation, the TLD's were harvested and their energy read at the Defence Research Establishment of Ottawa. Two other dosimetry experiments were done in a similar fashion, except the cadaver ferrets had not been previously irradiated.

Prodromal Effects of Irradiation

Quantifying the prodromal effects of irradiation can give important information about the animal's radiosensitivity. Ferrets were directly observed for a minimum of the first two hours post-irradiation. Some ferrets (in all groups) were directly observed for up to five hours post-irradiation, and a few were filmed on videotape for 48 hours PIRR. When ferrets could not be observed, the bedding in the cages containing the irradiated ferrets was periodically checked (up until the time

of the experiment) for evidence of vomitus or diarrhea. The prodromal events that were recorded in this investigation were retching, vomiting and bowel movements. In each case, the number of episodes, and the total number of events per episode were recorded, and averaged over a five minute interval. An episode was defined as a discrete time interval during which the ferret assumed and maintained the stereotypic posture for that particular event. For example, when ferrets were about to retch, they would generally orient themselves such that their heads were pointed at one corner of a cage (61 cm x 41 cm x 38 cm). The ferret would lower the upper half of its body and raise its lower half. A retching episode was therefore defined from the moment the ferret assumed this posture, to the moment it assumed another. The number of retches by the ferret while in the retching posture was counted as the total number of retches per episode. Vomiting and diarrhea episodes were also defined and recorded. A number of behavioral cues (burrowing, tongue-licking, drinking, level of activity) of nausea in irradiated ferrets, described by Bermudez et al. (1988), were also recorded in these experiments. Ferrets in the 48 hour PIRR group were offered a couple of tablespoons of wet cat food at 24 hours post-irradiation. The ferrets' reaction to the food was also used as an indicator of radiation-induced nausea (Davis, 1988). During the second hour of post-irradiation observation, the ferrets' level of response was tested by a series of auditory stimuli: clapping hands, running a pen along the edge of the cage, and normal ambient noise.

Surgical Protocol

Pre-operative Care

Ferrets were fasted (but had water *ad libitum*) 18 hours before surgery. This necessitated that animals in the 2 hour PIRR group were fasted prior to irradiation, while those in the 24 and 48 hour PIRR groups were irradiated in a fed state. This difference was controlled for by sham-irradiating ferrets (one at each PIRR time point) in a fasted state. At the appropriate time post-irradiation, ferrets were initially anesthetized with an intramuscular (i.m., hind leg) injection of 30 mg/kg ketamine HCl (Rogarsetic, 100 mg/mL of ketamine HCl, Rogar/STP Inc.), followed by halothane (3.0 - 5.0 %) delivered in oxygen (1.5 L/min) via a large anesthesia feline plastic mask. Once surgical anesthesia had been achieved, halothane (2 %) was administered via an endotracheal tube. A Vetrosan non-breathing anesthetic machine (Bain circuit system, Summit Hill Labs., Model STL-3000) was used for all of the experiments. The ferrets' fur was shaved (Oster Detachable Blade Electric Clipper, Model A5-08) around the neck and abdominal area. A YSI400 rectal probe connected to a tele-thermometer (YSI), was dipped in mineral oil and inserted approximately five cm into the rectum. Rectal temperature was maintained between 37 and 39.5 °C throughout the experimental procedure by means of a circulating water blanket (American Medical Systems, Aquamatic Model K-20-C) set at 39 °C, and by overhead heating from a study lamp (100 W bulb). Normal ferret body temperature is between 37.8 and 40.0 °C (Fox, 1988).

Blood Vessel Cannulations

Prior to the initial surgical incision, limb and jaw reflexes were tested to assure that surgical anesthesia had been achieved. A midline cervical incision (5 - 6 cm) was made from the suprasternal notch to just below the cricoid cartilage. The left jugular vein and the right carotid artery were cannulated[2]. Both cannulae were tested for patency by flushing with heparin saline (100 U/mL), and were secured in place by ligatures. The neck wound was then closed with one or two surgical staples (Royal Auto-Sutures, disposable skin sutures).

One end of the 3-way stopcock to which the jugular vein cannula was attached was connected to a Minitan flow drip selector (Flashball Device, Baxter, Model JC5402), set to deliver Lactated Ringer's (composition in mM: Na^+ 130, K^+ 4, Ca^{++} 1.5, Cl^- 109, Lactate 28, pH approximately 6.5, mOsm/L approximately 272) at a rate of 10 mL/kg/h. The tubing of the Minitan system and of the venous cannula were positioned on the water blanket such that they could be warmed before entering the circulation.

[2]Jugular vein cannula: Polyethylene-60 tubing, i.d. = 0.76 mm, o.d. = 1.22 mm.
Carotid artery cannula: Polyethylene-50 tubing, i.d. = 0.58 mm, o.d. = 0.965 mm.

Blood Pressure Recording

The other free end of the venous stopcock was connected to a Statham Pressure Transducer, which in turn was connected to a polygraph chart recorder. The polygraph was calibrated for blood pressures from a minimum of zero, to a maximum of 100 mmHg using a mercury manometer. Once the venous lines were connected, the arterial cannula was also connected to the transducer. A continuous chart recording of arterial pressure (AP)(systolic/diastolic), mean arterial pressure (MAP) and heart rate (HR) was made throughout the experiment. It was necessary to shut off temporarily the AP, MAP and HR recordings when either venous pressures (VP) were recorded or when a blood sample was withdrawn from the arterial line.

Abdominal Surgery

A midline laparotomy (7 - 8 cm long) was made just deep enough to expose the linea alba. The linea alba was gently picked up with Toothed Adson forceps and a small puncture wound was made using surgical scissors. Six to seven cm of the linea alba was cut, exposing the abdominal organs. A cloth, previously soaking in warmed (38 °C) water, was used to cover the abdominal organs. In order to expose both kidneys, it was necessary to move the abdominal organs gently (mainly small intestine) out of the way. Careful blunt dissection with a mosquito clamp was done to expose partially both the renal vein and artery of the right and left kidneys. Both renal pedicles were ligated in order to prevent the rapid excretion of the small

molecular weight probe ^{51}Cr-EDTA (vonRitter et al., 1988). To confirm that the renal vessels were effectively ligated, a urine sample (200 μL) was collected from the bladder (via a 20 gauge needle) at the end of each experiment and it was counted for both ^{51}Cr and ^{14}C.

Preparation of the in situ Luminal Perfused Loops

Intestinal Cannulae

Three types of intestinal cannulae were used: **an input cannula** (to deliver the perfusing solutions from the syringe pump to the cannulated segment), **a drainage cannula** (to collect, by gravity, any fluid from the portion proximal to the cannulated segment) and **an output cannula** (to collect, by gravity, the perfusates from the cannulated segment). To facilitate collection of the perfusates, the output cannulae were fitted with 2 - 3 side-ports located on the first 5 mm of the inserted end of the cannulae. All intestinal cannulae were made from silicon tubing (Pharmacia, i.d. = 2.7 mm, o.d. 4.7 mm) and were fitted with a cuff (5 mm long) made of the same tubing. The cuff was placed 5 mm from the insertion end and was used to secure the cannulae in place. The soft, flexible silicon tubing is ideal material for the intestinal cannulae as it causes minimal trauma during insertion. The disadvantage to cannulae made with the silicon tubing is that because the tubing is so soft, it offers no resistance to pressure, hence these cannulae cannot be used to measure the transmural pressure (of the intestinal wall), an important parameter used to assess changes in intestinal tone (Greenwood et al., 1990).

Rationale for Choice of Intestinal Segments

A regional difference in intestinal permeation of ^{51}Cr-EDTA was described by vonRitter et al. (1988). He and his colleagues found that the distal ileum of the rat was most sensitive to luminal challenge with a chemotactic agent N-FMLP (N-formyl methionyl-leucyl-phenylalanine), as reflected by a greater blood-to-lumen clearance of ^{51}Cr-EDTA in this region. As well, the effects of gamma radiation on electrolyte transport have been studied in the terminal ileum of rabbits (Gunter-Smith, 1986). Based on these studies, the distal ileum of the ferret was selected as one of the intestinal segments in which to study ^{51}Cr-EDTA permeation in response to "challenge" with radiation exposure. In order to make a regional comparison in radiation-induced changes in intestinal permeation, the jejunum was selected as the second intestinal segment. The jejunum was selected based on the large number of transport studies done on this tissue (Greenwood and Read, 1985; Nylander et al., 1989; Greenwood et al., 1990; Crowe et al., 1990; Perdue et al., 1990; Holtug and Skadhauge, 1991). It was not possible to study intestinal permeation in other regions of the ferret intestine for several reasons. First, both the duodenum and colon are too short (roughly 8 cm and 6 cm respectively) to obtain a satisfactory length (10 cm) of perfused intestine. Second, both of these segments are anatomically difficult (due to mesenteric attachments) to cannulate with minimal trauma. Third, cannulating and perfusing more than two intestinal segments simultaneously was considered to be too invasive. Fourth, time did not permit repetition of the experiments using different intestinal segments.

Identifying and Cannulating the Segments

The ileum of the ferret is approximately 120 cm long (An and Evans, 1988) and there is most likely differentiation of function along its length. Therefore, to minimize experimental error, it was extremely important to be able to perfuse the same length of ileum in each experiment. The first step in identifying the length of distal ileum used in this perfusion protocol was to identify the ileocolonic junction. As there is no cecum in the ferret, positive identification of the ileocolonic (IC) junction was made using other landmarks. First, there is a rather abrupt increase in intestinal diameter from the terminal ileum to the colon. Second, the vascular supply to the ileum is slightly greater than in the colon, causing the ileum to appear more pink in colour, compared to the slightly greyer colon. The vascular arcades on the ileal wall are also more visible than on the colon. Third, while the terminal ileum is not attached to the abdominal wall, the colon is suspended from the dorsal body wall by a short mesocolon (An and Evans, 1988). Fourth, the last 30 to 35 cm of terminal ileum contain Peyer's Patches which generally extend right up to the IC junction. Peyer's Patches (PP) were never observed on the colon.

A ligature was placed around the ileum approximately 35 - 45 cm oral to the IC junction (*this distance was selected in order to avoid perfusing an intestinal segment with PP)*[3]. This ligature effectively isolated the intestinal segment from the distal bowel, preventing reflux of intestinal secretions. All ligatures were pushed through

[3] The Peyer's Patches (aggregates of mucosal lymphoid follicles) are covered by specialized surface epithelial cells, called the "M" cells, which are believed to participate in absorption of luminal antigens (Madara and Trier, 1987). Thus the M cell presents a different type of barrier to intestinal permeation than normal enterocytes.

mesentery, minimizing damage to blood vessels and nerves. A small cut just proximal to the ligature was made with surgical scissors on the lateral surface of the ileal wall, avoiding any visible blood vessels. The output cannula was then gently inserted into the intestinal lumen, approximately 5 - 10 mm beyond the end of the silastic cuff and then secured with a second ligature, placed just behind the cuff. If the segment was sufficiently relaxed (low tone) or of large enough diameter, the intestinal cannulae slipped inside the intestinal lumen easily. Usually, however, the cut surface had to be gently lifted up with forceps in order to expose the lumen a bit more fully to the cannula. A second cut was made approximately 13 cm proximal to the end of the inserted output cannula. Both the drainage and input cannulae were inserted into the same opening, the input cannula advancing distally, the drainage cannula advancing proximally. Before the input cannula was inserted into the intestine, it was connected to a 60 mL Becton-Dickinson (BD) syringe previously filled with a balanced electrolyte solution (BES) (composition in mM: Na^+ 135, K^+ 5, Cl^- 115, HCO_3^- 25, mannitol 25, pH'd to 7.4) warmed to 40 °C. The BES was then injected into the input cannula, in order to minimize perfusing air into the intestinal segment. The opening for the input and drainage cannulae was made 13 cm proximal to the output cannula, so that the input cannula could be inserted 3 cm, leaving a 10 cm length of cannulated bowel for luminal perfusion.

Once the ileal segment was cannulated, the jejunal segment was identified. The ligament of Treitz, connecting the duodenum-jejunum junction to the dorsal abdominal wall, is quite prominent in the ferret. A large branch of the superior

mesenteric artery, hidden within the fat bed running along the inferior surface of the jejunum, can complicate cannulation of this segment. If the ligatures for securing the input and drainage cannulae were placed too proximally (i.e. around the branch), they could greatly reduce blood flow to a substantial portion of small intestine. Ligatures were secured approximately 2 cm distal to the ligament of Treitz, therefore the output cannula was placed 13 cm from this region, as previously described for the ileal segment. The input and drainage cannulae were placed such that the end of the input cannula was approximately 10 cm from the end of the output cannula.

The jejunum is more vascularized than the ileum. Locating a region on the jejunal wall relatively sparse of blood vessels is very difficult compared to the ileum. Therefore the cut on the jejunal wall for insertion of the jejunal cannulae was made slightly differently than on the ileal wall. Whereas the cut on the ileal wall was usually placed on the lateral surface (due to the pattern of the ileal vasculature), the jejunal cut was usually made on the anti-mesenteric border. Once a suitable region was found (sparse blood vessels), firm pressure was applied with a cool moist gauze to the jejunal region where the cut was to be made. This normally resulted in a short-lasting vasoconstriction of the prominent surface vessels on the jejunal wall. The incision was then made with minimal bleeding. Excessive bleeding was controlled with direct pressure from a cool moist piece of gauze.

Perfusing the Segments

Once all the intestinal cannulae were secured in place, the syringe pumps (Sage Instruments, Model 341A) - one for each intestinal segment - were turned on, and delivered the BES at a rate of 0.5 mL/min. As soon as the perfusates began to drip out of the two output cannulae, the segments (and rest of small bowel) were returned to the abdominal cavity. The perfused segments were placed as flat as possible on top of the rest of the small intestine, trying to minimize any kinking of cannulae or segment that could interfere with the delivery or collection of perfusates. To minimize heat and moisture loss, the abdominal incision was then closed with one or two surgical staples.

During the initial flushing phase (20 minutes long), both intestinal segments were perfused with 40 mL of BES, followed by 65 mL of BES containing the volume marker ^{14}C-Polyethylene glycol 4000 (PEG4000). The balanced electrolyte solution (BES) was made up as one litre volumes using distilled water, filtered through a 0.22 micron cellulose acetate membrane (Corning, disposable sterile filter system/stand) and bubbled for five to ten minutes with 95% O_2/5% CO_2. The solution was made to pH 7.40 with 0.1 Normal HCl, and stored (4 °C) in a capped bottle until use.

To maintain the perfusing BES at physiological temperature, the input cannulae delivering the pre-warmed BES were placed on the circulating water blanket. As well, an overhead heating lamp (100 W bulb) was positioned approximately 15 cm above the abdomen, warming the BES as it was delivered to the intestinal segments.

Perfusion Protocol

When surgery was complete, the perfusion was carried out according to the protocol outlined in Table 10.

Table 10. Experimental perfusion protocol.

	Time (min)	Perfusate (P) (Sample)	Blood (B) (Sample)
Flushing:	-80 → -60	----	B1 = 0.95 mL
Inject ^{51}Cr-EDTA →			
Perfuse ^{14}C-PEG4000 →	-60 → -45	E1	B2 = 0.55 mL
	-45 → -30	E2	B3 = 0.55 mL
	-30 → -20	E3	----
	-20 → -10	E4	----
	-10 → 0	P1	B4 = 0.55 mL
	0 → 10	P2	----
	10 → 20	P3	B5 = 0.55 mL
	20 → 30	P4	----
	30 → 40	P5	B6 = 0.55 mL
	40 → 50	P6	--
	50 → 60	P7	B7 = 0.75 mL

All perfusates were collected by gravity, dripping directly into plastic disposable containers. During the first twenty minutes (-80 to -60 minutes) of the perfusion protocol, the segments were flushed clean with BES. Immediately after the flush, the BES was replaced with the BES containing the volume marker ^{14}C-PEG4000. A bolus of 160 μCi ^{51}Cr-EDTA in 1 mL of Lactated Ringer's was then injected into the jugular vein. This amount of ^{51}Cr-EDTA was sufficient to maintain a ^{51}Cr plasma count of at least 15 000 (cpm/mL plasma), a count considered to be high enough to generate a gradient for ^{51}Cr-EDTA intestinal permeation (Nylander et al., 1989).

Equilibration of ^{51}Cr-EDTA

The first two collected samples (E1 and E2) were collected in the so-called equilibration ("E") phase, as this was the time period when the ^{51}Cr-EDTA was equilibrating within the blood volume (Figure 11). The counts of ^{51}Cr-EDTA had been previously reported in the rat to drop rapidly within the first 30 minutes of injection and then stabilize (Ramage et al., 1988). In these experiments, the counts of ^{51}Cr fell rapidly between 15 and 30 minutes post-injection. There was a non-statistically significant trend for plasma counts of ^{51}Cr in the 24 hour post-irradiation group to be elevated. Plasma counts of ^{51}Cr in the 24 hour PIRR group were still declining rapidly within the 30 to 40 minute post-injection interval. Therefore, another 30 minutes was allotted for equilibration (of ^{51}Cr-EDTA) and stabilization of the preparation (samples E3 and E 4). Therefore, as the ^{51}Cr counts were declining rapidly within the first 60 minutes of ^{51}Cr-EDTA injection, samples E1, E2, E3, and E4 were analyzed, but were not used in any final statistical analyses.

Analysis of Collected Perfusates

^{51}Cr-EDTA Clearance and Net Fluid Flux

After the equilibration period, all the remaining perfusates were collected at ten minute intervals. A 200 μL aliquot was counted for ^{51}Cr in a gamma counter (LKB Wallac, 1282 Compugamma, Universal Gamma Counter). Another 200 μL aliquot was mixed with 10 mL of scintillation fluid (Cytoscint, ICN Biomedicals Inc.) and counted in a scintillation counter (Beckman, Model LS 9000) to determine ^{14}C.

Figure 11.

Plasma excretion of ^{51}Cr-EDTA at various times post-irradiation (PIRR). Values are mean ± SE, n value of control group is 7, while the three PIRR groups have an n value of 6.

Plasma Excretion of ^{51}Cr-EDTA

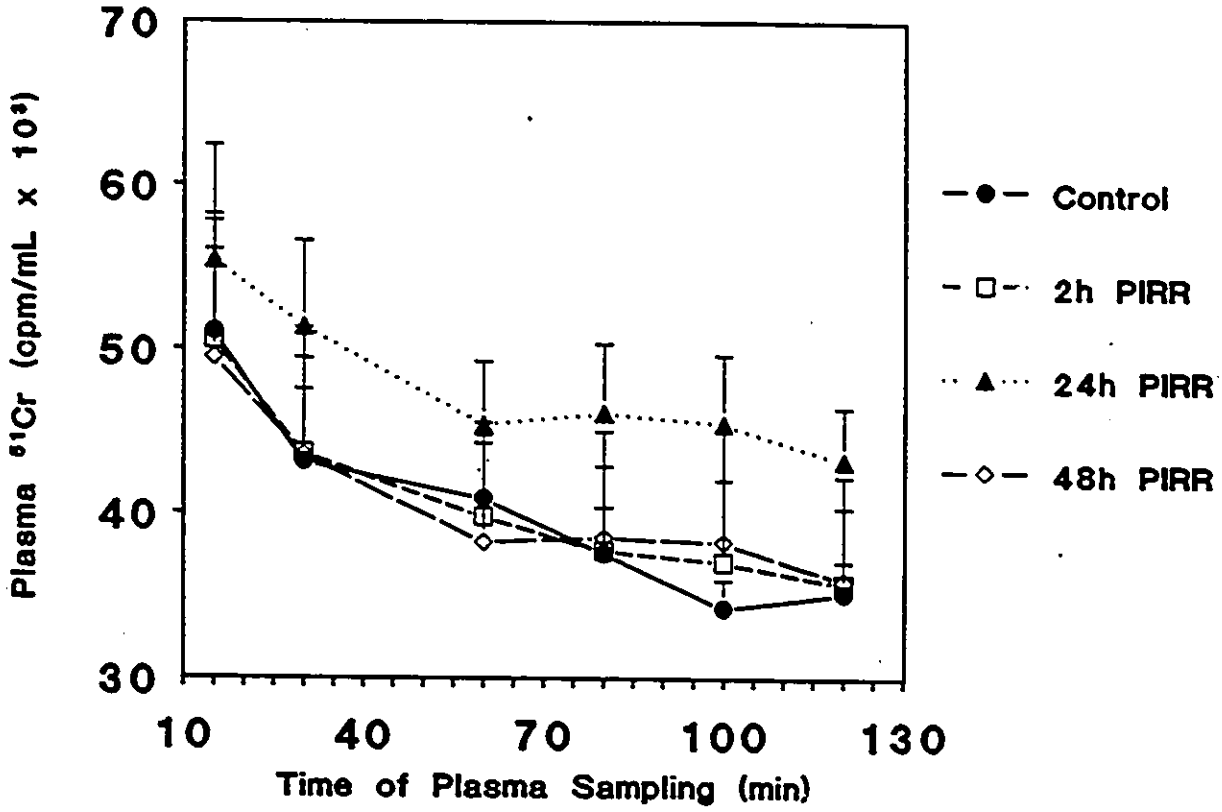

Figure 12 illustrates how ^{51}Cr-EDTA clearance and net fluid flux (J) were calculated. Fluid flux values were calculated at 10 minute intervals. ^{51}Cr-EDTA clearance values could only be calculated at 20 minute intervals because this was the frequency of blood sampling. Because the perfusate counts of ^{51}Cr (cpm/mL) were measured at 10 minute intervals, these values (the perfusate counts) were averaged for two consecutive samples (a 20 minute interval) for the determination of clearance (see Appendix II for sample calculations).

Both ^{51}Cr-EDTA clearance and net fluid flux were expressed per gram of dry tissue weight (of the intestinal segment). Some investigators express these measurements per gram of wet tissue weight (vonRitter et al., 1988) or per unit length of intestinal segment (Krugliak et al., 1990). However both wet weight and intestinal length measurements are difficult to standardize between experiments because they do not control for differences in fluid content nor for differences in intestinal tone. At the end of the experiment, the cannulae were removed and the perfused segment excised. Excess fluid was removed by gently compressing the segment. The segment was then patted dry with some gauze and wet weight was recorded. The segment was then dried overnight in an oven (55 °C) prior to determination of dry weight.

Biochemical Analyses

Generally, all biochemical analyses were done on the same day. When this was not possible, samples were frozen (-20 °C) until analyzed.

Figure 12.

Simplified schematic of intestinal loop preparation (modified from vonRitter et al., 1988) showing calculation of ^{51}Cr-EDTA clearance and net fluid flux (J). $^{14}C_i$ and $^{14}C_f$ respectively refer to the counts per minute (cpm) of ^{14}C in the initial perfusates (pre-perfusion) and in the final perfusates (collected).

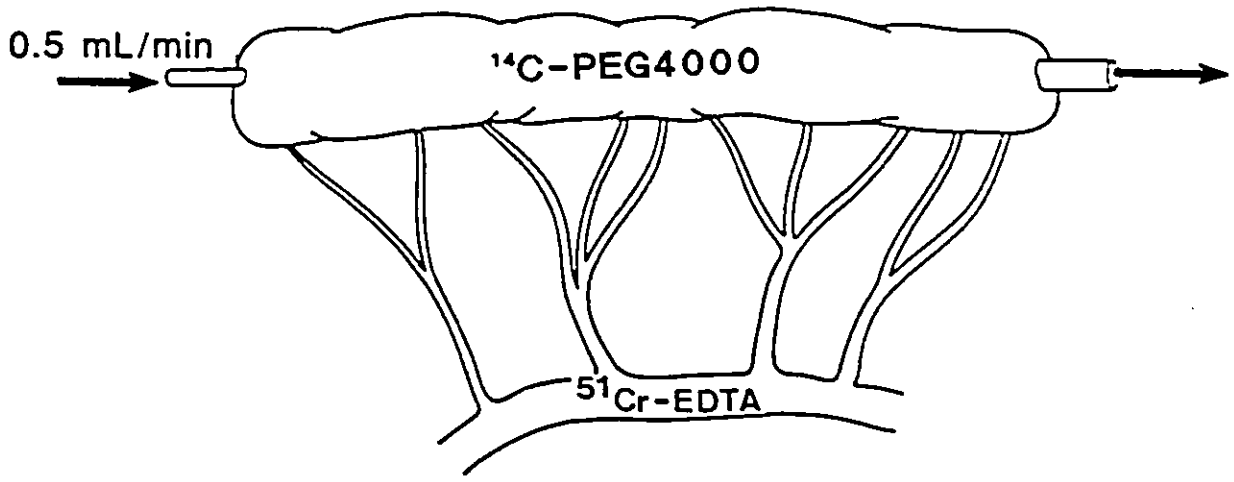

$$^{51}\text{Cr-EDTA Clearance} = \frac{(\text{cpm/mL perfusate } ^{51}\text{Cr} \times \text{perfusion rate})}{(\text{cpm/mL plasma } ^{51}\text{Cr} \times \text{tissue DW})}$$

$$\text{Net Fluid Flux (J)} = \frac{\text{perfusion rate} \times ([^{14}C_i / {}^{14}C_f] - 1)}{\text{tissue DW}}$$

Fractional Excretion of Electrolytes:

The collected perfusates were analyzed for Na^+ and K^+ (Corning, Model 480, flame photometer), and Cl^- (Chloride Analyzer, Corning Model 925). If the electrolytes were expressed only as absolute concentration, then any change in these values could be due to either: (1) a change in the net movement of the electrolyte; (2) a change in the net movement of fluid. To resolve this ambiguity, electrolytes were expressed as fractional excretion (FE), which will account for the movement of fluid across the intestinal wall.

$$FE = \frac{[ion]collected \,/\, [ion]stock}{[^{14}C]collected \,/\, [^{14}C]stock} \times 100\ \%$$

[ion]collected and $[^{14}C]$collected = the concentrations of ion (Na^+, K^+, Cl^-) and ^{14}C in the collected perfusates.

[ion]stock and $[^{14}C]$stock = the concentrations of ion (Na^+, K^+, Cl^-) and ^{14}C in the BES solution before it enters the intestine (i.e. in the bottle)

Thus expressing the electrolytes in terms of FE will indicate any changes in net electrolyte movement across the tissue. Values of FE greater than 100 % indicate net secretion of the ion (electrolyte), less than 100 %, net absorption.

Protein and Osmolality:

The collected perfusates were also assayed for protein content using a standard spectrophotometric technique (Bio-rad). Osmolality of the perfusates was

measured by freezing point depression (Precision Systems, Micro Osmometer).

Hemoglobin Analysis:

Blood in the perfusates (due to tissue injury during surgery) would most likely contribute to high ^{51}Cr-EDTA clearance values and possibly altered values for net fluid flux and fractional excretion. Thus permeability data from blood-contaminated perfusates would probably not reflect normal intestinal permeation. Therefore only perfusates that were free of blood (determined by visual observation) were used for analysis. However it was possible that even samples that appeared clear may have had some blood in them. A standard spectrophotometric hemoglobin (Hb) assay was done on the collected perfusates from selected experiments. Some of these perfusates appeared blood-free, others were of different intensities of pink (suggesting the presence of Hb). The Hb results were then statistically compared (simple regression analysis) with the permeation of ^{51}Cr-EDTA.

5-HT and 5-HIAA Assays:

Tissue samples from the stomach, jejunum, ileum, and colon were collected from ferrets irradiated at the different PIRR time points (sham, 2 hours, 24 hours, and 48 hours). The tissue assay for serotonin (5-HT) and its metabolite (5-hydroxyindoleacetic acid, 5-HIAA) was adapted from the established spectrofluorometric technique of Curzon and Green, (1970). See Appendix I for methodological details of this assay.

Blood Analysis

Blood Gas Analysis:

During the flushing phase, a 0.95 mL blood sample was withdrawn from the carotid artery cannula. Half of this volume was used for blood gas analysis. The blood sample for gas analysis was collected and capped in a 1 mL syringe, (to minimize the air content of the syringe). Blood gas analysis was started immediately after sampling. Blood pH was measured with a Ca^{++}/pH Analyzer (Ciba Corning Model 634). In order to obtain a plasma sample, the remaining blood sample (from the pH analysis) was transferred to an Eppendorf microfuge tube and centrifuged (14500 revolutions per minute) in a micro-centrifuge (Fisher, Model 235A) for three minutes. Fifty μL of the plasma sample was then measured for total CO_2 (tCO_2) with a Carbon Dioxide Analyzer (Corning Model 965). The pCO_2 and HCO_3^- concentration of the plasma sample were then calculated based on the measured values of pH and tCO_2 (see Appendix II for sample calculations).

Hematological Profile:

The other half of the original blood sample was transferred into a 3 mL Vacutainer (Becton Dickinson) containing a drop of a 7.5 % EDTA solution. This blood sample was then read on the Hematology Series Cell Counter (System 9000, Baker Inst.) for complete blood analysis. A few drops of this blood sample were also

used to prepare glass slides (stained with Wright's Stain) for differential counts of neutrophils, lymphocytes, eosinophils and basophils.

Plasma Analysis:

The remaining blood samples of 0.55 mL (the minimum blood volume necessary to accurately collect 200 μL of plasma for gamma counting of the ^{51}Cr.) were withdrawn to calculate the clearance of the ^{51}Cr-EDTA from the plasma. A larger volume of blood (0.75 mL) was withdrawn for the final blood sample, so that greater plasma sample could be collected (roughly 350 μL). This final plasma sample was combined with any extra plasma obtained from the other blood samples. This combined plasma sample was analyzed for Na^+, K^+, Cl^-, protein, and osmolality.

Euthanasia

After the last sampling of perfusate and blood, the ferret was euthanized by injecting into the jugular vein cannula, a 4 mL bolus of Euthanyl (240 mg/mL sodium pentobarbital, MTC Pharm.). Death of the animal was immediate.

Radiation Safety

All work with radioactive isotopes was in accordance with the safety regulations as outlined in the "Manual of Radiation Hazards Control at the University of Ottawa". Spot wipe tests for ^{51}Cr and ^{14}C were done on a weekly basis.

Statistics

All data are presented as mean ± standard error (SE) if the n value is four or greater, or ± standard deviation (SD) if the n value is three or less.

The effects of Granisetron on radiation-induced retching, vomiting and diarrhea were analyzed using the unpaired t-test. Clearance, net fluid flux and biochemical data from the different post-irradiation groups were compared by one-way analysis of variance (ANOVA). If the results from this test were significant ($p < 0.05$), a multiple comparison test (Newman-Keuls, corrected for unequal n size where appropriate) was applied. Statistical significance between post-irradiation groups is indicated on the presented tables and figures as a "star" symbol. Comparisons between the two tissues (jejunum vs ileum) were done using the unpaired t-test. Any significance using this test is indicated on the presented results as a "dagger" symbol. Data that were suspected as outliers (extreme observations) were tested using Dixon's criterion (Snedecor and Cochran, 1980), and were rejected or kept based on the probability result.

The clearance, net fluid flux, and biochemical results of sham-injected (SI) ferrets (Phase 3) were compared (unpaired t-test) to those results of non-injected (NI) ferrets (Phase 2). When there was no significant difference between these two groups, the data were pooled and this pooled group was used to make statistical comparisons against the drug-injected (DI) ferrets of Phase 3. If there was a statistical difference between SI and NI, then the results of the DI ferrets were compared against the SI ferrets.

Dosimetry

There was no significant difference in the delivered dose of radiation among different gut regions (Table 11). Only the results of a single dosimetry experiment are presented. The results of the two other dosimetry experiments were comparable.

Table 11. Dosimetry results of a 5 Gy irradiated ferret.

Tissue	Dose ± 10% (Gy)
Esophagus	4.8
Stomach - Fundus	5.1
Stomach - Antrum	5.5
Duodenum	5.3
Jejunum (mid segment)	5.3
Proximal Ileum	5.3
Ileum (mid segment)	5.1
Colon	5.3
Dorsal abdominal wall	5.3
Ventral abdominal wall	5.0
Background (Air)	0

Cardiovascular Parameters

During surgery, control ferrets had an average mean arterial pressure (MAP) of roughly 75 - 85 mmHg (80 - 95 mmHg systolic, 50 - 70 mmHg diastolic). Heart rate was generally 180 - 220 beats per minute. Venous pressures were always negative (-1 to -5 mmHg). These values were constant throughout the experiment (except for a transient (approximately 30 seconds) increase in MAP by about 30 to 50 mmHg during ligation of the renal pedicles), and there was no difference between the experimental groups.

Hematology Results

The hematology results presented in Figures 13, 14, and 15 are from non-injected ferrets (Phase 2). The hematological profile of sham- and Granisetron-injected ferrets was also assessed (Phase 3). There was no difference in the hematology results between Phase 2 and Phase 3, therefore only the results of Phase 2 are presented.

The total white blood cell count (WBC x $10^3/mm^3$) averaged 8.3 ± 0.5 (n=6) for control-irradiated animals (Figure 13). This value falls within the normal range reported by Fox (1988), however the reported data can have a substantial range: 1.7 to 11.9 (Fox, 1988), 7.7 to 15.4 (Lee et al., 1982). Total WBC dropped significantly, by approximately 75 %, within the first 2 hours of exposure to 5 Gy gamma radiation. The white cell count remained at this depressed level for at least two days post-irradiation. In control-irradiated ferrets, total polymorphonucleocytes (PMN) accounted for approximately half of the WBCs. By 2 hours post-irradiation (PIRR), PMN's had decreased from a control value of 4.3 x $10^3/mm^3$ ± 1.1 (n=4) to 0.6 x $10^3/mm^3$ ± 0.1 (n=4), an 85 % decrease, and accounted for only a third of the remaining white blood cells. However, by 24 hours PIRR, there was a modest increase in the total PMN count (1.9 ± 0.2 x $10^3/mm^3$ at 24 hours PIRR). In contrast, the lymphocyte population continued to decrease after 2 hours PIRR, such that by 24 and 48 hours PIRR, total lymphocyte count was effectively zero. At these later stages of radiation exposure, PMNs accounted for almost 100 % of the white blood cells (Figure 13). Monocytes also dropped to zero at 24 and 48 hours PIRR,

Figure 13.

Effect of whole body irradiation (5 Gy) on ferret differential blood counts. All values are expressed as mean ± SE, n values (% WBC): sham = 6, 2 h = 10, 24 h = 8, 48 h = 9; (% Polymorphonuclearcytes (PMN), % Lymphyocytes (Lymph), % Monocytes (Mono): control, 2 h, and 24 h all have n=4; 48 h, n= 5.

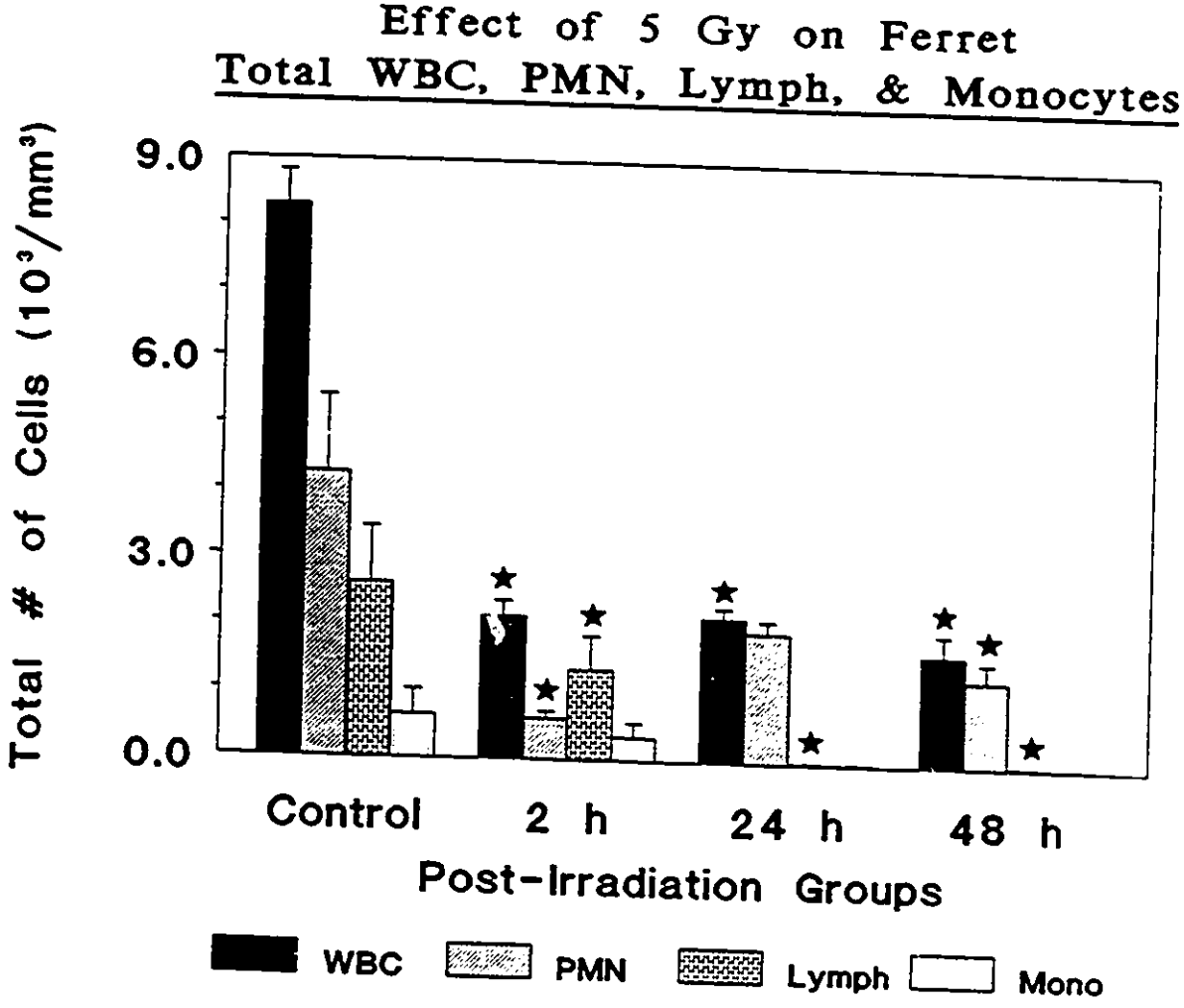
Effect of 5 Gy on Ferret
Total WBC, PMN, Lymph, & Monocytes
Total # of Cells (10^3/mm^3)
9.0
6.0
3.0
0.0
Control
2 h
24 h
48 h
Post-Irradiation Groups
WBC
PMN
Lymph
Mono

but this fall was not statistically significant compared to its low control value (0.6 ± 0.4 x $10^3/mm^3$) (Figure 13).

Platelets (PLT) and mean platelet volume (MPV) were unaffected by radiation exposure in the ferret (Figure 14). Mean corpuscular volume (MCV) and mean corpuscular hemoglobin concentration (MCHC), determinants of hematocrit and total hemoglobin, were likewise unaffected by whole-body radiation exposure to the ferret (Figure 15).

Blood Gas Analysis

Table 12 lists the measured values of arterial pH and total CO_2, and the calculated values of arterial pCO_2 and HCO_3^- of anesthetized ferrets. The control values (non-irradiated + sham-irradiated) suggest that the animals experienced respiratory acidosis (low pH, elevated pCO_2). The blood gas values for the irradiated groups were not significantly different from the control values, i.e. all animals had respiratory acidosis. Again, the results are only presented for non-injected ferrets (Phase 2). Blood gas analysis from ferrets in Phase 3 were not significantly different from Phase 2.

Plasma Analysis

The major electrolytes (Na^+, Cl^-, and K^+) and osmolality of ferret plasma from control-irradiated ferrets were within the normal range reported by Fox (1988) (Table 13). These values were not affected by radiation exposure (Table 13).

Figure 14.

Effect of whole body irradiation (5 Gy) on ferret platelet values (mean ± SE). n values (Platelet (PLT) and Mean Platelet Volume (MPV): control = 6, 2 h = 10, 24 h = 8, 48 h = 8.

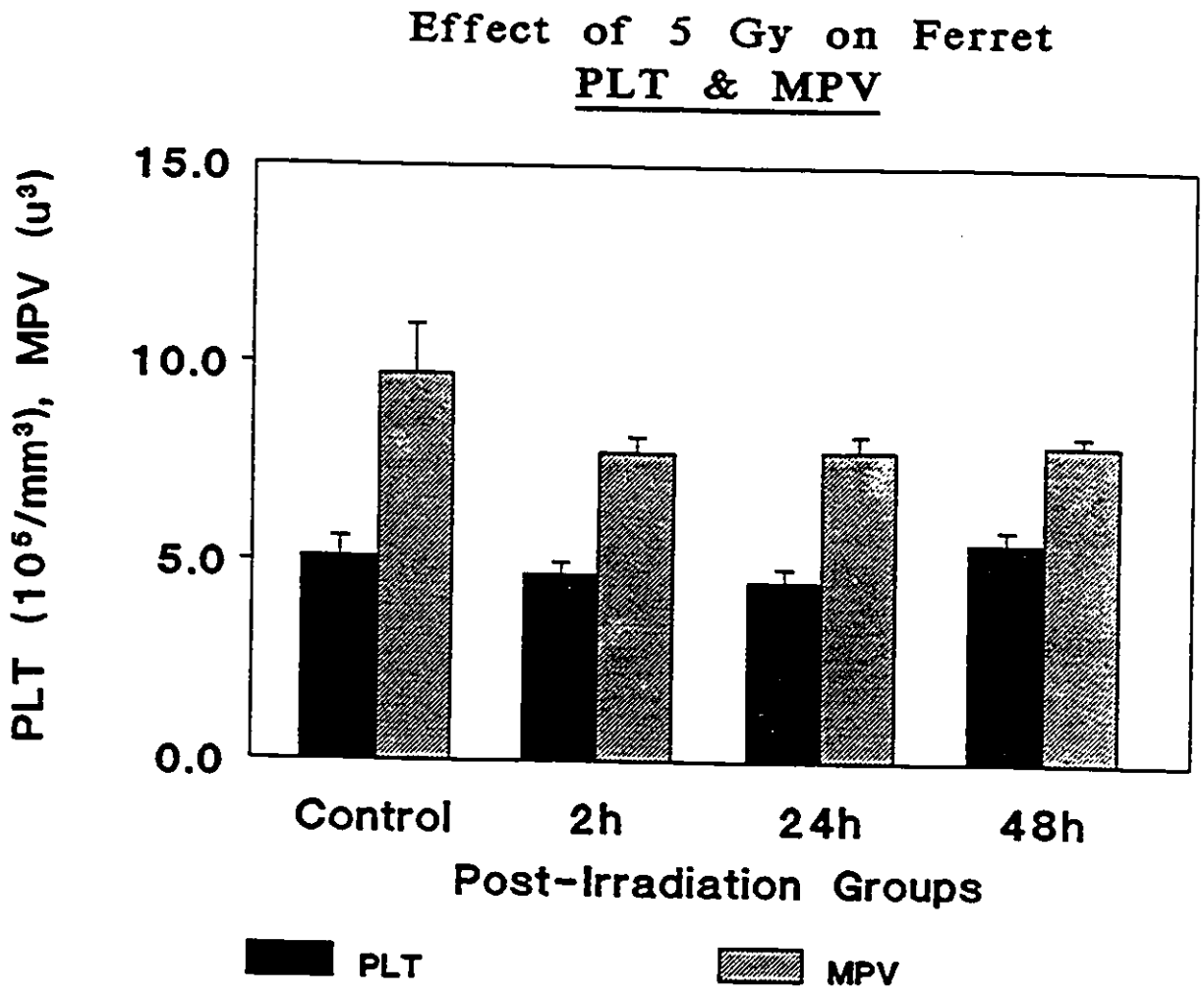
Effect of 5 Gy on Ferret
PLT & MPV
PLT (10⁶/mm³), MPV (u³)
15.0
10.0
5.0
0.0
Control
2h
24h
48h
Post-Irradiation Groups
PLT
MPV

Figure 15.

Effect of whole body irradiation (5 Gy) on ferret hematocrit parameters, MCV (mean corpuscular volume) and MCHC (mean corpuscular hemoglobin concentration). All values are mean ± SE, n values: control = 6, 2 h = 10, 24 h = 8, 48 h = 9.

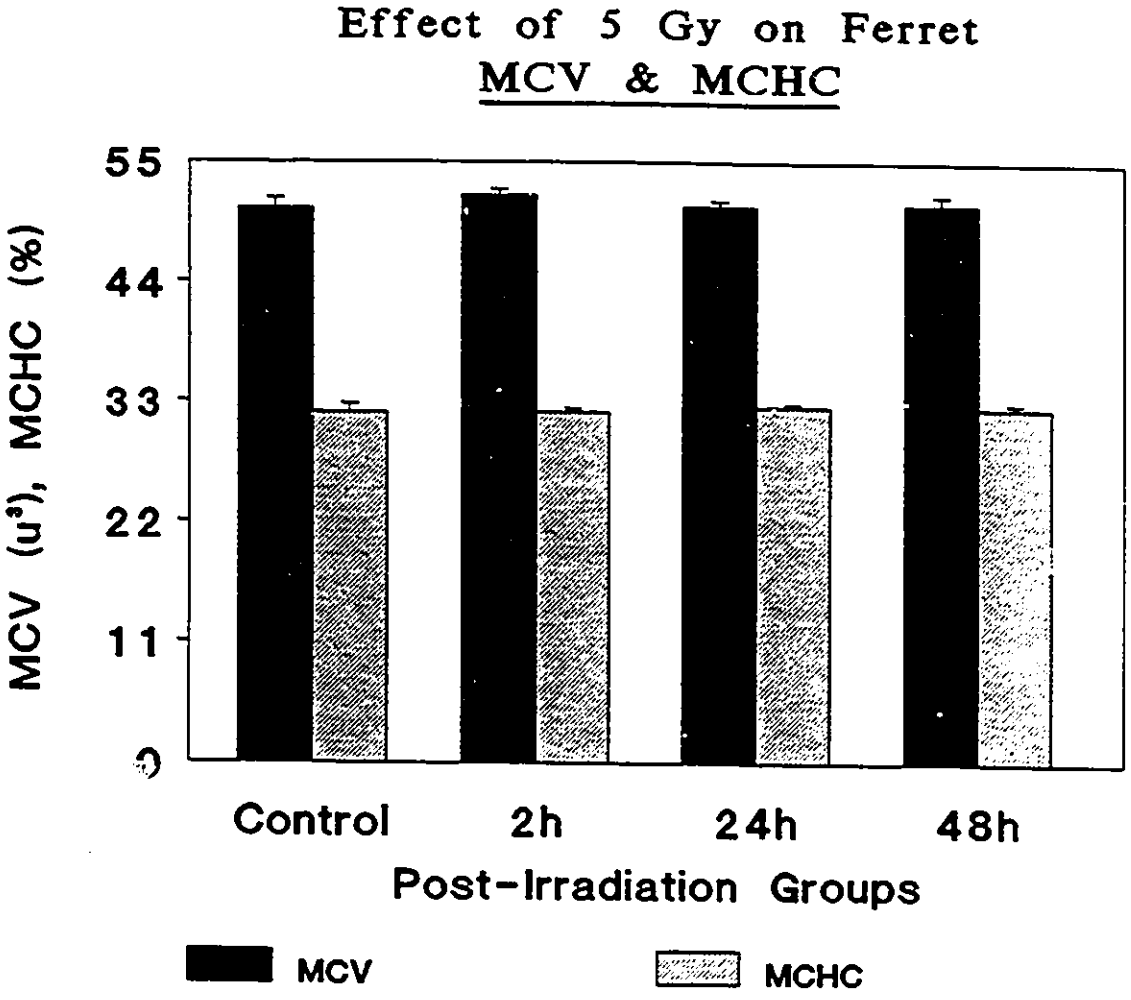
Effect of 5 Gy on Ferret
MCV & MCHC
MCV (u³), MCHC (%)
55
44
33
22
11
0
Control
2h
24h
48h
Post-Irradiation Groups
MCV
MCHC

Table 12. Acid-base status of anesthetized irradiated ferrets.

Arterial Blood

	pH	tCO_2	pCO_2	HCO_3^-
Control (n=7)	7.2 ± 0.02	26.2 ± 0.6	60.0 ± 3.0	24.4 ± 0.5
2 h PIRR (n=7)	7.3 ± 0.02	24.9 ± 0.5	54.5 ± 3.6	23.3 ± 0.5
24 h PIRR (n=11)	7.2 ± 0.02	23.8 ± 0.8	57.0 ± 4.1	22.1 ± 0.8
48 h PIRR (n=10)	7.2 ± 0.02	26.2 ± 0.9	64.5 ± 4.2	24.3 ± 0.8

Values are expressed as mean ± SE.

Table 13. Composition of major electrolytes in ferret plasma.

	(mM)			mOsm/kgH_2O
Group	Na+	Cl-	K+	Osmolality
Control (n=7)	150 ± 1	113 ± 1	6.3 ± 0.2	322 ± 2
2 h PIRR (n=7)	149 ± 1	114 ± 1	6.7 ± 0.1	325 ± 2
24 h PIRR (n=6)	149 ± 1	115 ± 1	6.5 ± 0.1	328 ± 3
48 h PIRR (n=5)	147 ± 2	113 ± 2	6.4 ± 0.2	320 ± 3

Values are expressed as mean ± SE, n values are indicated in brackets.

Prodromal Effects of Irradiation

Phase 2 (non-injected ferrets):

While nausea, one of the prodromata of radiation sickness, cannot be quantitated in animals, Bermudez et al. (1988) have documented several behavioral cues which suggest the severity of nausea: retching, drinking, defecation, posturing to defecate, urgent backing movements ("backing", related to defecation), urgent tunnelling under the wood shavings in the cage ("burrowing"), and vigorous licking (related to salivation). In this project, all irradiated ferrets (non- and sham-injected) retched. While retching always proceeded vomiting, some of the behavioral cues listed by Bermudez, very frequently proceeded retching. The most prominent behavioral responses were urgent tunnelling (burrowing) and vigorous licking. Burrowing was most frequent within the first 30 minutes post-irradiation, generally when retching episodes were a few minutes apart. Each burrowing episode was approximately 15 to 30 seconds long, and occurred just prior to retching. Vigorous tongue-licking occurred in roughly 75 % of the irradiated ferrets. Sometimes this response was so severe that the masseter and/or the temporalis muscles (of only one side) could be seen to contract and relax. This response generally occurred between 30 to 90 minutes post-irradiation. After the first hour post-irradiation, all irradiated ferrets appeared lethargic for several hours; most slept or dozed, and were unresponsive to auditory stimuli. The majority of ferrets in the 48 hour PIRR group ate the food that was offered to them at 24 hours PIRR. The ferrets at this time (24 hours PIRR) were generally active and curious. This suggested that the animals were

"feeling all right" by this time post-irradiation.

Retching commenced within the first 5 - 10 minutes following 5 Gy total body exposure and peaked within the 15 - 20 minute post-irradiation (PIRR) interval (Figure 16). An average of three to four retches were observed per retching episode. After approximately thirty minutes of intense retching (5 to 35 minutes PIRR), the retching response waned and only minor retching was observed occurring at approximately ten minute intervals for the remaining two hours of observation post-irradiation. Control irradiated (sham + non) ferrets were never observed to retch. The ferrets were frequently observed much longer than two hours PIRR. Five ferrets were filmed on videotape for several hours (up to 24) post-irradiation, however this practice was discontinued because the prodromal symptoms were very rare after two hours, and because the quality of observation from the videotape was poor. Quantification of prodromata from only the first two hours PIRR was therefore believed to be an accurate reflection of the prodromal effects of radiation. Three ferrets were sham-irradiated and 3 were non-irradiated. One ferret from each group (sham and non) was used for a 2 hour PIRR experiment. Therefore because of the protocol (see Methods) for the 2 hour PIRR experiments, these ferrets could not be observed for prodromal effects of irradiation. For this section post-irradiation observations were limited to the control animals used in the 24 hour and the 48 hour experiments, 2 from sham-irradiated ferrets, and 2 from non-irradiated ferrets.

Data were similarly obtained for vomiting (Figure 17) and bowel movements (Figure 18). The posture for vomiting was very similar to that for retching. Usually

Figure 16.

Retching responses of irradiated ferrets (n = 10, values are mean ± SE) observed during the first two hours post-irradiation (5 Gy). Two sham-irradiated ferrets were observed, neither retched.

Retching Responses of Irradiated Ferrets

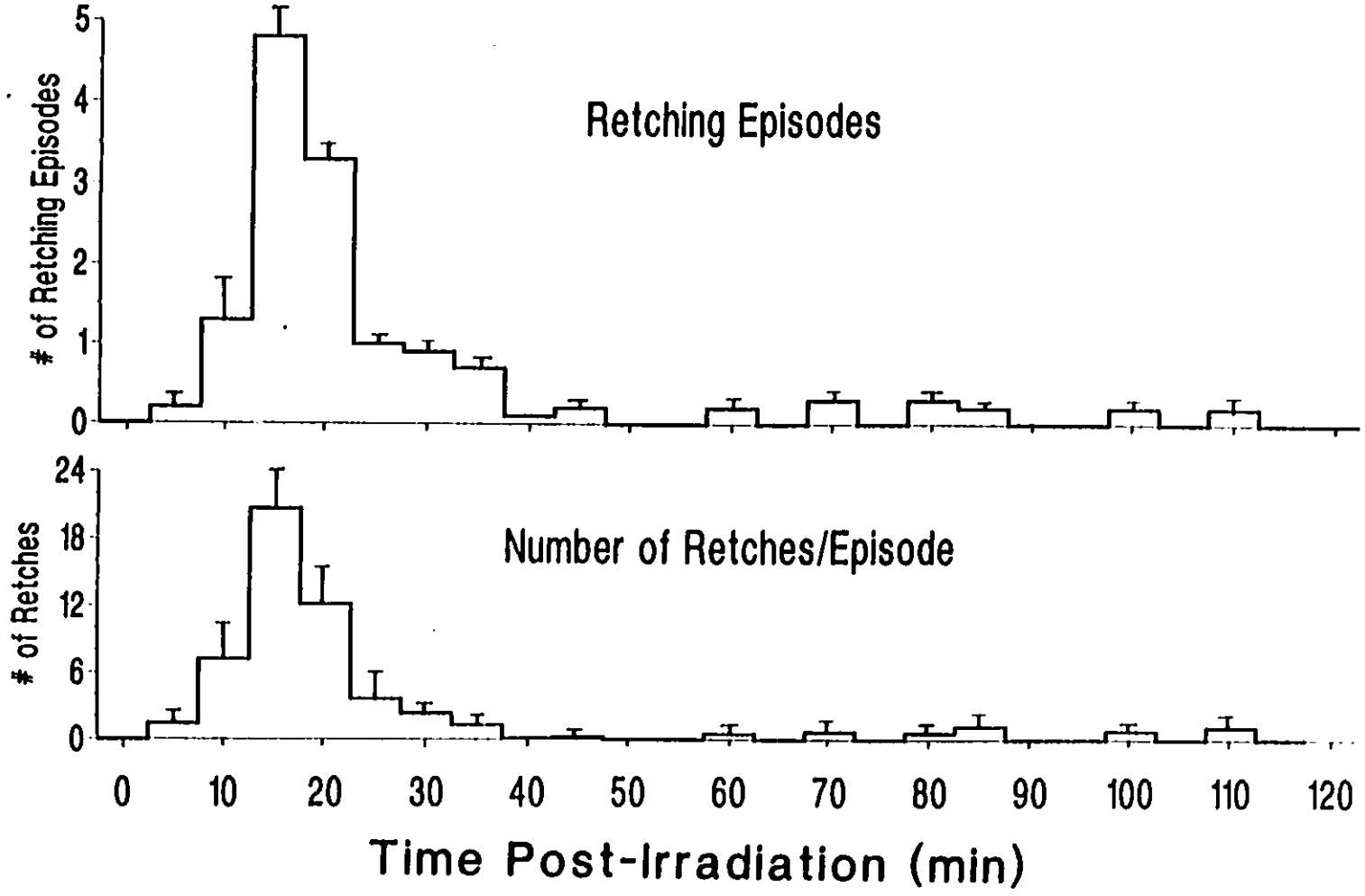

Figure 17.

Vomiting responses of irradiated ferrets (n = 10, mean ± SE) observed during the first two hours post-irradation (5 Gy). Two sham-irradiated ferrets were observed, neither vomited.

Vomiting Responses of Irradiated Ferrets

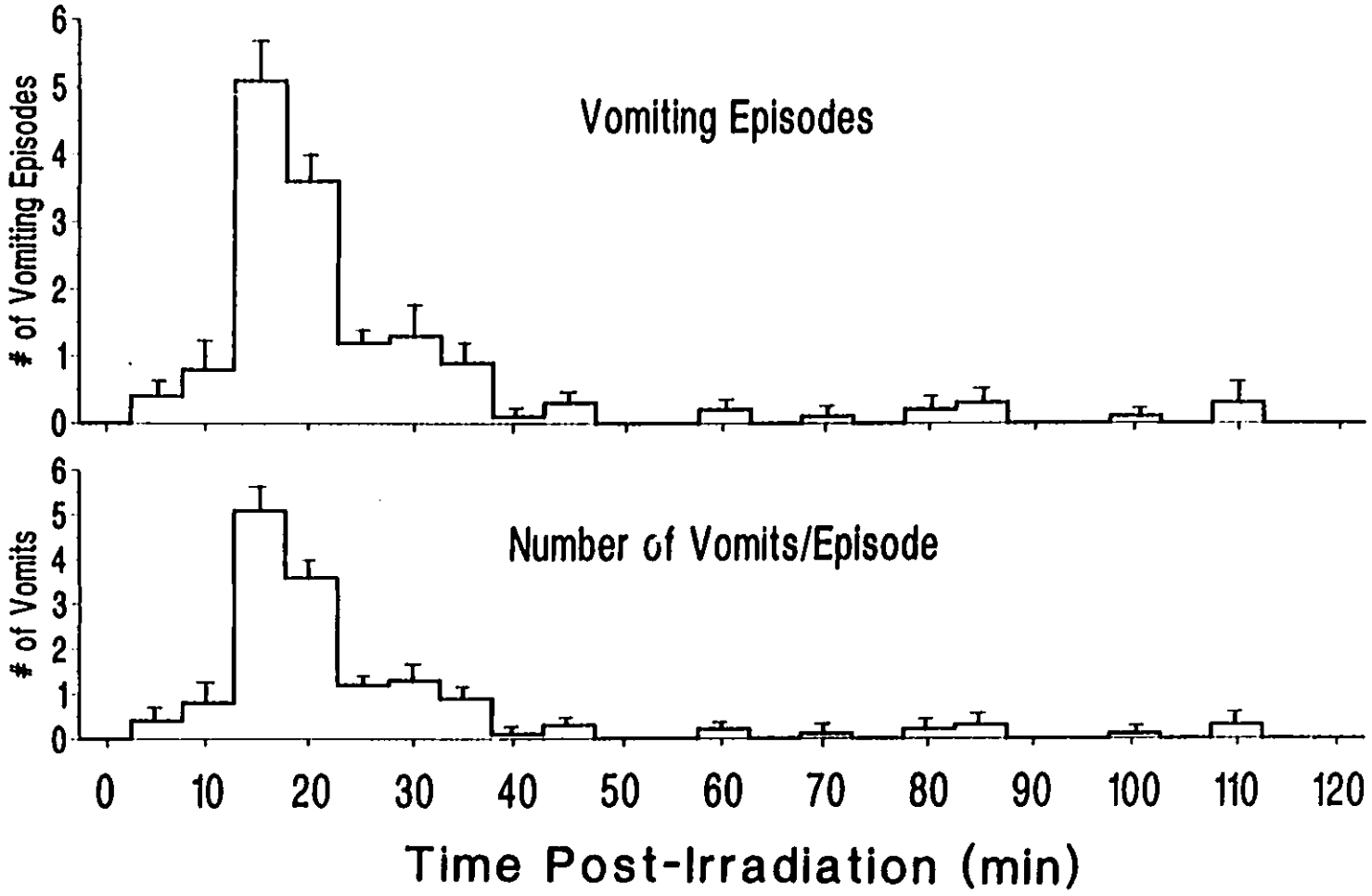

Figure 18.

Bowel resposes of irradiated ferrets (n = 10, mean ± SE) observed during the first two hours post-irradiation (5 Gy). On average, each irradiated ferret had two or three "normal" bowel movements during the first 30 minutes post-irradiation. All irradiated ferrets experienced a strained, pink mucoid diarrhea, starting around 25 - 30 minutes post-irradiation. Two sham-irradiated ferrets were observed, only one had a normal bowel movement at 70 minutes post-irradiation.

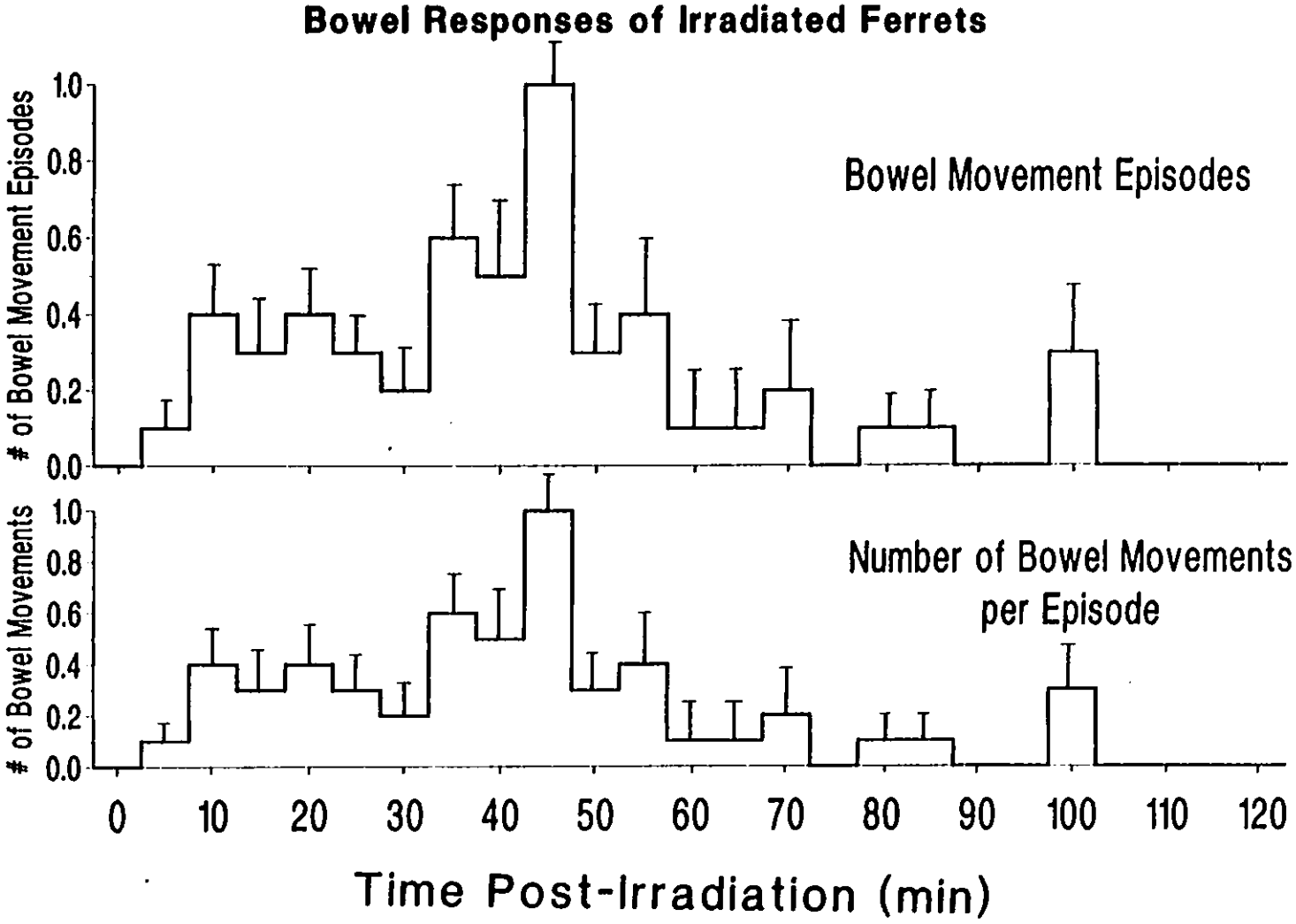
Bowel Responses of Irradiated Ferrets
# of Bowel Movement Episodes
1.0
0.8
0.6
0.4
0.2
0.0
Bowel Movement Episodes
# of Bowel Movements
1.0
0.8
0.6
0.4
0.2
0.0
Number of Bowel Movements per Episode
0
10
20
30
40
50
60
70
80
90
100
110
120
Time Post-Irradiation (min)

after a few retches, the ferrets (still in the retching posture) would arch their backs even more, raise their lower body and head, and then vomit. Vomiting often concluded the retching episodes, suggesting that retching was simply a primer for vomiting. Like retching, vomiting began within the first 5 - 10 minutes post-irradiation, and peaked within the first 15 - 20 minutes PIRR. There was a one-to-one relationship between the number of vomiting episodes and the total number of vomits per episode, i.e. the ferrets vomited only once while in the vomiting posture, following which they assumed another activity. Control-irradiated ferrets were never observed to vomit.

Bowel movement episodes were similarly defined, based on assuming and maintaining posture. The posture was very similar to that for retching, except that the ferret tried to position itself such that its feces (or diarrhea) would be deposited in a corner of the cage. Of the four control-irradiated ferrets that were observed post-irradiation, only one (apparently normal) bowel movement was recorded during the two hour observation period. During the first 25 minutes post-irradiation, ferrets in the irradiated groups produced on average two or three bowel movements. Although this represents an abnormal rate of defecation, there appeared to be no urgency, minimal straining (tenesmus), and the feces, though soft, were well-formed. The first bowel movement of this type generally occurred within the first 5 to 10 minutes post-irradiation (Figure 18). At approximately 25 to 30 minutes post-irradiation, the pattern and the product of defecation changed. Urgency and straining were apparent and there was no longer a well-formed stool, rather a mucoid

diarrhea was excreted. This diarrhea would often appear pink, or have fine red lines running through it, suggesting that either a direct or indirect effect of irradiation caused some bleeding into the intestinal lumen. This type of diarrhea response reached peak intensity at approximately 45 to 50 minutes PIRR. Although there was a decreased incidence of diarrhea after this peak response, pink mucoid diarrhea accompanied by straining, occurred up to 100 minutes post-irradiation (Figure 18). Ferrets observed longer than two hours PIRR were seen to have occasional mucoid diarrhea up to five hours PIRR (data recorded on video tape). As with the vomiting, there was a one-to-one relationship between bowel movement episodes and total number of bowel movements (Figure 18).

Phase 3 (BRL 43694 injected ferrets):

Although BRL 43694 has been previously demonstrated to be an effective anti-emetic in irradiated ferrets (Davis, 1988), it has never been tested at a dose of 0.4 mg/kg in 5 Gy irradiated ferrets. Pretreatment with the drug on prodromata was measured in order to test the hypothesis that BRL 43694 drug protocol could act as an effective anti-emetic with the radiation protocol used in these experiments. Subcutaneous (s.c.) injection of the anti-emetic compound, BRL 43694 (0.40 mg/kg) 30 minutes before irradiation, significantly reduced the frequency and severity (total numbers) of the retching response (Figure 19), but only during the peak response (15 - 25 minutes PIRR). The latency was also increased by about 10 minutes. Only two of the six ferrets pre-treated with Granisetron retched, but even in these animals the frequency of retching was reduced compared to non-injected ferrets (Table 14). Granisetron also significantly reduced the number of vomiting episodes and the total number of vomits (from 15 - 40 minutes PIRR), and also increased the latency (Figure 20). Of the six animals that were pre-treated with Granisetron and observed post-irradiation, only two vomited, but again with a

Figure 19.

Retching responses of irradiated ferrets (mean ± SE, n = 6) injected with BRL 43694 (dashed line) 0.4 mg/kg s.c. 30 minutes before irradiation. Retching was observed only in 2/6 ferrets treated with Granisetron. For comparison, solid line indicates the retching responses of non-injected ferrets of phase 2 (as presented in Figure 16).

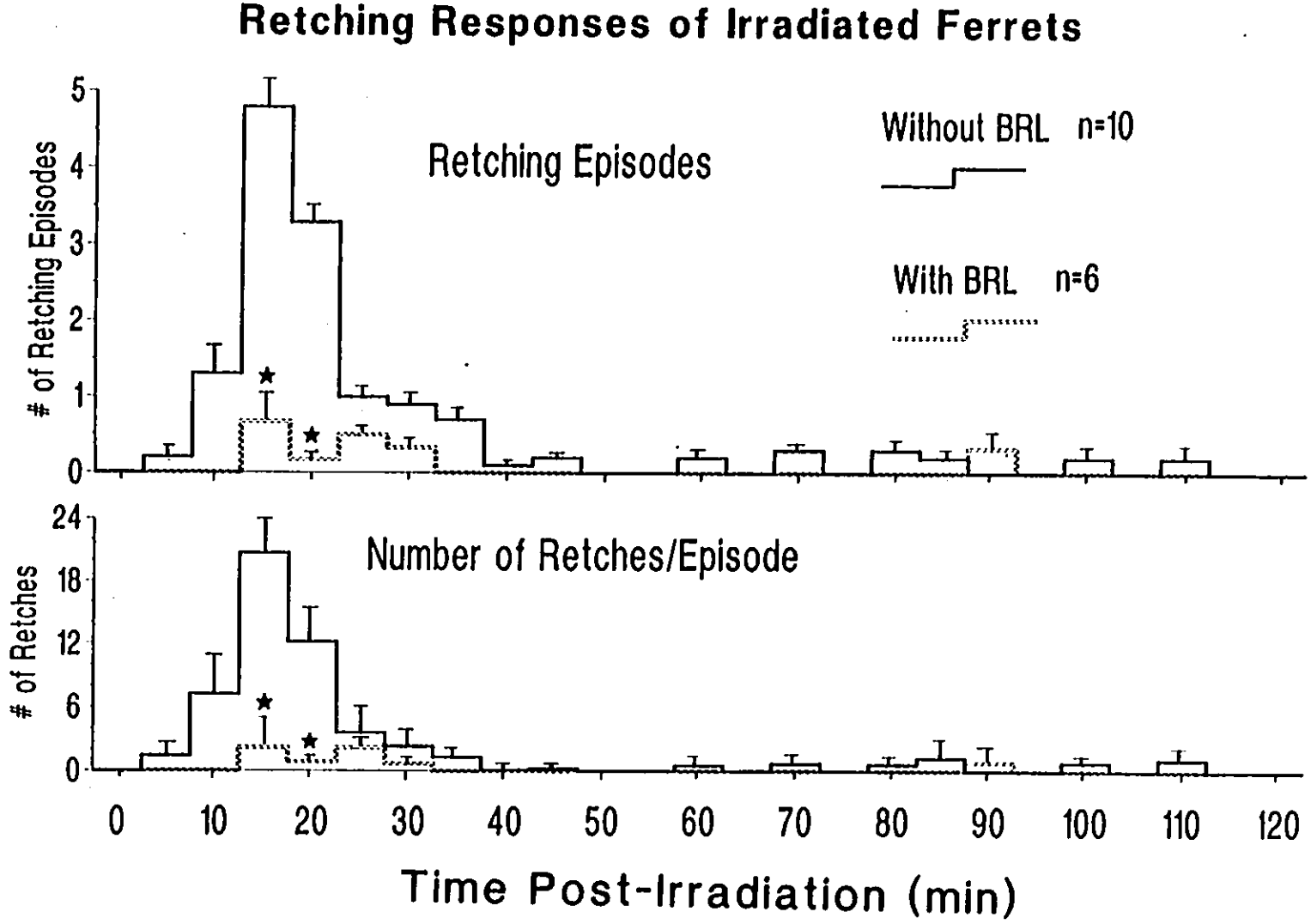
Retching Responses of Irradiated Ferrets
Retching Episodes
Without BRL n=10
With BRL n=6
# of Retching Episodes
0
1
2
3
4
5
Number of Retches/Episode
# of Retches
0
6
12
18
24
0
10
20
30
40
50
60
70
80
90
100
110
120
Time Post-Irradiation (min)

reduced frequency compared to non-injected ferrets (Table 14). These data are consistent with Granisetron's action as an anti-emetic. Pre-treatment with Granisetron significantly decreased the frequency of defecation at 45 - 50 minutes PIRR (Figure 21). The total number of bowel movements during the first two hours post-irradiation was not statistically different between non-injected and drug-injected ferrets (Table 14). However, an important but purely qualitative observation of the Granisetron-treated ferrets was that the diarrhea appeared to be less mucoid, and more watery. In addition, the volume of diarrhea excreted appeared to be lower than the non- and sham-injected ferrets. The behavioral cues of nausea that were frequently observed in non- and sham-injected ferrets (the burrowing and tongue-licking) were minimized in ferrets injected with Granisetron.

Table 14. Total number of prodromal events during the first two hours post-irradiation.

	Retching		Vomiting		Bowel Movements	
	Epi.	Total	Epi.	Total	Epi.	Total
NI	13.6	53.5	14.9	14.9	5.1	5.1
n=10	(1.1)	(7.7)	(1.0)	(1.0)	(0.7)	(0.7)
DI	2.0 *	6.7 *	1.5 *	1.5 *	3.2	3.2
n=6	(1.4)	(4.8)	(1.1)	(1.1)	(0.7)	(0.7)
DI #1	2	8	7	7	2	2
DI #2	4	11	2	2	5	5

Values are expressed as mean ± SE, SE indicated in brackets
Epi. = mean # of episodes during the first 2 hours PIRR
Total = total # of events during the first 2 hours PIRR
NI = non-injected ferrets, DI = drug-injected (Granisetron) ferrets
* = statistically lower from NI ferrets ($p < 0.001$)
Only 2 of the 6 DI ferrets retched or vomited, their data are presented: DI # 1 and DI # 2

Figure 20.

Vomiting responses of irradiated ferrets (mean ± SE, n = 6) injected with BRL 43694 (dashed line) 0.4 mg/kg s.c. 30 minutes before irradiation. Vomiting was only observed in 2/6 ferrets treated with BRL 43694. For comparison, the vomiting responses of non-injected ferrets from phase 2 are shown in the solid black line (as presented in Figure 17).

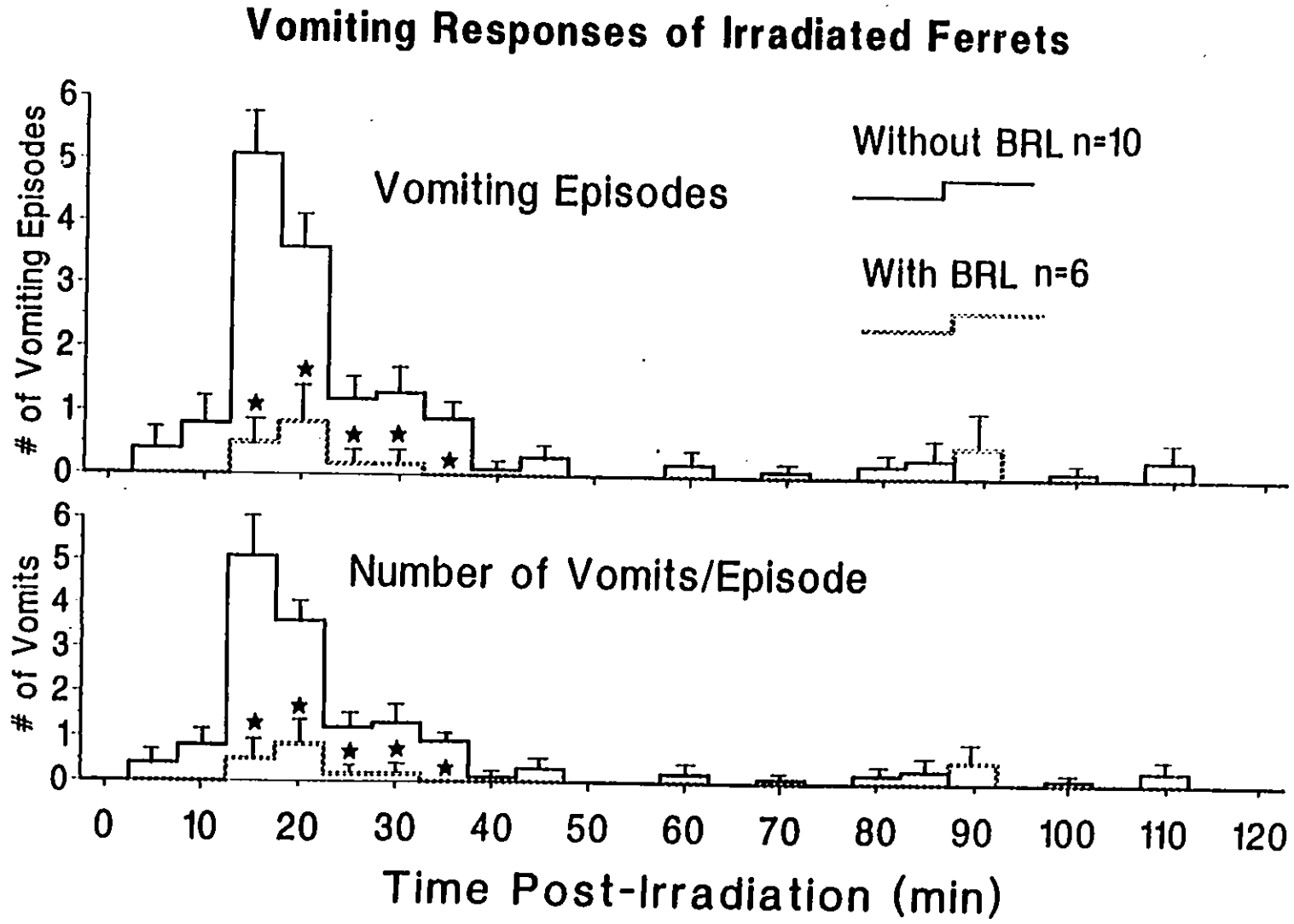
Vomiting Responses of Irradiated Ferrets
# of Vomiting Episodes
Vomiting Episodes
Without BRL n=10
With BRL n=6
# of Vomits
Number of Vomits/Episode
0 10 20 30 40 50 60 70 80 90 100 110 120
Time Post-Irradiation (min)

Figure 21.

Bowel responses of irradiated ferrets (mean ± SE, n = 6) injected with BRL 43694 (dashed line) 0.4 mg/kg s.c. 30 minutes before irradiation. Although all of the ferrets treated with BRL 43694 experienced diarrhea (commencing around 25 - 30 minutes post-irradiation), it was less mucoid, and less volume was excreted. For comparison, the bowel responses of non-injected ferrets of phase 2 are shown in the solid black line (as presented in Figure 18).

Bowel Responses of Irradiated Ferrets

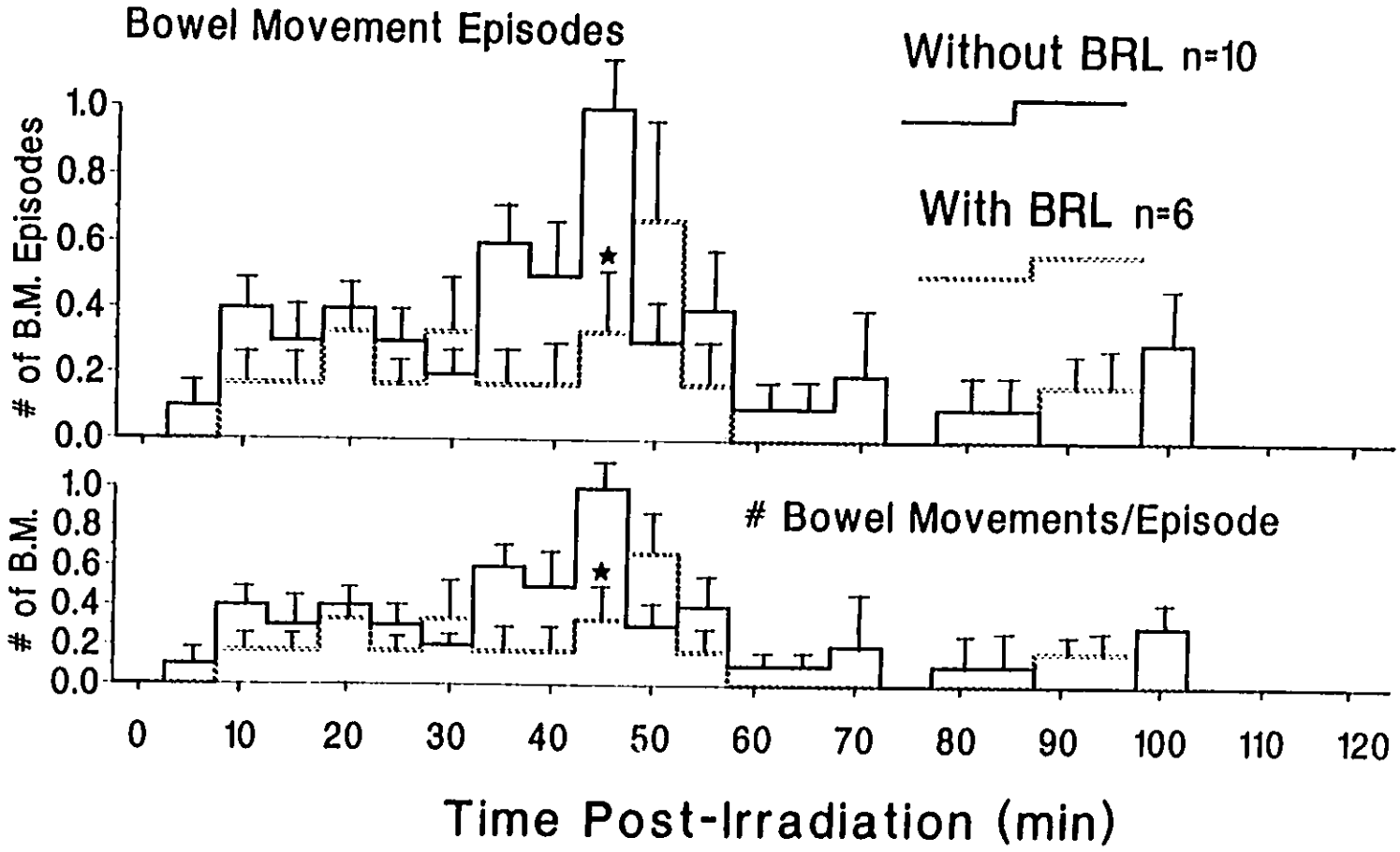

Clearance, Net Fluid Flux, and Biochemistry

Results for net fluid flux and biochemical analyses were calculated at 10 minute intervals of the 60 minute experimental perfusion phase, and at 20 minute intervals for the clearance of ^{51}Cr-EDTA. However because there were no statistical differences in the results over the 60 minutes of perfusion (see Appendix III), suggesting the stability of the experimental preparation, for clarity of presentation the results are presented only for the first sample (P1, collected at 0 minutes) and the last sample (P7, collected at 60 minutes) of the 60 minute experimental perfusion.

Clearance (Permeation) of ^{51}Cr-EDTA

Although the jejunum and ileum are both part of the small intestine, there are histological and functional differences between them, which may account for regional differences in permeability. Fordtran et al., (1965) and Loehry et al., (1973) have both suggested that the jejunum is more permeable than the ileum, whereas under experimental conditions (FMLP-induced intestinal inflammation) von Ritter et al., (1988) have suggested that the distal ileum is more permeable. Therefore, the permeation of ^{51}Cr-EDTA was measured in ferret jejunum and ileum in order to test the hypothesis that there are regional differences in ferret intestinal permeability. With the radiation protocol that was selected for these experiments, it is possible that radiation exposure to the intestine could cause changes in intestinal motility and blood flow, initiate inflammatory reactions, or stimulate release of secretagogues. All of these factors could possibly alter intestinal permeability. Therefore, the permeation of ^{51}Cr-EDTA was measured at different times post-irradiation to test the hypothesis that radiation exposure alters intestinal permeability.

Phase 2:

Both jejunum and ileum had virtually identical control values of ^{51}Cr-EDTA permeation (Figure 22). At 2 hours PIRR there was a significant increase in the permeation of ^{51}Cr-EDTA in the jejunum, the ileum had borderline significance, $p = 0.06$. Permeation at 24 hours PIRR was no different than control values. Clearance of ^{51}Cr-EDTA was dramatically increased at 48 hours PIRR in the ileum but not in the jejunum (Figure 22). This increased permeation was approximately 10-fold greater than in control ferrets (Figure 23).

Figure 22.

^{51}Cr-EDTA clearance in perfusion samples P1 (collected at 0 minutes) and P7 (collected at 60 minutes) of the jejunum (top) and ileum (bottom) of irradiated ferrets. Values are mean ± SE, n values for control, 2 h, 24 h, and 48 h post-irradiation groups are (in order) for jejunum: 5, 5, 6, 5; for ileum: 6, 6, 6, 6. † indicates significant difference from ileum at the corresponding PIRR time point, ⋆ indicates significant difference from other PIRR time groups within the same tissue.

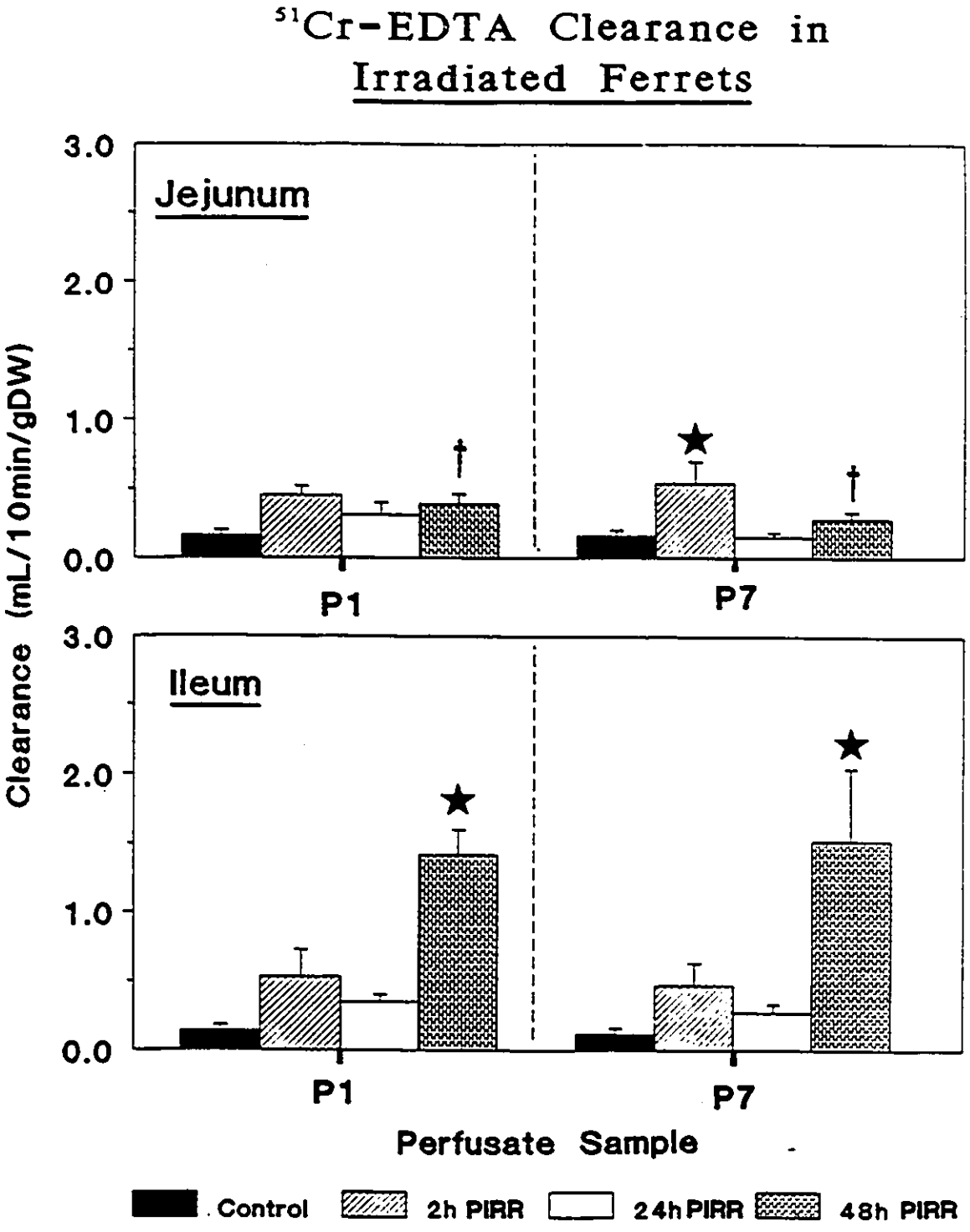
^{51}Cr-EDTA Clearance in Irradiated Ferrets
Jejunum
Ileum
Clearance (mL/10min/gDW)
3.0
2.0
1.0
0.0
P1
P7
Perfusate Sample
Control
2h PIRR
24h PIRR
48h PIRR

Figure 23.

^{51}Cr-EDTA clearance in perfusion samples P1 and P7 in the jejunum (top) and ileum (bottom) of irradiated ferrets. Values are expressed in relation to the control value (of Figure 22), as mean ± SE. n values for 2 h, 24 h, and 48 h post-irradiation groups are (in order) for jejunum: 5, 6, 5; for ileum 6, 6, 6. † indicates significant difference from ileum at the corresponding PIRR time point, ⋆ indicates significant difference from other PIRR time groups within the same tissue.

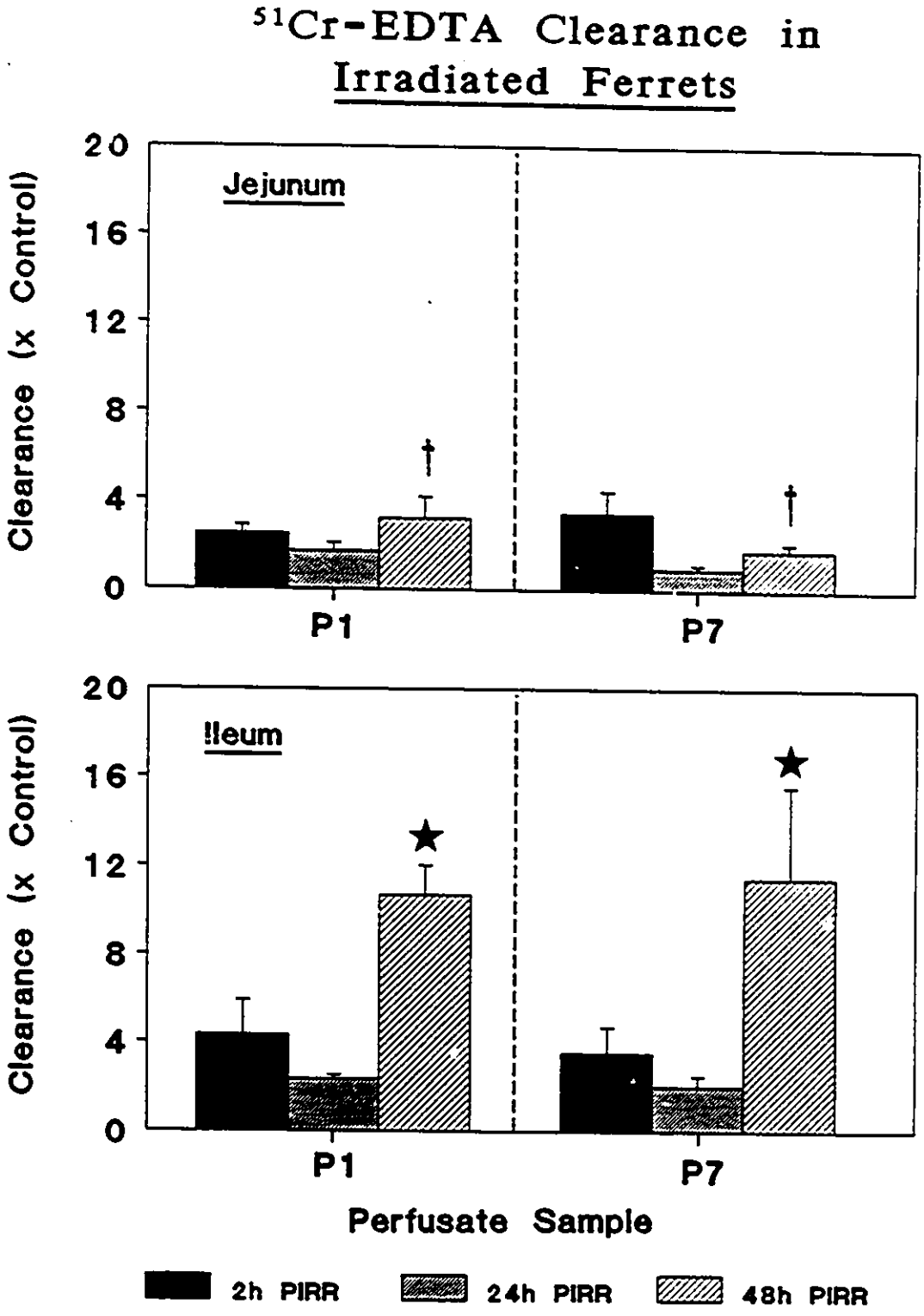
^{51}Cr-EDTA Clearance in Irradiated Ferrets
Jejunum
Ileum
Clearance (x Control)
20
16
12
8
4
0
†
★
P1
P7
Perfusate Sample
2h PIRR
24h PIRR
48h PIRR

Phase 3:

When there was no statistical difference between non-injected and sham-injected clearance results, these two groups were pooled and compared against the drug-injected ("DI") group. This was the case for all but two groups of clearance data. In one group (jejunum, sham-injected, control-irradiated for sample P1) the clearance value (of ^{51}Cr-EDTA) was statistically greater than in the corresponding group of non-injected ferrets; in the other group (jejunum, sham-injected, 2 hours PIRR for sample P1) the clearance value was significantly lower. Thus for some unknown reason there may have been a placebo effect. For these two (non-pooled) groups, statistical comparisons to the related DI group were made against the sham-injected (SI) results alone. Beubler and Horina (1990) have reported that a 5-HT$_3$ antagonist was effective in controlling the cholera-toxin stimulated intestinal secretion. The 5-HT$_3$ antagonist, Granisetron, was therefore tested to see if the radiation-induced secretion of ^{51}Cr-EDTA was mediated by 5-HT$_3$ receptors. In the jejunum of control-irradiated ferrets, Granisetron pre-treatment caused a significant decrease in the clearance of ^{51}Cr-EDTA (Figure 24). However, while this effect was significant for both P1 and P7 (and for the other collected samples, P3 and P5), the decrease may only be real for P5 and P7, due to the placebo effect in P1 (*the placebo effect was also present for sample P3, but not for sample P5*). Granisetron also caused a significant increase in clearance in the ileum at 48 hours PIRR, but this occurred only in the first collected sample (P1) - all other clearance values in this group (P3, P5, and P7) were statistically the same as control-injected (CI) ferrets.

Figure 24.

^{51}Cr-EDTA clearance in perfusion samples P1 (collected at 0 minutes) and P7 (collected at 60 minutes) of the jejunum (top) and ileum (bottom) of Granisetron pre-treated ferrets. CI refers to control-injected (pooled non-injected with saline-injected ferrets), SI refers to saline-injected ferrets, DI refers to drug-injected ferrets. Non-injected and saline-injected results were pooled for all groups except for 2 groups in the jejunum: control, perfusion sample P1 and 2 hours PIRR, perfusion sample P1. The data of these latter two groups are presented on the figure as saline-injected (SI) results.

Values are mean ± SE. Jejunum n values for control are: SI = 4, CI = 9 DI = 5; 2 h PIRR: SI = 4, CI = 9, DI = 4; 48 h PIRR: CI = 8, DI = 4. Ileum n values for control are: CI = 11, DI = 4; 2 h PIRR: CI = 11, DI = 6, 48 h PIRR: CI = 10, DI = 5. † indicates significant difference from ileum at the corresponding PIRR time point, ⋆ indicates significant difference from all other PIRR time groups within the same tissue. ‡ indicates significant difference between DI and SI, or between DI and CI.

^{51}Cr-EDTA Clearance in Granisetron Pre-Treated Ferrets

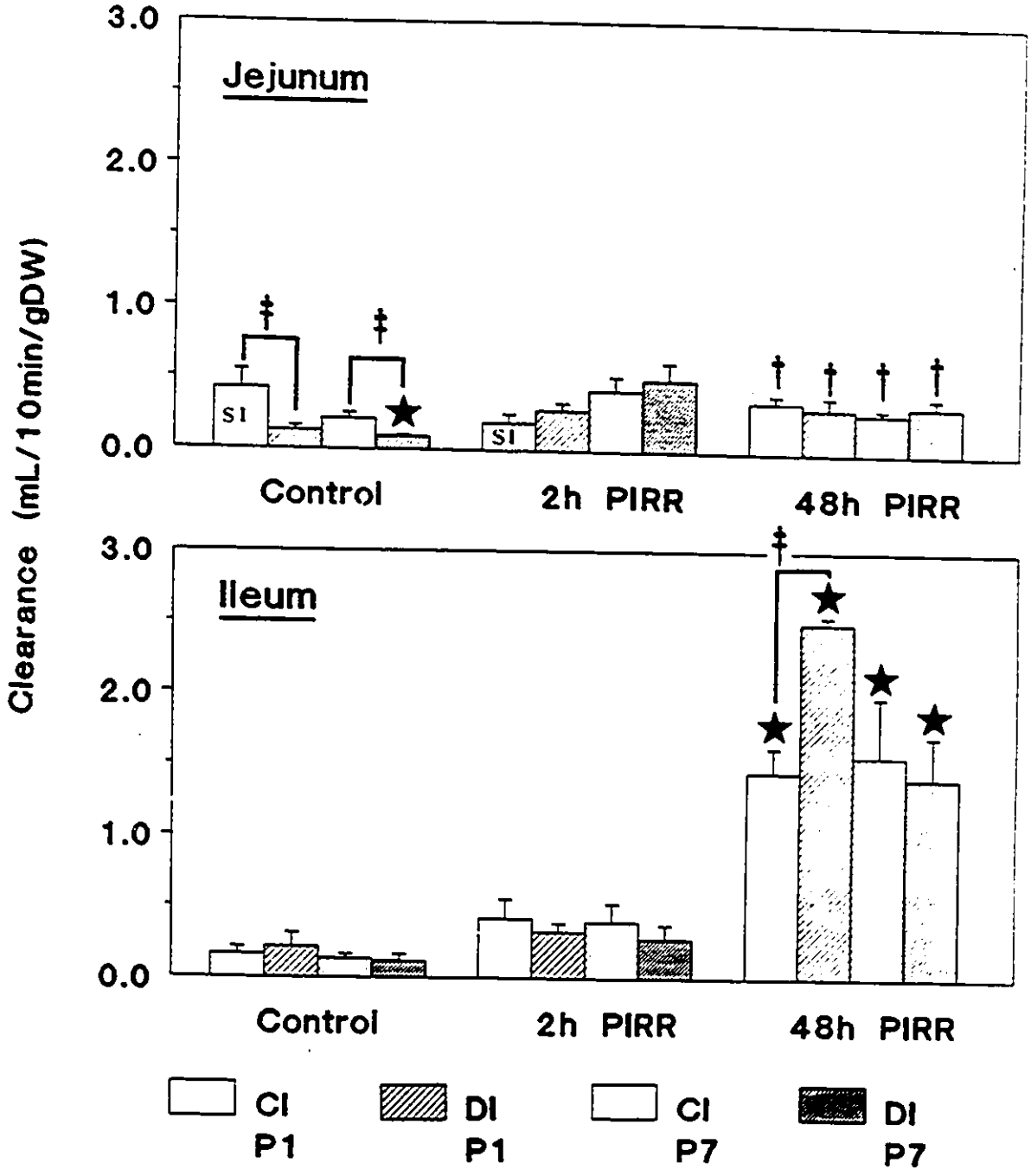

Analysis of ^{51}Cr in the Urine

The necessity of ligating the renal vessels was confirmed by one experiment, where the renal vessels were purposely left intact (not ligated), and the ^{51}Cr-EDTA was injected into the circulation. When the first plasma sample was taken 15 minutes after ^{51}Cr-EDTA injection, plasma counts of ^{51}Cr were six times lower than normal, and continued to decline rapidly throughout the experiment. The counts of the ^{51}Cr in the urine sample collected at the end of the experiment revealed that virtually all of the injected ^{51}Cr-EDTA had been excreted by the kidneys. Normally when the renal vessels were ligated, the urine counts of ^{51}Cr (and ^{14}C) were at normal levels of background radiation energy.

Fluid Movement in the Intestinal Segments

Phase 2:

In control-irradiated ferrets, both jejunum and ileum absorbed approximately 1.2 mL of fluid per gram dry weight of tissue, over the 10 minute perfusion interval (Figure 25, *negative flux values indicate net absorption of fluid*). In the ileum, fluid absorption was reduced, but not significantly ($p = 0.09$), at 2 hours post-irradiation, but had returned to control values by 24 and 48 hours PIRR. Compared to the ileum, the jejunum absorbed significantly less fluid at the later stages (24 and 48 hours) of radiation exposure. At 48 hours PIRR, the jejunum was bordering on a state of net fluid secretion (Figure 25).

Figure 25.

Net fluid flux (J) in perfusion samples P1 and P7 in the jejunum (top) and ileum (bottom) of irradiated ferrets. Positive J values indicate net secretion of fluid, negative values indicate net absorption of fluid. Values are mean ± SE, n values for control, 2 h, 24 h, and 48 h post-irradiation groups are in order: jejunum 5, 5, 6, 5; ileum 5, 6, 6, 5. † indicates significant difference from the same post-irradiation group in the ileum.

Net Fluid Flux in Irradiated Ferrets

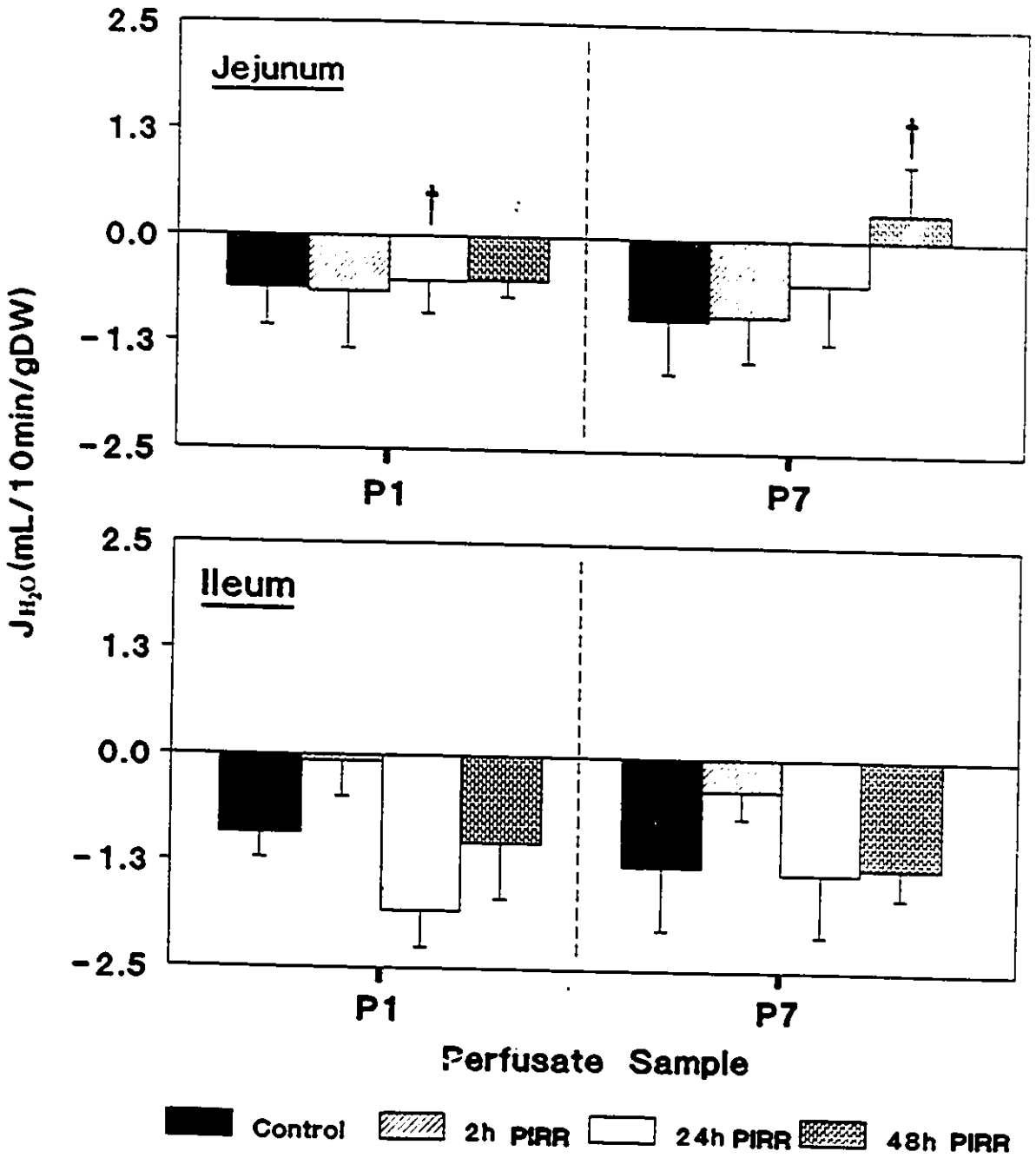

Phase 3:

There was no statistical difference in fluid flux data between non-injected ferrets of Phase 2, and the sham-injected ferrets of Phase 3. Therefore these groups were pooled (now called "control-injected", CI) and were statistically compared (unpaired t-test) against fluid flux data from drug-injected ("DI", Granisetron) ferrets (Figure 26). The only statistical effect of Granisetron pre-treatment was a modest increase in fluid absorption at 48 hours PIRR in the ileum. Fluid absorption continued to be reduced in the ileum at 2 hours PIRR, however this was only significant in the DI group of the final perfusion sample (P7). As well, at 48 hours PIRR in the jejunum fluid absorption was reduced compared to control-irradiated and 2 hour PIRR groups (significant only in CI, P7), and compared to the same time point in the ileum (significant only in the P7 groups) (Figure 26).

Biochemical Analyses

Fractional Excretion (FE)

Phase 2:

In non-injected (NI) ferrets there was no statistical difference in Na^+ FE (Table 15) or in Cl^- FE (Table 16) between post-irradiation (PIRR) groups or between tissues (jejunum vs ileum). The FE data for Na^+ and Cl^- suggest that movement of both electrolytes were in a steady state. FE of K^+ (Table 17) had the same trend as Na^+ and Cl^- except that at 48 h PIRR there was a significant secretion of K^+ in the ileum, where 4 of the 5 ferrets had a FE of K^+ > 120 %. The low n

Figure 26.

Net fluid flux (J) in perfusion samples P1 and P7 in the jejunum (top) and ileum (bottom) of Granisetron pre-treated ferrets. Positive J values indicate net secretion of fluid, negative values indicate net absorption of fluid. CI refers to control-injected (pooled non-injected with saline-injected ferrets), DI refers to drug-injected ferrets.

Values are mean ± SE for n ≥ 4, mean ± SD for n of 3. Jejunum n values for control are: CI = 8, DI = 5; 2 h PIRR: CI = 9, DI = 3; 48 h PIRR: CI = 8, DI = 4. Ileum n values for control are: CI = 11, DI = 3; 2 h PIRR: CI = 11, DI = 6; 48 h PIRR: CI = 10, DI = 5. † indicates significant difference from ileum at the corresponding PIRR time point, ⋆ indicates significant difference from all other PIRR time groups within the same tissue. • indicates significant difference from corresponding control and 2 h PIRR groups.

Net Fluid Flux in Granisetron Pre-Treated Ferrets

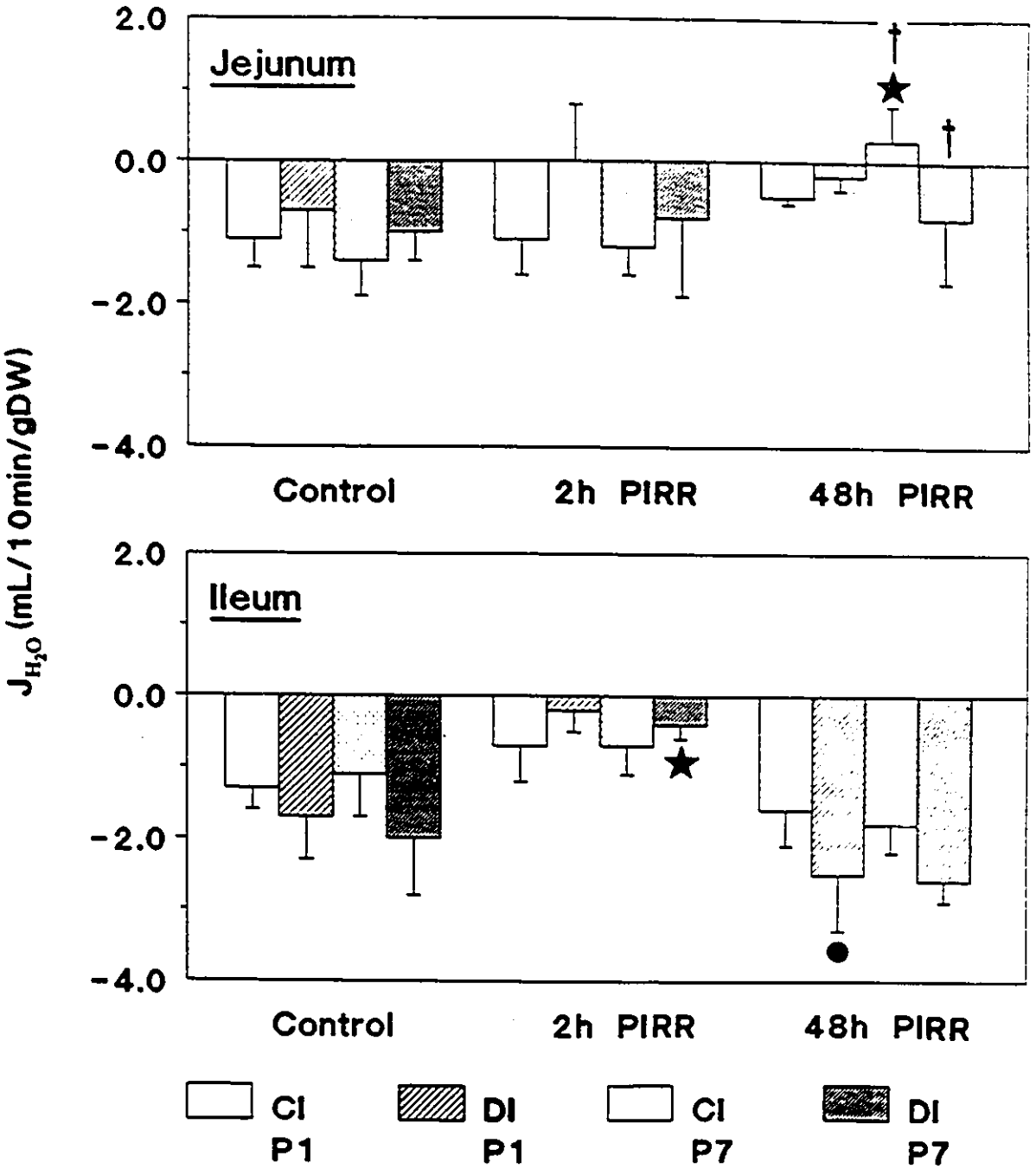

Table 15. Fractional excretion of Na^+ in perfused intestinal segments.

	Jejunum	Ileum
CONTROL		
P1	104.2 ± 2.9 (6)	104.7 ± 3.6 (6)
P7	106.5 ± 3.7 (6)	108.0 ± 4.0 (6)
2 h PIRR		
P1	103.8 ± 2.1 (5)	101.8 ± 2.5 (6)
P7	104.8 ± 2.5 (5)	105.5 ± 2.9 (6)
24 h PIRR		
P1	102.8 ± 1.6 (5)	103.0 ± 4.1 (5)
P7	103.6 ± 2.4 (5)	104.8 ± 2.0 (5)
48 h PIRR		
P1	102.5 ± 2.5 (6)	110.0 ± 9.3 (5)
P7	102.2 ± 3.1 (6)	109.2 ± 4.3 (5)

Values are expressed as percent mean ± SE, n values are indicated in brackets.
P1 = initial perfusate collected at t=0 min of 60 min perfusion
P7 = final perfusated collected at t=60 min of 60 min perfusion

Table 16. Fractional excretion of Cl^- in perfused intestinal segments.

	Jejunum	Ileum
CONTROL		
P1	97.7 ± 7.6 (3)	97.7 ± 5.7 (3)
P7	99.7 ± 10.0 (3)	107.0 ± 10.5 (3)
2 h PIRR		
P1	101.5 ± 3.5 (2)	95.7 ± 2.3 (3)
P7	96.3 ± 8.1 (2)	100.7 ± 1.5 (3)
24 h PIRR		
P1	102.2 ± 5.2 (4)	99.5 ± 8.2 (4)
P7	100.2 ± 5.3 (4)	102.5 ± 5.0 (4)
48 h PIRR		
P1	99.3 ± 7.5 (3)	100.0 ± 2.8 (2)
P7	95.3 ± 11.6 (3)	107.5 ± 0.7 (2)

Values are expressed as percent mean ± SE for n of 4 or greater, ± SD for n of 3 or less. n values are indicated in brackets.
P1 = initial perfusate collected at t=0 min of 60 min perfusion
P7 = final perfusated collected at t=60 min of 60 min perfusion

Table 17. Fractional excretion of K^+ in perfused intestinal segments.

	Jejunum	Ileum
CONTROL		
P1	109.8 ± 3.6 (6)	109.2 ± 3.1 (6)
P7	114.2 ± 5.2 (6)	113.3 ± 5.3 (6)
2 h PIRR		
P1	110.6 ± 2.6 (5)	110.5 ± 3.4 (6)
P7	112.4 ± 4.4 (5)	117.5 ± 4.6 (6)
24 h PIRR		
P1	108.4 ± 2.3 (5)	108.8 ± 5.8 (5)
P7	110.8 ± 2.9 (5)	110.2 ± 3.9 (5)
48 h PIRR		
P1	110.0 ± 3.5 (6) †	146.8 ± 15.4 (5) ★
P7	109.8 ± 3.4 (6) †	148.8 ± 9.6 (5) ★

Values are expressed as percent mean ± SE, n values are indicated in brackets.
P1 = initial perfusate collected at t=0 min of 60 min perfusion
P7 = final perfusated collected at t=60 min of 60 min perfusion
★ denotes statistical significance (by ANOVA, Newman-Keuls) from the other post-irradiation groups (PIRR)
† denotes statistical significance (by unpaired t-test) between tissues, but within the same PIRR group.

values of Cl^- FE were due to temporary equipment failure of the Chloride Analyzer. The samples for chloride analysis were frozen (-20 °C), but chloride measurements on the thawed samples were so extreme (75 - 100 % greater), suggesting an effect of freezing, that they were not included in the statistical analysis.

Phase 3:

In many groups the unpaired t-test indicated significant difference between NI and SI fractional excretion values for Na^+, Cl^-, and K^+. Therefore the FE data were not pooled and comparisons to DI were made against SI ferrets only. Generally, FE values for the electrolytes were lower (i.e. more net absorption) for SI ferrets compared to NI ferrets. Again, it is not clear how or why this apparent placebo effect occurred. This difference probably accounted for the significant difference in Na^+ FE at 2 hours PIRR between SI and DI ferrets (Table 18), and therefore it should not be considered as a real drug effect. The greater absorption in saline-injected animals may have also accounted for the differences in chloride movement seen at 48 hours PIRR. The SI groups at this time point had significantly lower absorption (almost secretion) in the jejunum than in the ileum. As well, this lower absorption in the jejunum was significantly different from the FE of Cl^- in the jejunal post-irradiation groups. No drug effect was seen in the FE of Cl^- (Table 19). There was also a placebo effect observed in the FE of K^+ (Table 20) and again this probably accounted for the difference in FE of K^+ between SI and DI ferrets in the 2 hour PIRR group. Unlike in non-injected ferrets, there was minimal secretion of

Table 18. Fractional excretion of Na^+ in perfused intestinal segments of drug-injected ferrets.

		Jejunum	Ileum
CONTROL			
P1	SI	93.3 ± 5.5 (3)	92.3 ± 3.8 (3)
	DI	99.4 ± 5.3 (5)	91.2 ± 2.1 (4)
P7	SI	94.3 ± 2.5 (3)	95.0 ± 1.0 (3)
	DI	96.6 ± 3.2 (5)	90.7 ± 3.0 (4)
2 h PIRR			
P1	SI	90.7 ± 2.5 (4) †	85.7 ± 12.7 (3) †
	DI	100.7 ± 3.0 (4)	99.6 ± 2.4 (6)
P7	SI	93.0 ± 4.8 (4)	91.5 ± 2.1 (2)
	DI	95.7 ± 7.6 (3)	99.2 ± 1.8 (5)
48 h PIRR			
P1	SI	100.2 ± 0.9 (4) **	92.5 ± 3.5 (4)
	DI	101.0 ± 4.0 (3)	81.0 ± 8.9 (4)
P7	SI	100.5 ± 3.5 (4)	93.7 ± 1.9 (4)
	DI	100.7 ± 6.6 (3)	85.5 ± 4.5 (4)

Values are expressed as percent mean ± SE for n of 4 or greater, ± SD for n of 3 or less. n values are indicated in brackets.

P1 = initial perfusate collected at t=0 min of 60 min perfusion

P7 = final perfusated collected at t=60 min of 60 min perfusion

** denotes statistical significance (by ANOVA, Newman-Keuls) from the 2 h SI post-irradiation group (PIRR)

† denotes statistical significance (by unpaired t-test) from DI ferrets within the same PIRR group

Table 19. Fractional excretion of Cl^- in perfused intestinal segments of drug-injected ferrets.

		Jejunum	Ileum
CONTROL			
P1	SI	92.0 ± 2.6 (3)	89.3 ± 3.8 (3)
	DI	96.4 ± 4.2 (5)	92.0 ± 2.1 (4)
P7	SI	91.7 ± 2.5 (3)	91.7 ± 0.6 (3)
	DI	94.2 ± 1.9 (5)	89.7 ± 3.3 (4)
2 h PIRR			
P1	SI	87.2 ± 2.9 (4)	82.7 ± 12.8 (3)
	DI	97.0 ± 3.4 (4)	95.3 ± 3.0 (6)
P7	SI	90.5 ± 5.3 (4)	88.5 ± 2.1 (2)
	DI	92.0 ± 7.9 (3)	95.6 ± 2.1 (5)
48 h PIRR			
P1	SI	102.7 ± 2.1 (4) ★ †	91.2 ± 4.1 (4)
	DI	96.3 ± 5.0 (3)	78.0 ± 8.7 (4)
P7	SI	103.2 ± 2.9 (4) ** †	92.0 ± 2.5 (4)
	DI	95.7 ± 6.9 (3)	82.2 ± 4.2 (4)

Values are expressed as percent mean ± SE for n of 4 or greater, ± SD for n of 3 or less. n values are indicated in brackets.

P1 = initial perfusate collected at t=0 min of 60 min perfusion

P7 = final perfusated collected at t=60 min of 60 min perfusion

★ denotes statistical significance (by ANOVA, Newman-Keuls) from the corresponding SI jejunal post-irradiation groups (PIRR)

** denotes statistical significance (by ANOVA, Newman-Keuls) from the corresponding group at 2 h PIRR

† denotest statistical significance (by unpaired t-test) from the corresponding ileal group

Table 20. Fractional excretion of K^+ in perfused intestinal segments of drug-injected ferrets.

		Jejunum	Ileum
CONTROL			
P1	SI	98.7 ± 6.4 (3)	96.3 ± 2.8 (3)
	DI	107.4 ± 7.1 (5)	95.0 ± 2.4 (4)
P7	SI	99.7 ± 3.1 (3)	99.7 ± 1.5 (3)
	DI	105.8 ± 5.7 (5)	94.2 ± 3.7 (4)
2 h PIRR			
P1	SI	97.5 ± 3.4 (4) †	93.7 ± 12.7 (3)
	DI	109.2 ± 1.3 (4)	105.3 ± 2.5 (6)
P7	SI	103.2 ± 5.4 (4)	103.0 ± 12.7 (2)
	DI	106.0 ± 0.0 (3)	106.0 ± 2.3 (5)
48 h PIRR			
P1	SI	106.7 ± 2.2 (4)	108.7 ± 7.2 (4)
	DI	111.0 ± 7.9 (3)	116.5 ± 10.3 (4)
P7	SI	105.7 ± 3.1 (4)	111.7 ± 7.8 (4)
	DI	111.0 ± 9.6 (3)	122.2 ± 6.5 (4) *

Values are expressed as percent mean ± SE for n of 4 or greater, ± SD for n of 3 or less. n values are indicated in brackets.

P1 = initial perfusate collected at t=0 min of 60 min perfusion

P7 = final perfusated collected at t=60 min of 60 min perfusion

* denotes statistical significance (by ANOVA, Newman-Keuls) from CONTROL group, P7 DI ileum.

† denotes statistical significance (by unpaired t-test) from DI ferrets within the same group

K^+ at 48 hours in the ileum from SI and DI ferrets (Table 20). In SI ferrets only 1 of 4, and in DI only 2 of 4 ferrets had a FE of K^+ > 120 %. Consequently in injected animals only ferrets in the DI 48 h PIRR group have a FE of K^+ that was significantly greater than in control DI ferrets.

Osmolality

Osmolality of the collected perfusates from both intestinal segments were unaffected by radiation exposure and by Granisetron pre-treatment (Table 21). Osmolality results are shown only for Phase 3. The results from Phase 2 were similar.

Protein

Phase 2:

Protein content was significantly elevated at 2 hours PIRR in the ileum of non-injected (NI) animals (Table 22). There were no significant differences between ileum and jejunum in NI animals.

Phase 3:

As there was no statistical difference in the protein content between NI and SI groups, these two groups were pooled. This pooled group, referred to as control injected (CI), was not different at any of the PIRR time points, from drug injected (DI) ferrets. Protein content of the CI groups was only significantly greater at 2

Table 21. Osmolality (mOsm/kg H_2O) of collected luminal perfusates.

		Jejunum	Ileum
CONTROL			
P1	CI	294 ± 1 (4)	292 ± 2 (4)
	DI	300 ± 6 (3)	289 ± 2 (2)
P7	CI	298 ± 2 (4)	295 ± 2 (4)
	DI	306 ± 8 (3)	294 ± 0 (2)
2 h PIRR			
P1	CI	290 ± 2 (4)	292 ± 4 (3)
	DI	292 ± 4 (4)	296 ± 2 (5)
P7	CI	299 ± 8 (3)	299 ± 7 (2)
	DI	297 ± 8 (3)	297 ± 2 (4)
48 h PIRR			
P1	CI	298 ± 6 (3)	294 ± 4 (3)
	DI	298 ± 3 (4)	293 ± 2 (5)
P7	CI	302 ± 10 (3)	301 ± 3 (3)
	DI	296 ± 5 (4)	299 ± 3 (5)

Values are expressed as mean ± SE for n of 4 or >, ± SD for n 3 or <.
n values are indicated in brackets.
CI = control injected (non-injected pooled with saline injected) ferrets.
DI = drug (BRL 43694) injected ferrets.
P1 = initial perfusate collected at t=0 min of 60 min perfusion
P7 = final perfusate collected at t=60 min of 60 min perfusion

Table 22. Protein concentration (μg/mL) of collected luminal perfusates.

	Jejunum	Ileum
CONTROL		
P1	46.9 ± 13.9 (6)	17.5 ± 8.8 (7)
P7	20.4 ± 12.7 (6)	9.7 ± 5.3 (7)
2 h PIRR		
P1	45.2 ± 10.7 (6)	68.9 ± 19.9 (7) *
P7	48.6 ± 7.5 (6)	62.4 ± 16.0 (7) *
24 h PIRR		
P1	26.8 ± 10.2 (5)	98.9 ± 56.0 (6)
P7	31.8 ± 15.8 (6)	37.6 ± 25.1 (6)
48 h PIRR		
P1	20.1 ± 8.6 (5)	25.1 ± 6.9 (5)
P7	16.8 ± 9.4 (5)	41.7 ± 12.3 (6)

Values are expressed as mean ± SE n values are indicated in brackets.
P1 = initial perfusate collected at t=0 min of 60 min perfusion
P7 = final perfusate collected at t=60 min of 60 min perfusion
* = significantly greater than the corresponding CONTROL ileal group

hours PIRR in the ileum (Table 23). In the control PIRR group, protein content was greater in the CI jejunum than in the CI ileum. Protein content was also greater in the DI 2 hour PIRR jejunal group than in the corresponding ileal group. However, protein content was significantly lower by P7 in the jejunum compared to the ileum in CI 48 hour PIRR ferrets (Table 23).

Hemoglobin

Although perfusates that were used in the final analysis were clear, suggesting the absence of blood, in order to confirm this, perfusates from three experiments were analyzed for hemoglobin (Hb) content. By visual inspection, some of the perfusates from these selected experiments were obviously contaminated with blood (consequently they were not used for final statistical analysis). The hemoglobin (Hb) concentration of these contaminated samples ranged from 0.04 mg/mL to 0.15 mg/mL. The perfusates that appeared clear, i.e. presumed blood-free, had a Hb concentration that ranged from 0.01 to 0.05 mg/mL. Therefore even samples that appear blood-free, have some hemoglobin in them. However, by regression analysis, Hb concentration was not related to the calculated clearance of ^{51}Cr-EDTA.

Tissue 5-HT and 5-HIAA

Serotonin (5-HT) and its metabolite 5-hydroxyindoleacetic acid (5-HIAA) were assayed in the stomach, jejunum, ileum, and colon of irradiated ferrets (Table 24), in order to test the hypothesis that radiation exposure stimulates the release of

Table 23. Effects of Granisetron on luminal protein concentration (μg/mL) of collected luminal perfusates.

		Jejunum	Ileum
CONTROL			
P1	CI	73.8 ± 20.00 (10) †	19.2 ± 5.8 (11)
	DI	60.0 ± 21.0 (5)	46.9 ± 46.9 (4)
P7	CI	40.1 ± 16.0 (10)	10.8 ± 3.9 (11)
	DI	30.1 ± 11.2 (4)	0.0 ± 0.0 (3)
2 h PIRR			
P1	CI	43.6 ± 10.3 (11)	61.5 ± 15.2 (10) *
	DI	50.6 ± 9.5 (4)	49.8 ± 16.5 (5)
P7	CI	49.0 ± 12.3 (11)	95.1 ± 39.9 (9) **
	DI	59.3 ± 22.9 (3) †	8.1 ± 4.9 (4)
48 h PIRR			
P1	CI	24.1 ± 9.6 (9)	19.6 ± 5.2 (8)
	DI	27.4 ± 17.2 (4)	48.8 ± 31.1 (5)
P7	CI	14.0 ± 6.2 (9) †	43.6 ± 10.7 (8)
	DI	44.6 ± 22.2 (4)	28.6 ± 26.5 (5)

Values are expressed as mean ± SE for n of 4 or >, ± SD for n 3 or <.
n values are indicated in brackets.
CI = control injected (non-injected pooled with saline injected) ferrets.
DI = drug (BRL 43694) injected ferrets.
P1 = initial perfusate collected at t=0 min of 60 min perfusion
P7 = final perfusate collected at t=60 min of 60 min perfusion
* = significantly greater than the P1 CI CONTROL and 48 h PIRR ileal groups.
** = significantly greater than the PIRR CI CONTROL ileal group
† = significantly different from the corresponding group in the ileum

Table 24. 5-HT and 5-HIAA concentration in the gut of irradiated ferrets.

Group	Tissue	5-HT	5-HIAA
Control	Stomach	4.3 ± 0.9 (7)	53.4 ± 23.0 (7)
	Jejunum	3.8 ± 0.3 (7)	175.7 ± 55.5 (7)
	Ileum	3.1 ± 0.4 (7)	260.2 ± 72.8 (7)
	Colon	6.2 ± 0.9 (7) †	131.4 ± 47.6 (7)
2 h	Stomach	2.4 ± 0.6 (6)	39.7 ± 21.4 (6)
	Jejunum	2.8 ± 0.3 (6)	128.4 ± 45.2 (6)
	Ileum	2.4 ± 0.2 (6)	71.2 ± 29.5 (6)
	Colon	5.2 ± 1.2 (6) †	82.8 ± 30.3 (6)
24 h	Stomach	5.3 ± 2.0 (6)	74.5 ± 27.6 (6)
	Jejunum	3.4 ± 0.4 (6)	189.1 ± 86.9 (6)
	Ileum	2.3 ± 0.3 (6)	69.4 ± 18.8 (6)
	Colon	7.0 ± 1.0 (6) ‡	174.6 ± 54.2 (6)
48 h	Stomach	4.9 ± 1.4 (6)	62.9 ± 28.1 (6)
	Jejunum	7.2 ± 1.4 (6) ⋆	209.8 ± 69.9 (6)
	Ileum	3.5 ± 0.2 (6) *	95.7 ± 68.0 (6)
	Colon	7.4 ± 0.9 (6)	85.6 ± 14.2 (6)

Values are expressed as mean ± SE, n values are indicated in brackets.
5-HT is expressed as μg of amine per gram tissue, 5-HIAA is expressed as ng of amine per gram tissue
† = statistically greater than other tissues in the same PIRR group
‡ = statistically greater than the jejunum and ileum in the same PIRR group
⋆ = statistically greater from all other PIRR time points
* = statistically greater from 2 and 24 hours PIRR groups

serotonin from the ferret gastrointestinal tract. At 48 hours PIRR, the 5-HT content was significantly greater in the jejunum (than all other PIRR groups) and in the ileum (than the 2 and 24 hour PIRR groups). Among the tissues that were assayed, the colon had the highest 5-HT content. Radiation exposure did not have any effect on tissue levels of serotonin's metabolite, 5-HIAA.

Other Findings

Bile-Contaminated Perfusates:

In control and 2 hour PIRR experiments, fluid was rarely collected from the drainage cannulae. However in experiments from 24 and 48 hour PIRR ferrets (particularly in the 48 hour PIRR group), usually 0.1 to 0.5 mL of bilious fluid was collected from both the jejunal and ileal drainage cannulae. As well, intestinal perfusates from 24 and 48 hour PIRR experiments were frequently tinged a light to a dark yellow-green. These subjective observations suggested the presence of an unusually high amount of bile (hypersecreted or malabsorbed) in the intestinal lumen.

DISCUSSION

Radiotherapy patients and radiation accident victims may present with radiation-induced diarrhea in the first hours to days following irradiation (Anno et al., 1989). This side-effect, for both physiological and psychological reasons, can result in an alteration of the radiation protocol so that the radiation-induced diarrhea is minimized. Consequently, the therapeutic benefits of radiotherapy may also be affected. This project was designed to investigate the role of intestinal permeability as a causal mechanism of radiation-induced diarrhea. The post-irradiation time points that were examined in these experiments were selected to permit comparisons between the "early" (2 hours PIRR) and "late" (24 and 48 hours PIRR) effects of a therapeutic radiation protocol. Ongoing histological studies in our laboratory of irradiated ferrets demonstrated that with the radiation protocol used in these experiments, there is minimal morphological damage in the ferret intestine following irradiation (at either 2, 24, or 48 hours PIRR) (unpublished observations). Although villar height and intestinal mucosal surface area were reduced by 48 hours PIRR, the epithelium was intact. Therefore, effects investigated in this thesis are more related to pathophysiology than to histopathology.

Prodromal Effects of Radiation Exposure

All irradiated ferrets (not treated with Granisetron) retched and vomited in response to 5 Gy whole-body irradiation. Both retching and vomiting had similar

profiles in terms of time to first response, time of peak response, and time of diminution of response. It was frequently observed that vomiting often concluded the retching episodes, supporting the concept that retching is simply a priming mechanism for vomiting (McCarthy and Borison, 1974).

Andrews and Hawthorn (1987) reported that abdominal vagotomy almost totally abolished vomiting by ferrets during the first 30 minutes post-irradiation (8 Gy, whole body X-irradiation). However, abdominal vagotomy was without effect on the vomiting responses that occurred during the 30 minute to 60 minute PIRR phase. Retching responses by the ferrets were similarly affected. Andrews and Hawthorn (1987) thus proposed that radiation-induced vomiting could be divided into a vagally-dependent (0 to 30 minutes PIRR) and a vagally-independent phase (30 to 90 minutes PIRR). The results of the present project demonstrate that the ferrets exhibited minimal vomiting and retching episodes more than 40 minutes post-irradiation with a dose of 5 Gy. This suggests that the emetic episodes that were recorded were mediated by the vagus and that the vagally-independent phase reported by Andrews and Hawthorn (1987) was absent in this protocol. Worthy of note is that when Davis (1988) tested the ferret vomiting responses to 2 Gy irradiation, only the vagally-dependent phase was observed. These results suggest that the dose of 5 Gy that was used in the present experiments was more similar to the 2 Gy than to the 8 Gy used by Davis (1988).

The ferret has been the primary animal model used to develop the new class of serotonin type 3 receptor ($5\text{-}HT_3$) antagonist anti-emetics (Miner et al., 1987).

These drugs have proved to be potent and specific, and have implicated serotonin as an important mediator of the emetic response. Andrews et al. (1988) have proposed that radiation, through some as yet unknown mechanism, causes the release of serotonin from enterochromaffin cells. Serotonin would thus be released in close proximity to nerve endings (enteric interneurons, vagal afferent neurons) located in the mucosa, bind to its specific receptor, and given sufficient stimulus, elicit vomiting.

Evidence supporting serotonin's involvement in emesis comes from recent studies by Cubeddu et al. (1990). They found that chemotherapy patients (treated with cisplatin) had a significant increase in the urinary excretion of 5-HIAA (the metabolite of 5-HT). As well, the rise in 5-HIAA excretion paralleled the onset and development of emesis in the patients. In the present experiments, the tissue assay for 5-HIAA could not be adapted for urine measurements, therefore confirmation of the results of Cubeddu et al. (1990) could not be obtained in the irradiated ferret. However, tissue analysis suggested that at 2 and 24 hours post-irradiation, serotonin content in the ileum tended to be lower than in control ferrets. Although not statistically significant, this trend suggested that radiation exposure may in fact cause release of serotonin from gut tissues, confirming the results of Matsuoka et al. (1962); Penttila et al. (1975); and Kocmierska-Grodzka et al. (1976). The fact that the 5-HT_3 antagonist Granisetron was effective in abolishing radiation-induced emesis also suggested that serotonin was released post-irradiation.

Since vomiting is proposed to be mediated by 5-HT_3 receptors, Granisetron was injected *pre-irradiation*. By blocking the 5-HT_3 receptors before serotonin can

bind to them, radiation-induced emesis, and possibly other responses (as yet unknown) mediated by these receptors, could be minimized or abolished. Radiation-induced retching and vomiting were completely abolished in two thirds (4/6) of Granisetron pre-treated ferrets. In the other two ferrets, the frequency and severity of radiation-induced retching and vomiting were significantly reduced compared to non-injected ferrets. These data support Granisetron's action as an anti-emetic drug and its potential therapeutic benefit to radiotherapy patients and suggest that the dose of Granisetron (0.4 mg/kg) was appropriate for the amount of emetic stimulus (5 Gy irradiation) used in these experiments. Since Granisetron is a highly specific 5-HT_3 receptor antagonist, these data further support the role of serotonin in radiation-induced emesis.

Recent evidence (Leslie et al., 1990) suggests that Granisetron may elicit its anti-emetic action by binding to centrally-located 5-HT_3 receptors. Binding of the 5-HT_3 antagonist Granisetron in the medulla oblongata of the ferret brain is highly localized to the dorsal vagal complex. The most concentrated binding is located in the dorsomedial portion of the nucleus of the solitary tract, less so in the area postrema and dorsal motor nucleus of the vagus (Leslie et al., 1990). Because the dorsomedial portion of the nucleus of the solitary tract receives the largest number of vagal afferent fibers from the stomach, it is plausible to assume that the Granisetron binding sites are located on gastric vagal afferent fiber terminals. These vagal afferent fibers relay information regarding the activity of the muscular wall of the gut (Andrews et al., 1986), and the chemical nature of the luminal contents

(Grundy, 1988). This afferent information concerns visceral sensations including irritation, the extrinsic reflex control of gut function, and for the generation of responses such as the vomiting reflex. Thus, 5-HT_3 receptors are possibly involved in modulating these effects (Leslie et al., 1990). However, simply because it is documented that the anti-emetic, Granisetron binds to centrally located 5-HT_3 receptors, it is not proved that this is the only, or predominant, site for anti-emetic activity. It has also been hypothesized, that emetic stimuli released by radiation or cytotoxic drugs, may activate 5-HT_3 receptors located on peripheral termini of vagal afferents (Andrews et al., 1988). The binding profile of Granisetron to peripheral 5-HT_3 receptors has yet to be reported in the literature. Thus at the present time it is undetermined what is the actual site of the anti-emetic action of Granisetron.

Bermudez et al. (1988), induced emesis by irradiating ferrets with soft X-rays (greater than 1000 Roentgens[4]). The emetic response was comparable to the emesis data obtained in this thesis. Bermudez et al. (1988) found that Granisetron administered i.v. (0.5 mg/kg) 5 minutes before radiation exposure prevented vomiting in all four animals tested. Further, emesis could be stopped if Granisetron (same dose) was injected during the peak of an emetic period (i.e. post-irradiation). It was also interesting that when the Granisetron was administered with the above protocols, it dramatically reduced the incidence of the various behavioral cues for nausea (Bermudez et al., 1988). These authors suggested that the 5-HT_3 antagonist

[4]Roentgens (R) are units of radiation exposure, and are related to the ability of X-rays to ionize air (Hall, 1988).

may be an effective nausea treatment for cancer patients. In the present study, it appeared that Granisetron pretreatment did reduce the number of behavioral cues for nausea. However, since these cues were only observed to precede retching or vomiting episodes, their reduction may also be related to the decreased frequency of retching and vomiting.

If vomiting can be considered as a defence mechanism for clearing the upper gut of potentially toxic substances, then diarrhea is the defence mechanism for the lower gut (Read, 1989). Radiation-induced diarrhea could result from changes in intestinal motility, altered active cellular transport mechanisms, or simply from leakage of fluid and electrolytes caused by an altered mucosal permeability (Gunter-Smith, 1986). The bowel movements experienced by the irradiated ferrets during the first 20 to 30 minutes post-irradiation were characterized as normal, though the rate of defecation was higher than in the sham-irradiated group. After 30 minutes PIRR, the rate of defecation was still high among irradiated ferrets, and the feces was a mucoid diarrhea. Thus irradiated ferrets had an abnormally high rate of defecation, suggesting that normal intestinal motility patterns were somehow disrupted by the radiation exposure.

The effects of radiation exposure on intestinal motility have been analyzed by other investigators. Fractionated irradiation of the abdomen (9 x 2.5 Gy) significantly increased the frequency of giant migrating contractions and retrograde giant contractions in the dog (Otterson et al., 1988). This abnormal motor pattern may have been responsible for the radiation-induced diarrhea which occurred as early as

after the first dose of radiation (Otterson et al., 1988). Recent studies have reported that 10 Gy whole-body irradiation accelerated pellet expulsion from the guinea-pig colon (Moore, 1990, unpublished observations). The mechanism of radiation-induced alterations in intestinal motility is not known, but serotonin may be a possible mediator.

Serotonin can induce disruptions in intestinal motility. Serotonin released by mast cell degranulation has been shown to inhibit intestinal motility and abolish the migrating motor complex in fasted rats. This disruption in intestinal motility could be reversed by pretreatment with 5-HT_1 and 5-HT_3 receptor antagonists (Bueno et al., 1991). In the rabbit, 5-HT stimulated colonic circular muscle, (a direct effect on the muscle 5-HT_1 receptors and indirectly through enteric nerves), with greater efficiency than longitudinal muscle (Ng et al., 1991). Clinical studies with the 5-HT_3 antagonist Ondansetron (Zofran®, GR38032F) have demonstrated that this drug can result in constipation (thought to be related to an increase in colonic transit time) as a side-effect to anti-emetic therapy (Smith, 1989), and may be an effective treatment for diarrhea predominant irritable bowel syndrome (Steadman et al., 1990).

In these experiments, pretreatment with the 5-HT_3 antagonist Granisetron significantly reduced the frequency of diarrhea at the time of the peak diarrheal response. The total number of bowel movements during the first 2 hours post-irradiation however was not significantly different between non-injected and Granisetron pre-treated ferrets. This latter finding may be explained by the fact that radiation-induced alterations in intestinal motility may be partially mediated via 5-

HT_1 receptors (Bueno et al. 1991, Ng et al., 1991), to which Granisetron has no reported antagonistic action.

The increased rate of defecation following irradiation suggested that hypermotility contributed to the diarrhea. Decreased transit time however results in less intestinal absorption, and therefore the excreted product of hypermotility is normally watery (Binder, 1989). Therefore, because the diarrhea was mucoid and not watery in consistency, it is possible that altered intestinal secretion of mucus was involved (Binder, 1989). Whereas the villus goblet cells are the primary source of the normal mucous blanket, the crypt goblet cells are the major contributors to the production of an emergency layer of mucus. This latter response occurs during acute cholinergic stimulation (Kemper and Specian, 1991). Radiation has been shown to accentuate cholinergic-mediated motility events in the intestine (Conrad, 1951), and perhaps in these experiments, cholinergic transmission was affected by radiation exposure.

Qualitative and subjective observation of the consistency of the excreted diarrhea in pre-treated ferrets, indicated that Granisetron did offer some therapeutic benefit concerning the radiation-induced diarrhea: the diarrhea was less mucoid, and there was a decrease in excreted volume, suggesting that Granisetron had an anti-secretory effect. Another 5-HT_3 antagonist (ICS 205-930, Sandoz) has been reported to be effective in controlling the secretory diarrhea associated with the carcinoid syndrome (Anderson et al., 1987). These results suggest that the radiation-induced diarrhea may be a consequence of both altered motility and secretion. Therefore,

Granisetron appears to be not only an effective anti-emetic, but may also offer therapeutic benefit in radiation-induced diarrhea.

In this project, neither hematocrit, urine Na^+ and K^+, nor plasma electrolytes, were affected by radiation exposure. Severe vomiting and diarrhea can cause reductions in plasma volume. In such circumstances, compensation is achieved by the absorption of fluid and electrolytes first from the interstitial space and then from the intracellular space. Severe redistributions in body fluids, can result in hemoconcentration and hyponatremia (Geraci et al., 1988). The results of the present experiments indicate that there was no significant decrease in ferret plasma volume following irradiation with 5 Gy. Most radiotherapy patients receive medical intervention before vomiting and diarrhea can result in these severe redistributions of body fluids. Davis (1988) reported that a radiation dose of 8 Gy gamma irradiation, caused ferrets to have vomiting and diarrhea (often bloody), that lasted for several hours post-irradiation. Compared to those studies, the prodromal results reported in this thesis are more representative of the prodromata experienced by some radiotherapy patients. Therefore, these data indicate that vomiting and diarrhea in this project were not severe, and support the argument that the radiation protocol that was selected for these experiments was physiologically relevant to the condition of the radiotherapy patient.

Fluid Flux

In these experiments, fluid absorption in the ileum was reduced to almost zero at 2 hours post-irradiation. This decrease was only statistically significant from the other PIRR groups at one perfusion time point ("P7") in the Granisetron pre-treated ferrets. Nevertheless, this reduced fluid absorption was a constant feature of all 2 hour PIRR experiments, and may have been related to the radiation-induced

diarrhea. Biochemical analysis of the diarrhea was not attempted, but its appearance suggested that it consisted predominantly of mucus. Goblet cells synthesize and secrete high-molecular weight glycoproteins known as mucins. Once secreted, the mucins hydrate and gel, generating a protective mucus "blanket" overlying the epithelial surface. Other components within the mucus gel are water, electrolytes, sloughed epithelial cells, and secreted immunoglobulins (Specian and Oliver, 1991). When the ileal segments from 2 hour irradiated ferrets were prepared for cannulation, it was observed that the initial perfusates were cloudy and that they had a significantly greater protein content than in control-irradiated ferrets. It is possible that the secreted mucus may have retarded normal fluid absorption at 2 hours post-irradiation in the ileum, by increasing the thickness of the unstirred water layer, a barrier to normal intestinal permeation (Csaky, 1984). Increased resistance of the unstirred water layer has been previously speculated to be involved in malabsorption syndromes (Westergaard and Dietschy, 1987).

In the present experiments, the time required for surgery, equilibration and baseline data collection, dictated that 2 hours PIRR was the earliest possible time to collect luminal perfusates for experimental analyses. However, retching, vomiting, and diarrhea rarely occurred in un-operated animals at this time. Therefore direct correlation analyses could not be made between permeability changes and prodromal events. It is difficult to speculate to what extent the prodromal effects contributed to the reduced fluid absorption and other permeability changes. It should be recalled that the permeability studies in 2 hour PIRR ferrets were accomplished in animals

anesthetized immediately after irradiation, and that they did not experience the prodromal effects of irradiation.

Fractional Excretion of Electrolytes

In this protocol, there was no net movement of Na^+ and Cl^- across the intestinal mucosa. Normally, the permeability characteristics of the small intestine are such that both Na^+ and Cl^- are absorbed from the intestinal lumen: isosmotically in the jejunum, and against a concentration gradient in the ileum (Powell, 1987). Bidirectional movement of electrolytes across the intestinal wall is very rapid (Binder, 1989). Considering that the collected perfusates were analyzed for Na^+ and Cl^- in an already physiological solution (the BES), detection of any change in their concentration in the collected perfusates, may only occur if the net movement of Na^+ and Cl^- across the intestinal wall was relatively high. It has been suggested that normal, basal fluxes of the electrolytes cannot be determined by FE measurements across the *in situ* perfused intestinal segment, and perhaps *in vitro* experiments (Ussing chambers) would be more informative regarding electrolyte flux post-irradiation (Greenwood, personal communication). However, Curran et al. (1960) used a similar intestinal perfusion technique to that used in the present experiments (*in situ* perfused intestinal segments) and reported that there was a significant reduction in Na^+ and fluid absorption in the rat distal ileum, but not until 4 days following high dose abdominal X-irradiation (25 to 30 Gy). These investigators also noted that there was a noticable, but not significant reduction in Na^+ and fluid

absorption as early as 13 hours post-irradiation. This observation of "early" inhibition of active transport could not be explained by epithelial cell death and the authors suggested that radiation exposure had a direct effect on the active transport process (Curran et al., 1960). Five Gy whole-body irradiation was reported not to have any significant effect on rabbit fluid and electrolyte flux studies in Ussing Chambers (Gunter-Smith, 1986). It was not until this investigator irradiated the rabbits with a dose of 7.5 Gy, that active secretion of fluid and chloride was observed (Gunter-Smith, 1986). However, both these latter two experiments (Curran et al., 1960 and Gunter-Smith, 1986) used an animal model other than the ferret and there are considerable differences in electrolyte and fluid permeability between species (Powell, 1987). As well, the time to onset of radiation-induced diarrhea varies between species: two to three days post-irradiation for rats and rabbits, but within a few hours for both the ferret and man. Since the present experiments were the first to examine the effects of irradiation on ferret intestinal permeability, comparisons to other projects using the ferret as an animal model cannot be made.

Numerous studies have documented the effects of serotonin on electrolyte transport (Kisloff and Moore, 1976; Donowitz et al., 1977; Donowitz et al., 1980; Hardcastle et al., 1981). The serotonin receptor(s) that mediates these transport changes is/are unknown. Therefore, the effect of a 5-HT_3 antagonist (Granisetron) was assessed in the present experiments. Pre-treatment with Granisetron was without effect on any parameter of intestinal permeability: fluid flux, fractional excretion of electrolytes, permeation of ^{51}Cr-EDTA. As previously mentioned, possible binding

sites of Granisetron are the abdominal vagal afferent fibers (Andrews et al., 1988). Abdominal vagotomy significantly reduces radiation-induced emesis in the ferret (Andrews and Hawthorn, 1987), an effect mimicked by pre-treatment with Granisetron. Thus, Granisetron has been said to cause a chemical vagotomy and this explains, at least in part, its anti-emetic properties (Davis, 1988). Therefore, unless the factors that were responsible for intestinal permeability mediated their effects via a similar afferent/efferent vagal pathway, they might be unaffected by Granisetron treatment. It was surprising that fluid flux was not affected by Granisetron pre-treatment, as the dorsal motor nucleus of the vagus (DMNV) and the nucleus tractus solitarius (NTS) are the central regulatory sites for intestinal fluid absorption (Martin et al., 1989). Thus experiments with other doses of Granisetron should be considered.

The acid-base status of animals should be monitored during experiments of intestinal permeation, as many of the intestinal transport mechanisms in the ileum and colon are affected by changes in these parameters (Donowitz and Welsh, 1987, DeSoignie and Sellin, 1990). Respiratory acidosis can increase Na^+ and Cl^- absorption, and decrease HCO_3^- secretion. These changes in electrolyte transport may be due to intracellular availability of H^+ for the Na^+-H^+/Cl^--HCO_3^- exchange system (Powell, 1987). In this protocol all ferrets were diagnosed with respiratory acidosis, presumably due to the effects of surgery and anesthesia (Booth and McDonald, 1988) yet in most ferrets there was no detectable absorption of either Na^+ or Cl^-. This again may be attributed to species differences, as the work of

Donowitz and Welsh (1987) and DeSoignie and Sellin (1990) is based on experiments on animals other than ferrets. Some of the saline-injected ferrets of phase 3 had a significantly greater absorption of these electrolytes than in the non-injected ferrets of phase 2. This could not be attributed to the respiratory acidosis as the ferrets in both phases had the same level of acid-base disturbance. The cause of this placebo effect in phase 3 is undetermined.

Unlike Na^+ and Cl^-, net movement of K^+ was detected in this protocol. The FE of K^+ suggested that potassium was secreted into the ileum at 48 hours PIRR. The intracellular concentration of potassium is relatively high (approximately 140 mEq/L). Therefore, a possible source of the luminal potassium was from sloughing of surface epithelial cells. However, the protein content at 48 hours PIRR was not significantly greater than in control animals, suggesting that there was minimal cell loss. This suggested that there was an abnormal potassium permeability in the ileum at 48 hours PIRR. Although normal ileal enterocytes are not known to have any apical permeability to potassium, it is possible that (as a consequence of radiation exposure), membrane defects occurred, and that these resulted in secretion of intracellular potassium. Such membrane effects could include changes in hydroxy fatty acids, increased intracellular cAMP and Ca^{2+} levels, as well as villus adenomas and intestinal inflammation (Powell, 1987). Wills (1970) has proposed three possible mechanisms for radiation-induced membrane injury. Radiation exposure may: 1) alter lipid conformation such that lipids are susceptible to autoxidative processes; 2) destroy antioxidants (primarily vitamin E); 3) initiate membrane peroxidation by

altering some membrane component so that it may become an effective catalyst for peroxidative processes. Abdominal irradiation has been shown to increase the phospholipid content of intestinal brush-border membranes in the rat (Keelan et al., 1986). Other postulated mechanisms involved in radiation-induced altered transport are changes in the fatty acyl constituents of the intestinal brush-border membrane, as well as lipid peroxidation of this membrane (Thomson et al., 1989). Thomson et al., (1989) also reported that at three days post-irradiation (6 Gy, abdominal), the villi of both rat jejunum and ileum expressed membrane transport molecules at an earlier age, and at a position much closer to the base of the villi. Therefore, even though there were a lower number of enterocytes (the villi are shorter), as an adaptive response to irradiation, a greater proportion of the enterocytes were involved in transport (Thomson et al., 1989). It is possible, therefore, that altered membrane function may have also occurred in the present experiments (48 hours PIRR in the ileum).

Radiation-Induced Alterations of ^{51}Cr-EDTA Permeation

The increased permeation of ^{51}Cr-EDTA observed at 2 hours and 48 hours post-irradiation, occurred before substantial morphological alterations were observed by light microscopy (Harding, unpublished observations). Alterations in the permeation of ^{51}Cr-EDTA are believed to reflect irregularities in mucosal morphology before they are revealed by histological examination (Bjarnason et al., 1983; Elia et al., 1987). At 48 hours post-irradiation, both the jejunum and ileum

were absorbing fluid at the same rate as in the control animals, suggesting that the mucosa was functional. Therefore, it is most possible that some "physiological" mechanism was responsible for the increased secretion of ^{51}Cr-EDTA and that a histopathological explanation (broken or incomplete mucosal barrier) is less likely.

Serotonin tissue levels determined in control ferrets corresponded to unpublished results of Andrews' (personal communication). Confirmation of Andrews's results validates the suitability of the serotonin assay used in these experiments. At 48 hours PIRR, there was a statistical increase in serotonin content in the jejunum. A post-irradiation increase in serotonin content has been previously reported in the rat small intestine (Ershoff and Gal, 1962). The increase in serotonin content may be caused by an increase in serotonin synthesis, or an impairment in its release from cellular stores. The changes in serotonin tissue content however were not related to the permeability changes that were observed at different times post-irradiation, nor to regional differences in permeability.

The cause of the increased permeation of ^{51}Cr-EDTA at 2 hours PIRR in the jejunum and ileum is not known. Nor is it known why permeation was normal at 24 hours PIRR, and why only the ileum and not the jejunum exhibited the enhanced permeation of ^{51}Cr-EDTA at 48 hours PIRR. The counts of ^{51}Cr in the luminal perfusates were not related to the Hb concentration of the perfusates, reaffirming that the measured counts (of chromium) were not simply due to the presence of blood, but rather represented an actual permeation of ^{51}Cr-EDTA. The increased permeation may be a result of changes in several possible physiological factors,

including intestinal blood flow, vascular permeability, malabsorption of bile acids, and inflammatory reactions. These are discussed below.

Blood Flow:

No quantitative techniques were used to measure intestinal blood flow in these experiments. However, there was no macroscopic evidence of hyperemia or ischemia. These subjective observations do not exclude the possibility that there were changes in blood flow, perhaps attributed to radiation exposure or surgical manipulation. Radiation exposure has been documented to affect blood flow, but unfortunately the data assessing these changes are limited to supralethal doses of whole-body irradiation (80 to 100 Gy). One study found that there was a significant decrease in cerebral blood flow (Cockerham et al., 1986), while another study examining intestinal blood flow, reported that there was a significant increase in canine submucosal blood flow (Cockerham et al., 1984) at 90 minutes post-irradiation. The relevance of these studies to this protocol, which used a therapeutically relevant radiation dose, is uncertain. It is certainly possible that radiation exposure at the dosage used in this protocol (5 Gy) was followed by release of some vasoactive agents (for example, histamine, serotonin, norepinephrine, prostaglandins, and leukotrienes) (Timmermans and Gerber, 1980).

Hypoxic tissues are more resistant to radiation-induced tissue damage (Earnest and Trier, 1989). This property is related to the involvement of oxygen in the production of free radicals, which are mediators of radiation-induced tissue damage

(Earnest and Trier, 1989). Post-irradiation free radical generation is an acute event which may be related to the permeation changes seen at 2 hours PIRR. The events would not be evident at 24 hours, and this perhaps explains the normal values seen in all tissues at this time.

Free radical generation is not a likely explanation for the large increase in permeation seen at 48 hours PIRR in the ileum. The fact that there was no permeation change in the jejunum at 48 hours PIRR supports the contention that a region specific effect is involved. With the recent development of laser-Doppler flowmetry, blood flow can now be measured instantaneously and continuously (DiResta et al., 1987). Such a technique is ideally suited for investigating the effects of irradiation on intestinal blood flow, and will allow correlation analyses to be made between intestinal blood flow and intestinal permeability changes, within and between gut regions.

Vascular Permeability:

Although the vascular endothelium does not normally represent a physical barrier to ^{51}Cr-EDTA permeation (Nylander et al., 1989), it is possible that upon radiation exposure, changes in vascular permeability might alter intestinal permeation of ^{51}Cr-EDTA. Vascular corrosion casts, and light and transmission electron microscopy studies of blood vessels from rat duodenal villi 3 days post-X-irradiation (whole-body, 10 Gy) revealed that vessels became tortuous, vertical inter-capillary distance was decreased, capillary lumen diameter was increased, the endothelium was

irregular, and that there was evidence of plasma leakage (Abbas et al., 1990). An increase in intestinal vascular permeability (as demonstrated by leakage of trypan blue dye) was demonstrated in X-irradiated (abdominal, 15 Gy) rats at 24, 48, and 72 hours post-irradiation. Histamine was implicated as the mediator of vascular damage at 24 hours PIRR (Willoughby, 1960). Buell and Harding (1989) have also demonstrated an increase in microvascular permeability in the irradiated rat. Such experiments have yet to be done in the ferret.

Bile:

In these experiments, the luminal perfusates of both the jejunum and ileum at 24 hours, but more frequently from 48 hour PIRR experiments, typically exhibited a variable intensity of yellow colour. The feces of 48 hour PIRR animals were also pigmented a dark green. These observations suggest that bile acids were prominent in the lumen post-irradiation, perhaps because of increased bile salt synthesis, hypersecretion of bile, or bile malabsorption. Normally bile acids are absorbed with greater than 90 % efficiency in the small intestine, predominantly via active Na^+ dependent transport in the terminal ileum. Disease or resection of this segment frequently causes bile acid malabsorption and subsequent diarrhea (van Tilburg et al., 1990). Abdominal irradiation does affect the intestinal permeability of bile acids in the rat. Cheeseman et al. (1984), and Mulholland et al. (1984) have reported that luminal bile acids can enhance the small-bowel injury observed in radiation enteritis. Therefore it is possible that the permeability changes that were observed in the ileum at 48 hours PIRR may have been due to the presence of an inordinate amount of

bile acids. It would be interesting to repeat these experiments using a luminal perfusing solution with the addition of a known amount of bile salt, and observe if it would further alter the intestinal permeability.

Inflammation:

In control-irradiated ferrets, polymorphonucleocytes (PMN) comprised roughly 50 % of the total WBC count, and lymphocytes roughly 30 %. By 2 hours post-irradiation, there was more than an 80 % decrease in the total number of PMNs in the peripheral circulation. Buell and Harding (1989) have reported that within the first few hours post-irradiation there was an emigration of PMNs (from the peripheral circulation) into the mucosa of the rat jejunum and ileum, where they may have contributed to local inflammatory reactions. Although in the present experiments, histological sections of ferret intestine were not stained for neutrophils, perhaps the decrease in peripheral PMNs was also related to their emigration into the intestinal mucosa, as occurred in the rat experiments of Buell and Harding, (1989). Radiation enteritis and inflammatory bowel disease are both associated with large numbers of PMNs infiltrating the mucosa. PMNs can be stimulated to produce and release superoxide and hydrogen peroxide (H_2O_2). As well, activated PMNs secrete myeloperoxidase which catalyses the oxidation of chloride by H_2O_2 to yield hypochlorous acid (HOCl). All of these products can be cytotoxic to a variety of cell types, and may be involved in enhanced mucosal permeability associated with acute inflammation of the bowel (Milks et al., 1986; Buell and Harding, 1989;

Grisham et al., 1990; Killackey and Killackey, 1990). ^{51}Cr-EDTA intestinal permeation has previously been reported to increase as the degree of intestinal inflammation increases (Bjarnason et al., 1986; Jenkins et al., 1987). This effect can be reversed by intraluminal adminstration of misoprostol, an analog of prostaglandin E_1 (Bjarnason et al., 1989; Miller et al., 1991).

Lymphocytes in the peripheral circulation of the ferret were significantly reduced at all PIRR time points. By 24 and 48 hours PIRR lymphocytes were barely detectable in the peripheral circulation. This represents a certain compromise to immune responses and could make the ferrets more susceptible to post-irradiation infections. At present it is unknown if like PMNs, lymphocytes emigrate from the circulation and permeate the intestinal mucosa. In patients with coeliac disease, which is characterized by intestinal inflammation, there is an increase in intraepithelial lymphocyte count in the intestinal mucosa. Separate studies have found a significant correlation between the increased intraepithelial lymphocyte count and increased mucosal permeability to ^{51}Cr-EDTA (Bjarnason et al., 1983) and to sugars (Strobel et al., 1984). However, this mechanism of altered intestinal permeability is not a likely explanation for the effects observed here since numerous studies have demonstrated that the mature lymphocyte is more sensitive to radiation-induced death than any other cell type.

These studies and the present results suggest that the increased mucosal permeation of ^{51}Cr-EDTA that was observed here may be related, at least in part, to radiation-induced intestinal inflammation. Future studies could be directed at

quantification of inflammatory mediators (for example, leukotrienes, prostaglandins, and thromboxanes) in ferret gastrointestinal tissue at the post-irradiation times used in these experiments. This would give an estimate of the degree of intestinal inflammation that occurred in these animals post-irradiation, and determine if the increased permeation of ^{51}Cr-EDTA was related to intestinal inflammation.

Regional Differences in ^{51}Cr-EDTA Permeation

No difference was observed in the ^{51}Cr-EDTA clearance between the distal ileum and the jejunum in control irradiated ferrets. There was no regional difference (between jejunum and ileum) in ^{51}Cr-EDTA permeation at 2 hours PIRR, nor at 24 hours PIRR. Both tissues had a similar increase in ^{51}Cr-EDTA permeation at 2 hours PIRR (although only statistically significant in the jejunum), and a similar return to control values at 24 hours PIRR. It was not until 48 hours post-irradiation that large regional differences in ^{51}Cr-EDTA permeation became apparent. Whereas in the ileum there was a significant increase (10 times control) in ^{51}Cr-EDTA clearance, in the jejunum at 48 hours PIRR there was no statistical change from control values. The different results between jejunum and ileum cannot be explained on the basis of delivered dose, as the dosimetry experiments confirmed that all gut tissues were exposed to the same amount of radiation (5 Gy).

It had been hypothesized based on the work of Fordtran et al., (1965) and Loehry et al. (1973) that the jejunum would have a greater permeability than the

ileum, both in the control and irradiated states. Fordtran et al. (1965) expanded Hober and Hober's (1937) original idea that the membranes of the intestinal mucosa were perforated with water-filled pores through which small molecules can diffuse. In order to simplify the pore theory, the intestinal barrier was considered as a single membrane perforated by pores of uniform dimensions. This allowed an effective pore radius of the intestine to be calculated. Using this model, it was conceptually determined that the effective pore radius of the jejunum was twice as great as that in the ileum. Powell (1987) has reported that the average pore radius of jejunum is 0.8 nm, while it is only 0.3 nm for the ileum. Reflection coefficients have also been calculated for substances (mannitol, NaCl, urea, erythritol) placed in the lumen of the jejunum and ileum. The reflection coefficient values for all of the solutes were higher in the ileum than in the jejunum, further supporting the concept that the jejunum has a greater basal permeability than the ileum (Fordtran et al., 1965).

An explanation for decreasing permeability along the length of the small intestine was proposed by Loehry et al. (1973). They suggested that in the small intestine, permeation routes are formed by many small pores, a moderate number of medium-size pores, and a few larger pores, and that a greater number of these pores are found in the proximal intestine compared to the distal intestine. Although the surface area of the jejunum is approximately 25 % greater than the ileum (Fisher and Parsons, 1950), by correlation analyses with permeability studies, surface area does not solely account for regional differences in permeability (Loehry et al., 1973). Another possibility for regional differences in intestinal permeation is structural

differences in the junctional complex. The junctional complex is not as well developed in the jejunum as it is in the ileum. The depth and strand numbers of villar tight junctions are greater in the ileum than in the jejunum (Madara et al., 1980). This could possibly cause a greater permeation through the paracellular pathway in the jejunum than in the ileum. The data on regional differences in intestinal permeability described and hypothesized by Fordtran et al., (1965) and Loehry et al., (1973), may be applicable only for normal, non-pathological states.

The data and literature discussed above suggest that the effects seen here in the ileum warrant further study. Just as in the present experiments, vonRitter et al. (1988) reported that the rat terminal ileum had a greater basal clearance of ^{51}Cr-EDTA than other more proximal intestinal regions and suggested that this may explain why this intestinal region is predominantly affected in inflammatory bowel disease.

In the present protocol, the blood-to-lumen clearance of ^{51}Cr-EDTA in the control ferrets was approximately 20 ± 5 mL/min/g DW x 10^{-2}, while in vonRitter's (1988) control rats, the basal clearance was roughly 40 ± 5 mL/min/g wet weight x 10^{-4}. Experimental procedures were very similar between these two investigations, suggesting that the large difference (a 50-fold) between the control values could be attributed to species differences. The ferret's gastrointestinal system is more similar to man's, than is the rat's (Davis, 1988). This suggests that experiments in the rats, may underestimate the severity of permeability changes, and that the ferret should be considered as a favoured animal model for permeability studies.

vonRitter et al. (1988) challenged the rat terminal ileum with a chemotactic agent (FMLP, 1 μM) and reported that the blood-to-lumen clearance of ^{51}Cr-EDTA was approximately 120 mL/min/gram wet tissue weight x 10^{-4}, approximately three-fold greater than the control value. In the present experiments in the ileum at 2 hours PIRR, the blood-to-lumen clearance of ^{51}Cr-EDTA was approximately 4 times greater than the control value. This permeability defect was 65-fold greater than vonRitter's results obtained with luminal challenge by FMLP. If the species difference accounts for a 50-fold change in ^{51}Cr-EDTA clearance, then the 65-fold difference between the respective challenges, FMLP (vonRitter) and radiation (present experiments) represents an extra 1.5-fold change. Thus compared to luminal challenge with FMLP, a standard model of acute intestinal inflammation, a therapeutic dose of radiation results in a greater intestinal permeability defect.

The increased secretion of ^{51}Cr-EDTA in the ileum at 48 hours post-irradiation occurred at a time when the ferrets had no outward manifestations of illness. It is possible that the permeability changes at 48 hours were transient, and that at later times post-irradiation, intestinal permeability would return to control values. However it is also possible that the abnormal permeation of ^{51}Cr-EDTA would continue, or even become worse, at later times post-irradiation, and that diarrhea might re-appear. Therefore, it would be interesting to pursue these experiments at 72 or 96 hours post-irradiation. These experiments at later times post-irradiation however, introduce a complicating variable, that of a failing immune system. Even in the present experiments, by 24 hours post-irradiation the total

number of white blood cells in the circulation had dropped by approximately 70 percent. In addition, histopathological effects in the intestinal mucosa will likely become factors affecting permeation at these later time points.

Route of ^{51}Cr-EDTA Permeation

The increased clearance in the irradiated intestine may be a result of an exaggerated permeation through the same route as in non-irradiated ferrets, or it may reflect permeation through an additional route uncovered subsequent to radiation damage. Normally as older villar enterocytes are sloughed off, they are replaced by new recruits. However, as a consequence of radiation exposure and the reduction of proliferation, the number of recruits will be reduced, and those that are available will not be as well developed (Thomson et al., 1989). This could lead to the development of cell extrusion zones, or intercellular gaps, through which abnormal permeation may occur (Csaky, 1984). However, under light microscopy, both tissues appeared to have an intact mucosa, suggesting that these permeation routes proposed by Csaky (1984) were not available in these experiments.

Morphological studies of intestinal mucosa isolated from irradiated mice, revealed a decrease in the integrity of the junctional complex between adjacent absorptive and goblet cells (Porvaznik, 1979). Although comparable morphological studies are not available for ferret tissue, such breaks in the strands of the junctional complex could also serve as a route for ^{51}Cr-EDTA permeation. However, this would seem to be an unlikely permeation route, as such changes in the junctional

complex would also lead to alterations in fluid and electrolyte flux, which were not observed in these experiments.

It is not clear what the relative role of crypt versus villar cells is, in ^{51}Cr-EDTA permeation. The tight junctions of villi are composed of a greater number of strands which are more highly structurally organized, than the strands of the crypt cells (Marcial et al., 1984; Madara et al., 1980). Since it is generally accepted that ^{51}Cr-EDTA permeates the mucosa through large aqueous pores located in the junctional complex, it is not known if the structural differences in the junctional complex, along the crypt-villar axis and in the jejunal-ileal axis, can influence ^{51}Cr-EDTA permeation. Also, it is not known if the "pores" through which ^{51}Cr-EDTA is assumed to permeate (Maxton et al., 1986), vary in number along the crypt-villar and jejunal-ileal axes. Further experiments must be completed to answer these questions and to clarify the route of ^{51}Cr-EDTA permeation. The molecular dimensions of ^{51}Cr-EDTA are comparable to monosaccharides (eg. sucrose). Therefore, by quantifying the leakage of ^{51}Cr-EDTA from the blood, these experiments have also estimated the loss of nutrients following radiation exposure. Although the permeation routes and barriers are considered to be the same regardless of the direction of permeation (Csaky, 1984), it would be interesting to repeat this protocol with the ^{51}Cr-EDTA in the luminal perfusion solution. By quantifying the permeation of ^{51}Cr-EDTA from the luminal side, one could estimate the severity of malabsorption and sepsis, which are potentially life-threatening conditions post-irradiation.

CONCLUSIONS

The ferret is a superior animal model for the study of radiation-induced intestinal pathologies. This project has reported for the first time the effects of irradiation on ^{51}Cr-EDTA permeation. Radiation exposure increased the permeation of ^{51}Cr-EDTA in both the jejunum and ileum at 2 hours post-irradiation. There was a regional difference in permeation at 48 hours post-irradiation; only in the ileum was there a significant increase in ^{51}Cr-EDTA permeation at 48 hours post-irradiation. Except for a significant secretion of potassium in the ileum at 48 hours PIRR, radiation exposure had no significant effect on fluid flux or fractional excretion of electrolytes. Morphological studies, conducted by others in the laboratory, of the ferret intestinal mucosa, have shown that the mucosa was not significantly affected by radiation exposure and that histopathological mechanisms could not explain the radiation-induced changes in ^{51}Cr-EDTA permeation. These experiments also supported Granisetron's anti-emetic effect in the irradiated ferret, and suggested that it may offer some therapeutic benefit for radiation-induced diarrhea. Granisetron did not have any statistically significant effect on fluid flux, fractional excretion of electrolytes, nor on intestinal permeation of ^{51}Cr-EDTA, suggesting that in this protocol, these parameters of intestinal transport were not mediated by 5-HT_3 receptors. These studies further suggest that changes in intestinal permeability consequent to radiation exposure, are not directly involved in radiation-induced diarrhea.

REFERENCES

Abbas B., Boyle F.C., Wilson D.J., Nelson A.C., and Carr K.E. Radiation induced changes in the blood capillaries of rat duodenal villi: a corrosion cast, light and transmission electron microscopical study. J Submicrosc Cytol Pathol 22(1):63-70, 1990.

Ahlman H., Lundberg, J.M., Dahlstrom A., and Kewenter J. A possible vagal adrenergic release of serotonin from enterochromaffin cells in the cat. Acta Physiol Scand 98:366-376, 1976.

An N.Q., and Evans, H.E. Anatomy of the ferret. *In*: Biology and Diseases of the Ferret, edited by J.G. Fox. Philadelphia: Lea and Febiger, 1988, pp 14-65.

Anderson J.V., Coupe M.O., Morris J.A., Hodgson H.J.F., and Bloom S.R. Remission of symptoms in carcinoid syndrome with a new 5-hydroxytryptamine M receptor antagonist. Br Med J 294:1129, 1987.

Andrews P.L.R., Davis C.J., and Hawthorn J. Abdominal vagotomy modifies the emetic response to radiation in the ferret. J Physiol 378:16P, 1986.

Andrews P.L.R., and Hawthorn J. Evidence for an extra-abdominal site of action for the 5-HT_3 receptor antagonist BRL 24924 in the inhibition of radiation-evoked emesis in the ferret. Neuropharmacology 26(9):1367-1370, 1987.

Andrews P.L.R., Rapeport W.G., and Sanger G.J. Neuropharmacology of emesis induced by anti-cancer therapy. TIPS 91:334-341, 1988.

Anno G.H., Baum S.J., Withers H.R., and Young R.W. Symptamatology of acute radiation effects in humans after exposure to doses of 0.5-30 Gy. Health Phys 56(6):821-838, 1989.

Armstrong W.M. Cellular mechanisms of ion transport in the small intestine, *In*: Physiology of the Gastrointestinal Tract, 2nd Ed., edited by by L.R. Johnson. New York: Raven Press, 1987, pp 1251-1265.

Bacq Z.M. The amines and particularly cysteamine as protectors against roentgen rays. Acta Radiologica 41:47-55, 1954.

Barnes J.H. The physiology and pharmacology of emesis. Mol Aspects Med 7:397-508, 1984.

Becciolini-A., Fabbrica D., Cremonin D., and Balzi M. Quantitative changes in the goblet celis of the rat small intestine after irradiation. Acta Radio Oncol 24:291-299, 1985.

Bermudez J., Boyle E.A., Miner W.D. and Sanger G.J. The anti-emetic potential of the 5-hydroxytryptamine$_3$ receptor antagonist BRL 43694. Br J Cancer 58:644-650, 1988.

Berne R.M., and Levy M.N. Gastrointestinal motility. *In*: Physiology, St. Louis: Mosby, 1983, p 743.

Berthrong M. Pathologic changes secondary to radiation. World J Surg 10:155-170, 1986.

Beubler E., and Horina G. 5-HT$_2$ and 5-HT$_3$ receptor subtypes mediate cholera toxin-induced intestinal fluid secretion in the rat. Gastroenterology 99:83-89, 1990.

Binder H.J. Absorption and secretion of water and electrolytes by small and large intestine. *In*: Gastrointestinal Disease, 4th edition, volume 2, edited by M.H. Sleisenger, and J.S. Fordtran. Philadelphia: W.B. Saunders, 1989, pp 1022-1045.

Bjarnason I., Peters T.J., and Veall N. A persistent defect in intestinal permeability in coeliac disease demonstrated by a ^{51}Cr-labelled EDTA absorption test. Lancet j:323-325, 1983.

Bjarnason I., Peters T.J., and Levi A.J. Intestinal permeability; clinical correlates. Dig Dis 4:83-82, 1986.

Bjarnason I., Smethurst P, Fenn C.G., Lee C.E., Menzies I.S., and Levi A.J. Misoprostol reduces indomethacin-induced changes in human small intestinal permeability. Dig Dis Sci 34(3):407-411, 1989.

Booth N.H., and McDonald L.E. Veterinary Pharmacology and Therapeutics, 6th Ed. Iowa: Iowa State University Press, 1988, p 268.

Borison H.L. and Wang S.C. Physiology and pharmacology of vomiting. Pharmac Rev 5:193-230, 1953.

Borison H.L. Area postrema: chemoreceptor circumventricular organ of the medulla oblongata. Progress in Neurobiol 32:351-390, 1989.

Buell M.G., and Harding R.K. Proinflammatory effects of local abdominal irradiation on rat gastrointestinal tract. Dig Dis Sci 34(3):390-399, 1989.

Bueno L., Fargeas M.J., Theodorou V., and Fioramonti J. Involvement of 5-hydroxytryptamine in the intestinal motor disturbances induced by mast cell degranulation in rats. Eur J Pharm 192:263-269, 1991.

Bulbring E., and Crema A. Observations concerning the action of 5-hydroxytryptamine on the peristaltic reflex. Br J Pharmacol 13:444-457, 1958.

Bulbring E., and Crema A. The release of 5-hydroxytryptamine in relation to pressure exerted on the mucosa. J Physiol 146:18-28, 1959.

Burks T.F., and Long J.P. Catecholamine-induced release of 5-hydroxytryptamine from perfused vasculature of isolated dog intestine. J Pharm Sci 55:1383-1391, 1966.

Cassidy J., Raina V., Lewis C., Adams L., Soukop M., Rapeport W.G., Zussman B.D., Rankin E.M., and Kaye S.B. Phamacokinetics and anti-emetic efficacy of BRL 43694, a new selective 5-HT_3 antagonist. Br J Cancer 58(5):651-653, 1988.

Cheeseman C.I., Walker K., and Thomson A.B.R. Intestinal uptake of bile acids in rats: effect of external abdominal irradiation. Gastroenterology 86(5):1045, 1984.

Churnratanakul S., Wirzba B., Lam T., Walker K., Fedorak R., and Thomson A.B.R. Radiation and the small intestine. Dig Dis 8:45-60, 1990.

Cockerham L.G., Doyle T.F., Trumbo R.B., and Nold J.B. Acute post-irradiation canine intestinal blood flow. Int J Radiat Biol 45(1):65-72, 1984.

Cockerham L.G., Cerveny T.J., and Hampton J.D. Postradiation regional cerebral blood flow in primates. Aviat Space Environ Med 57:578-582, 1986.

Conrad R.A. Effect of x-irradiation on intestinal motility of the rat. Am J Physiol 165:375-385, 1951.

Costall B., Domeney A.M., Naylor R.J., and Tattersall F.D. Emesis induced by cisplatin in the ferret as a model for the detection of anti-emetic drugs. Neuropharmacology 26:1321-1326, 1987.

Crowe S.E., Sestini P., and Perdue M.H. Allergic reactions of rat jejunal mucosa: ion transport responses to luminal antigen and inflammatory mediators. Gastroenterology 99:74-82, 1990.

Csaky T.Z. Methods for investigation of intestinal permeability. *In*: Handbook of Experimental Pharmacology: Pharmacology of Intestinal Permeation,vol 70/1, edited by T.Z. Csaky. Berlin: Springer-Verlag, 1984, pp 91-111.

Cubeddu L.X., Hoffman I.S., Fuenmayor N.T. and Finn A.L. Efficacy of ondansetron (GR38032F) and the role of serotonin in cisplatin-induced nausea and vomiting. N Engl J Med 322:810-816, 1990.

Curran P.F., Webster E.W., and Hovespian J.A. The effect of X-irradiation on sodium and water transport in rat ileum. Radiat Res 13:369-380, 1960.

Curran P.F., and MacIntosh J.R. A model system for biological water transport. Nature 193:347-348, 1962.

Curzon, G. and Green A.R. Rapid method for the determination of 5-hydroxytryptamine and 5-hydroxyindolacetic acid in small regions of the rat brain. Brit J Pharm 39:653-655, 1970.

Davis C.J., Harding R.K., Leslie R.A., and Andrews P.L.R. The organization of vomiting as a protective reflex. *In*: Nausea and Vomiting: Mechanisms and Treatment, edited by C.J. Davis, G.V. Lake-Bakaar, and D.G. Grahame-Smith. Berlin: Springer-Verlag, 1986, pp 65-75.

Davis C.J. Neuropharmacological investigations into the mechanisms of emesis caused by cytotoxic drugs and radiation. Ph.D. Thesis, Oxford University, 1988.

DeSoignie R., and Sellin J.H. Acid-base regulation of ion transport in rabbit ileum in vitro. Gastroenterology 99:132-141, 1990.

Diamond J.M. The epithelial junction: Bridge, gate, and fence. Physiologist 20:10-18, 1977.

DiResta G.R., Kiel J.W., Riedel G.L., Kaplan P., and Shepherd A.P. Hybrid blood flow probe for simultaneous H_2 clearance and laser-Doppler velocimetry. Am J Physiol 253:G573-G581, 1987.

Doe W.F. The intestinal immune system. Gut 30:1679-1685, 1989.

Donowitz M., Charney A.N., and Hefferman J.M. Effect of serotonin treatment on intestinal transport in the rabbit. Am J Physiol 232(1):E85-E94, 1977.

Donowitz M., Tai Y.H., and Asarkof N. Effect of serotonin on active electrolyte transport in rabbit ileum, gallbladder, and colon. Am J Physiol 239:G463-G472, 1980.

Donowitz M., and Welsh M.J. Regulation of mammalian small intestinal electrolyte secretion. *In*: Physiology of the Gastrointestinal Tract, 2nd Ed., edited by L.R. Johnson, New York: Raven Press, 1987, pp 1351-1388.

Drapanas T., McDonald J.C., and Steward J.D. Serotonin release following instillation of hypertonic glucose into the proximal intestine. Ann Surg 156:528-536, 1962.

Dumuis A., Sebben M., and Bockaert J. BRL 24924: a potent agonist at a non-classical 5-HT receptor positively coupled with adenylate cyclase in colliculi neurons. Eur J Pharm 162:381-384, 1989.

Earnest D.L., and Trier J.S. Radiation enteritis and colitis. *In*:Gastrointestinal Disease, 4th Ed., edited by M.H. Sleisenger M.H., and J.S. Fordtran. New York: W.B.Saunders, 1989, pp 1369-1382.

Elia M., Behrens R., Northrop C., Wraight P., and Neale G. Evaluation of mannitol, lactulose and ^{51}Cr-EDTA as markers of intestinal permeability. Clin Sci 73:197-204, 1987.

Ershoff B.H., and Gal E.M. Effects of radiation on tissue serotonin levels in the rat. Proc Soc Exp Biol and Med 107:160-162, 1962.

Fisher R.B., and Parsons D.S. The gradient of mucosal surface area in the small intestine of the rat. J Anat 84:272-282, 1950.

Florczyk A.P, Schurig J.E., and Bradner W.T. Cisplatin-induced emesis in the ferret: A new animal model. Cancer Treat Rep 66:187-189, 1982.

Fordtran J.S., Rector F.C., Ewton, M.F., Soter N., and Kinney J. Permeability characteristics of the human small intestine. J Clin Invest 44(12):1935-1944, 1965.

Fox J.G. Normal clinical and biological parameters. *In*: Biology and Diseases of the Ferret, edited by J.G. Fox. Philadelphia: Lea and Febiger, 1988,pp 159-173.

Fozard J.R., and Mobarok Ali A.T.M. Receptors for 5-hydroxytryptamine on the sympathetic nerves of the rabbit heart. Naunyn-Schmiedeberg's Arch of Pharm 301:223-235, 1978.

Fozard J.R., Mobarok Ali A.T.M., and Newgrosh G. Blockade of serotonin receptors on autonomic neurones by (-)-cocaine and some related compounds. Eur J Pharm 59:195-210, 1979.

Fozard J.R., Loisy C., and Tell G.P. Blockade of neuronal 5-hydroxytryptamine receptors with MDL 72222. A novel approach to the symptomatic treatment of migraine. *In*: Proceedings of the 5th Migraine Symposium, edited by C.F. Rose. Basel: Karger, 1985, pp 264-272.

Fozard J.R. The development and early clinical evaluation of selective 5-HT_3 receptor antagonists. *In*: The Peripheral Actions of 5-Hydroxytryptamine, edited by J.R. Fozard. New York: Oxford Medical, 1989, pp 354-376.

Fujita T. and Kobayashi S. The cells and hormones of the GEP endocrine system: The current of studies. *In*: Gastroentero-Pancreatic Endocrine System: A Cell-Biological Approach, edited by T. Fujita. Tokyo: Igaku Shoin, 1973, pp 1-16.

Furness J.B., and Costa M. Neurons with 5-hydroxytryptamine-like immunoreactivity in the enteric nervous system - their projections in the guinea-pig small intestine. Neuroscience 7(2):341-349, 1982.

Gaddum J.H. and Picarelli Z.P Two kinds of tryptamine receptor. Br J Pharmacol Chemother 12:323-328, 1957.

Geraci J.P, Jackson K.L., and Mariano M.S. Protection against the physiological derangements associated with acute intestinal radiation injury. Pharmac Ther 39:45-57, 1988.

Gershon M.D., and Erde S.M. The nervous system of the gut. Gastroenterology 80:1571-1594, 1981.

Gershon M.D., Wade P.R., Kirchgessner A.L., and Tamir H. 5-HT receptor subtypes outside the central nervous system. Role in the physiology of the gut. Neuropsychopharm 3(5/6):385-395, 1990.

Gordon J.L. Intestinal epithelial differentiation: new insights from chimeric and transgenic mice. J Cell Biol 108:1187-1194, 1989.

Gozlan H., Schechter L.E., Bolanos F., Emerit M.B., Miquel M.C., Nielsen M., and Hamon M. Determination of the molecular size of the 5-HT_3 receptor binding site by radiation inactivation. Eur J Pharm 172:497-500, 1989.

Gray J.L., Tew J.T., and Jensen H. Protective effect of serotonin and of para-aminopropriophenone. Proc Soc Exp Biol Med 80:604-607, 1952.

Green C.J. Animal Anaesthesia. Laboratory Animal Handbooks (8), Laboratory Animals Ltd, London, 1979, pp 17-27.

Greenwood B., and Read N.W. Vagal control of fluid transport, transmural potential difference, and motility in the ferret jejunum. Am J Physiol 249:G651-G654, 1985.

Greenwood B., Doolittle T., See N.A., Koch T.R., Dodds W.J., and Davison J.S. Effects of substance P and vasoactive intestinal polypeptide on contractile activity and epithelial transport in the ferret jejunum. Gastroenterology 98:1509-1517, 1990.

Grisham M.B., Gaginella, T.S. vonRitter C., Tamai H., Be R.M., and Granger D.N. Effects of neutrophil-derived oxidants on intestinal permeability, electrolyte transport, and epithelial cell viability. Inflammation 14(5):531-542, 1990.

Gronstad K.O., Zinner M.J., Nilsson O., Dahlstrom A., Jaffe B.M., and Ahlman H. Vagal release of serotonin into gut lumen and portal circulation via separate control mechanisms. J Surg Res 43:205-210, 1987.

Grundy D. Speculations on the structure/function relationship for vagal and splanchnic afferent endings supplying the gastrointestinal tract. J Auto Ner Syst 22:175-180, 1988.

Gumbiner B. Stucture, biochemistry, and assembly of epithelial tight junctions. Am J Physiol 253:C749-C758, 1987.

Gunter-Smith P.J. Gamma radiation affects active electrolyte transport by rabbit ileum: basal Na and Cl transport. Am J Physiol 250:G540-G545, 1986.

Gylys J.A., and Gidda J.S. Radiation induced emesis in ferrets: an experimental model of emesis. Gastroenterology 90(5,#2):A1446, 1986.

Hall E.J. The physics and chemistry of radiation absorption. *In*: Radiobiology for the Radiologist, 3rd Ed., edited by E.J. Hall. New York: J.B. Lippincott Company, 1988, p 5.

Hardcastle J., Hardcastle P.T., and Redfern J.S. Action of 5-hydroxytryptamine on intestinal ion transport in the rat. J Physiol 320:41-55, 1981.

Harding R.K. Prodromal effects of radiation: pathways, models, and protection by antiemetics. Pharmac Ther 39:335-345, 1988.

Hober R., and Hober J. Experiments on the absorption of organic solutes in the small intestine of rats. J Cell Comp Physiol 10:401-420, 1937.

Hollander D., Ricketts D., and Boyd C.A.R. Importance of "probe" molecular geometry in determining intestinal permeability. Can J Gastroenterol 2(Suppl A):35A-38A, 1988.

Holtug K., and Skadhauge E. Ion transport across isolated pig jejunum. Am J Physiol 260:G220-G231, 1991.

Holzheimer G., and Winne D. Influence of distension on absorption and villous structure in rat jejunum. Am J Physiol 256:G188-G197, 1989.

Hopkinson G.B., Hinsdale J., and Jaffe B.M. Contraction of canine stomach and small bowel by intravenous administration of serotonin. A physiological response ? Scand J Gastroenterol 24:923-932, 1989.

Hoyer D. Serotonin 5-HT_3, 5-HT_4, and 5-HT-M receptors. Neuropsychopharm 3(5/6):371-383, 1990.

Jenkins R.T., Goodacre R.L., Rooney PJ., Bienenstock J., Sivakumaran T., and Walker C. Studies of intestinal permeability in inflammatory diseases using polyethlyene glycol 400. Clin Bioch 19:298-302, 1986.

Jenkins R.T., Jones D.B., Goodacre R.L., Collins S.M., Coates G., Hunt R.H., and Bienenstock, J. Reversibility of increased intestinal permeability to ^{51}Cr-EDTA in patients with gastrointestinal inflammatory diseases. Am J Gastroenterology 82(11):1159-1164, 1987.

Jensen M.H., Sauer T., Devik F., and Nygaard K. Late changes following single dose roentgen irradiation of rat small intestine. Acta Radio Oncol 22:299-303, 1983.

Kabal J., Parkhurst L.J., and Wyant D.E. Measurement of canine intestinal capillary blood flow in the terminal phase of the gastrointestinal radiation syndrome. AFRRI SR73-18, 1973.

Keelan M., Walker K., and Thomson A.B.R. Intestinal morphology, marker enzymes and lipid content of brush border membranes from rabbit jejunum and ileum: effect of aging. Mech Aging Dev 31:49-68, 1985.

Kemper A.C., and Specian R.D. Rat small intestinal mucins: a quantitative analysis. Anat Rec 229:219-226, 1991.

Killackey J.J.F. and Killackey B.A. Neutrophil-mediated increased permeability of microcarrier-cultured endothelial monolayers: a model for in vitro study of neutrophil-dependent mediators of vasopermeability. Can J Physiol Pharmacol 68:836-844, 1990.

King G.L. Characterization of radiation-induced emesis in the ferret. Radiat Res 114:599-612, 1988.

Kinsella T.J., and Bloomer W.D. Tolerance of the intestine to radiation therapy. Surg Gynecol Obst 151:273-284, 1980.

Kisloff B. and Moore E.W. Effect of serotonin on water and electrolyte transport in the in vivo rabbit small intestine. Gastroenterology 71:1033-1038, 1976.

Kockmierska-Grodzka D., Siegienczuk M., and Szewko A. The influence of protease inhibitor on hydroproteolytic activity and serotonin content in the intestine of rats after fractionated irradiation. Arch Imm Ther Exp 24:259-265, 1976.

Krugliak P., Hollander D., Schlaepfer C.C., Katz D.K., Dadufalza V.D., and Ma T.Y. Polyethylene glycol 400 permeation of the colonic epithelial barrier of the rat. Gastroenterology 99:1001-1007, 1990.

Lee E.J., Moore W.E., Fryer H.C., and Minocha H.C. Hematological and serum chemistry profiles of ferrets (*Mustela putorius furo*). Lab Anim 16:133-137, 1982.

Leslie R.A., Reynolds D.J.M., Andrews P.L.R., Grahame-Smith D.G., Davis C.J., and Harvey J.M. Evidence for presynaptic 5-hydroxytryptamine$_3$ recognition sites on vagal afferent terminals in the brainstem of the ferret. Neuroscience 38(3):667-673, 1990.

Lincoln J., Crowe R., Kamm M.A., Burnstock G., and Lennard-Jones J.E. Serotonin and 5-hydroxyindoleacetic acid are increased in the sigmoid colon in severe idiopathic constipation. Gastroenterology 98:1219-1225, 1990.

Loehry C.A., Kingham J., and Baker J. Small intestinal permeability in animals and man. Gut 14(9):683-688, 1973.

Madara J.L., Trier J.S., and Neutra M.R. Structural changes in the plasma membrane accompanying differentiation of epithelial cells in human and monkey small intestine. Gastroenterology 78(5):964-975, 1980.

Madara J.L., and Trier J.S. Functional morphology of the mucosa of the small intestine. *In*: Physiology of the Gastrointestinal Tract, 2nd Ed. edited by L.R. Johnson. New York: Raven Press, 1987, pp 1209-1249.

Marcial M.A., Carlson S.L., and Madara J.L. Partitioning of paracellular conductance along the ileal crypt-villus axis: a hypothesis based on structural analysis with detailed consideration of tight junction structure-function relationships. J Membrane Biol 80:59-70, 1984.

Martin K., Kong T.H., Renehan W., Schurr A., Dong W., Zhang X., and Fogel R. Identification and function of brain stem neurons regulating rat ileal water absorption. Am J Physiol 257:G266-G273, 1989.

Matsuoka O., Tsuchiya T., and Furukawa Y. The effect of X-irradiation on 5-hydroxytryptamine (serotonin) contents in the small intestines of experimental animals. J Radiat Res 3:104-108, 1962.

Maxton D.G., Bjarnason I., Reynolds A.P, Catt S.D., Peters T.J., and Menzies I.S. Lactulose ^{51}Cr-labelled ethylenediaminetetra-acetate, L-rhamnose and polyethylene glycol 500 as probe markers of assessment in vivo of human intestinal permeability. Clin Sci 71:71-80, 1986.

McCarthy L.E., and Borison H.L. Respiratory mechanisms of vomiting in decerebrate cats. Am J Phyiol 226(3):738-743, 1974.

Milks L.C., Conyers G.P., and Cramer E.B. The effect of neutrophil migration on epithelial permeability. J Cell Biol 103(6):2729-2738, 1986.

Miller A.D., and Wilson V.J. "Vomiting center" reanalyzed: An electrical stimulation study. Brain Res 270:154-158, 1983.

Miller M.J.S., Adams J., Gu X., Zhang X.J., and Clark D.A. Hemodynamic and permeability characteristics of acute experimental necrotizing enterocolitis. Dig Dis Sci 35:1257-1264, 1990.

Miller M.J.S., Zhang X., Gu X., and Clark D.A. Acute intestinal injury induced by acetic acid and caesin: prevention by intraluminal misoprostol. Gastroenterology 101:22-30, 1991.

Miner W.D., Sanger G.J., and Turner D.H. Evidence that 5-hydroxytryptamine$_3$ receptors mediate cytotoxic drug and radiation-evoked emesis. Br J Cancer 56:159-162, 1987.

Moe O.W., Preisig PA., and Alpern R.J. Cellular model of proximal tubule sodium chloride and sodium bicarbonate absorption. Kidney Int 38:605-611, 1990.

Mulholland M.W., Levitt S.H., Song C.W., Potish R.A., and Delaney J.P. The role of luminal contents in radiation enteritis. Cancer 54:2396-2402, 1984.

Naftalin R.J., and Tripathi S. Passive water flows driven across the isolated rabbit ileum by osmotic, hydrostatic and electrical gradients. J Physiol 360:27-50, 1985.

Ng W.W., Jing J., Hyman P.E., and Snape W.J. Effect of 5-hydroxytryptamine and its antagonists on colonic smooth muscle of the rabbit. Dig Dis Sci 36(2):168-173, 1991.

Nilsson O., Cassuto J., Larsson P.A., Jodal M., Lidberg P., Ahlman H., Dahlstrom A., and Lundgren O. 5-Hydroxytryptamine and cholera secretion: a histochemical and physiological study in cats. Gut 24:542-548, 1983.

Nylander O., Kvietys P., and Granger N. Effects of hydrochloric acid on duodenal and jejunal mucosal permeability in the rat. Am J Physiol 257:G653-G660, 1989.

Otterson M.F., Sarna S.K., and Moulder J.E. Effects of fractionated doses of ionizing radiation on small intestinal motor activity. Gastroenterology 95:1249-1257, 1988.

Penttila A., and Kormano M. Effect of X-irradiation of the exteriorized jejunal loop on the morphology and 5-hydroxytryptamine content of the enterochromaffin cells in the mouse. Strahlentherapie 142(2):238-247, 1971.

Penttila A., Kormano M., and Ahonen A. Effects of 400 R whole-body X-irradiation on 5-hydroxytryptamine content of the rat gastrointestinal tract. Strahlentherapie 49(4):426-437, 1975.

Perdue M.H., Ramage J.K., Burget D., Marshall J., and Masson S. Intestinal mucosal injury is associated with mast cell activation and leukotriene generation during Nippostrongylus-induced inflammation in the rat. Dig Dis Sci 34(5): 724-731, 1989.

Perdue M.H., Marshall J., and Masson S. Ion transport abnormalities in inflamed rat jejunum. Gastroenterology 98:561-567, 1990.

Pettersson G.B., Newson B., Ahlman H., and Dahlstrom A. In vitro studies of serotonin release from rat enterochromaffin cells: studies of gut serotonin release. J Surg Res 29:141-148, 1980.

Porvaznik M. Tight junction disruption and recovery after sublethal gamma-irradiation. Radiat Res 78:233-250, 1979.

Powell D.W. Barrier function of epithelia. Am J Physiol 241:G275-G288, 1981.

Powell D.W. Intestinal water and electrolyte transport. *In*: Physiology of the Gastrointestinal Tract, 2nd Ed., edited by L.R. Johnson. New York: Raven Press, 1987, pp 1267-1305.

Quastler H. The nature of intestinal radiation death. Radiat Res 4:303-320, 1956.

Quastler H., and Hampton J.C. Effects of ionizing radiation on the fine structure and function of the intestinal epithelium of the mouse. Radiat Res 17:914-931, 1962.

Ramage J.K., Stanisz A., Scicchitano R., Hunt R.H., and Perdue M.H. Effect of immunological reactions on rat intestinal epithelium. Correlation of increased permeability to ^{51}Cr-EDTA and ovalbumin during acute inflammation and anaphylaxis. Gastroenterology 94:1368-1375, 1988.

Read N. Hypersecretion in the gut: diarrhea. Pathophysiology of Gut and Airways Symposium, 1989.

Richardson B.P, Engel G., Donatsch P., and Stadler P.A. Identification of serotonin M-receptor subtypes and their specific blockade by a new class of drugs. Nature 316:126-131, 1985.

Rodriguez-Boulan E., and Nelson J.W. Morphogenesis of the polarized epithelial cell phenotype. Science 245:718-725, 1989.

Sanger G.J. and King F.D. From metoclopramide to selective gut motiltiy stimulants and 5-HT_3 receptor antagonists. Drug Design and Delivery 3:273-295, 1988.

Schmidt A.W., and Peroutka S.J. 5-Hydroxytryptamine receptor "families". FASEB J 3:2242-2249, 1989.

Smith R.N. Safety of Ondansetron. *In*: Ondansetron Symposium. Cheshire: Gardiner-Caldwell, 1989, pp 55-59.

Smith D.H. and DeCosse J.J. Radiation damage to the small intestine. World J Surg 10:189-194, 1986.

Snedecor G.W. and Cochran W.G. Statistical Methods, 7th Ed. Iowa: Iowa State University Press, 1980, pp 281-283.

Specian R.D. and Oliver M.G. Functional biology of intestinal goblet cells. Am J Physiol 260:C183-C193, 1991.

Steadman C.J., Talley N.J., Phillips S.F., and Mulvihill C. Trial of a selective serotonin type 3 (5-HT_3) receptor antagonist ondansetron (GR38032F) in diarrhea predominant irritable bowel syndrome (IBS). Gastroenterology 98(5,#2):A394, 1990.

Stephens R.L., Garrick T., Weiner H., and Tache Y. Serotonin depletion potentiates gastric secretory and motor responses to vagal but not peripheral gastric stimulants. J Pharm and Exp Ther 251(2):524-530, 1989.

Strobel S., Brydon W.G., and Ferguson A. Cellobiose/mannitol sugar permeability test complements biopsy histopathology in clinical investigation of the jejunum. Gut 25:1241-1246, 1984.

Summers R.W., Flatt A.J., Prihoda M.J., and Mitros F.A. Effect of irradiation on morphology and motility of canine small intestine. Dig Dis Sci 32(12):1402-1410, 1987.

Tansy M.F., Rothman G., Bartlett J., Farber P., and Hohenleitner F.J. Vagal adrenergic degranulation of enterochromaffin cell system in guinea-pig duodenum. J Pharm Sci 60:81-84, 1971.

Taylor A.E., and Townsley M.I. Evaluation of the Starling fluid flux equation. NIPS 2:48-52, 1987.

Thompson J.H. Serotonin and the alimentary tract. Res Comm Chem Path Pharm 2:687-781, 1971.

Thomson A.B.R., Keelan M., Lam T., Cheeseman C.I., Walker K., and Clandinin M.T. Saturated fatty acid diet prevents radiation-associated decline in intestinal uptake. Am J Physiol 256:G178-G187, 1989.

Timmermans R., and Gerber G.B. Reaction of blood pressure and mesenteric blood flow to infusion of biogenic amines in normal and supralethally X-irradiated rats. Radiat Res 82:81-92, 1980.

Trier J.S., and Browning T.H. Morphologic response of the mucosa of human small intestine to X-ray exposure. J Clin Invest 45(2):194-204, 1966.

Upward J.W. The clinical pharmacology of Granisetron (BRL 43694), a novel specific 5-HT_3 receptor antagonist. *In*: Update in Emesis Control Symposium, SmithKline Beecham Pharmaceuticals, 1990, pp 17-19.

Ussing H.H., and Zeranhn K. Active transport of sodium as the source of electric current in the short-circuited isolated frog skin. Acta Physiol Scand 23:110-127, 1951.

Van Tilburg A.J.P, De Rooij F.W.M., van Blankenstein M.V., van Den Berg J.W.O., and Bosman-Jacobs E.P. Sodium-dependent bile acid transport in the ileum: the balance between diarrhea and constipation. Gastroenterology 98:25-32, 1990.

Vigneulle R.M., Herrera J., Gage T., MacVittie T.J., Taylor P., Zeman G., Nold J.B., and Dubois A. Nonuniform irradiation of the canine intestine. Radiat Res 121:45-53, 1990.

Von Ritter C., Sekizuka E., Grisham M.B., and Granger N. The chemotactic peptide N-formyl-methionyl-leucyl-phenylalanine increases mucosal permeability in the distal ileum of the rat. Gastroenterology 95:651-656, 1988.

Warren T.M. and Stoelting R.K. Hemodynamic effects of general anesthetics. *In*: Cardiovascular Actions of Anesthetics and Drugs Used in Anesthesia, vol 1, edited by B.M. Altura and S. Halevy. New York: Karger, 1986, pp 1-16.

Westergaard H. and Dietschy J.M. Malabsorption syndromes. *In*: Clinical Disorders of Membrane Transport Processes, edited by T.E. Andreoli, F.F. Hoffman, D.D. Fanestil, and S.G. Schultz. New York: Plenum Medical Book, 1987, pp 107-119.

Willoughby D.A. Pharmacological aspects of the vascular permeability changes in the rat's intestine following abdominal radiation. Br J Radiol 23:515-519, 1960.

Wills E.D. Effects of irradiation on subcellular components. I. Lipid peroxide formation in the endoplasmic reticulum. Int J Radiat Biol 17:217-228, 1970.

Zunini G.S., Roth S.H., and Lucier G.E. The inhibitory effect of halothane on the emetic response in the ferret. Can J Physiol Pharmacol 68:374-378, 1990.

Appendix I

Details of Methodology

Choice of Anesthetic

The first choice of anesthetic for this protocol was urethane, an injectable anesthetic commonly used in ferret experiments (Greenwood and Read, 1985; Greenwood et al., 1990). Urethane is also a carcinogen and this was the rationale offered by the Animal Care Facility, University of Ottawa, for not permitting its use in this protocol. An alternate choice was the injectable anesthetic Inactin, widely used in renal microperfusion experiments. Like urethane, Inactin minimally depresses cardiovascular parameters (Booth and McDonald, 1988). In microperfusion experiments on inactin-anesthetized rats, mean arterial blood pressure and heart rate are minimally depressed, ensuring good blood flow (hence solute delivery) to the tubule being perfused. These same principles apply to the present experiment. Changes in blood flow to the perfused intestine must be kept to a minimum in order to maintain normal electrolyte and fluid flux across the bowel. Unfortunately, at the time that this protocol was submitted, Inactin was no longer being manufactured and an ensured supply for the duration of this project could not be obtained (Inactin production started again in the winter of 1990).

Isoflurane is a gaseous anesthetic known to have minimal cardiovascular effects (Warren and Stoelting, 1986). However this anesthetic has recently been shown to alter gastrointestinal motility (MacKay, 1990, personal observation). Therefore, it was decided to use halothane combined with ketamine (as a pre-anesthetic) in the surgical anesthetic. This anesthetic combination was used in other studies of radiation-induced emesis (Andrews and Hawthorn, 1987; Bermudez et al.,

1988). It must be noted though that anesthetics themselves are emetic stimuli (Green, 1979), but it was recently suggested that at clinical concentrations (as used in this protocol), halothane does not stimulate emesis in the ferret (Zunini et al., 1990).

Blood Vessel Cannulations

The left jugular vein was isolated by blunt dissection. Compared to the rat and dog, the ferret jugular was more difficult to cannulate: more sensitive to collapse, surrounded by thicker, tougher connective tissue, and had numerous branches. To cannulate the vein, it was extremely important to remove as much of the connective tissue as possible from the area where the cut was to be made. The vein was cannulated proximal to any large branches. Once the vein was ready to be cannulated, a single ligature was placed and secured proximally. To prevent the vein from collapsing, it was necessary that a surgical assistant pump the vein in order to fill it with blood. When the vein was engorged with blood, a pair of small forceps was slipped underneath the vein where the cut was to be made. Using a pair of fine dissecting scissors, a cut was made on the ventral surface of the vein, large enough that the lumen of the vein was visible to the naked eye. Any excess blood was quickly dabbed away. The upper proximal surface of the cut vein was gently lifted up with a pair of fine forceps. With the other hand, the venous cannula previously dipped in mineral oil, was inserted into the vein using a forward, twisting motion. The venous cannula was 45 cm long and had a "blister" (made with a cannula heater on the outer surface of the cannula to assist in proper positioning and attachment)

7 cm from the bevelled end. The cannula was inserted just beyond the bubble (approximately 7.5 cm) and then a second ligature was secured around the cannulated vein at this point, i.e., distal to the bubble. For cannulation of jugular vein, King (1988) recommended that the tip of the cannula should be where the left and right jugular veins join to form the precava, a distance of approximately 10 cm of intravascular length. This was relatively difficult to achieve in our ferrets, hence the compromise to 7 cm. The external end of the cannula was connected to a 3-way luer stopcock via a 20 gauge tubing adapter (Becton-Dickinson). The cannula which had been previously filled with heparin saline (100 U/mL, 0.9 % saline), was then flushed and tested for patency. The cannula was then further secured in place by using the distal ligature.

The cannula used for the right carotid artery was made from PE-50 tubing (i.d. = 0.58 mm, o.d. 0.965 mm), and connected to a 3-way luer stopcock via a 22 gauge tubing adapter (Becton-Dickinson). In all other respects, the arterial cannula was constructed in an identical manner to the jugular vein cannula. Larger diameter arterial cannulae were attempted (PE-60, PE-90, PE-120), but only the PE-50 cannula could be reliably advanced the minimum distance (7 cm) to within 1 cm of the common carotid artery. To expose the right carotid artery, a midline incision was made through the sternohyoid. Blunt dissection with pediatric mosquito clamps was done on the right side of the trachea. The artery was attached relatively firmly to the vagus nerve via connective tissue. Care must be taken to separate the artery from the nerve, as mechanical stimulation of the nerve via handling, could result in

altered heart rate, ventilation, and GI function. The carotid artery was cannulated in the same manner as the jugular vein, except that initially three ligatures were s ipped around the artery. Pumping the high pressure artery was not necessary, but even the small diameter cannula must be well dipped in mineral oil in order for it to be advanced past the bubble (7 cm).

Details of Intestinal Loop Preparation

The input cannulae were 45 cm long, and both the drainage and output cannulae were 15 cm long. To minimize plugging of the output cannulae, two or three side-ports were constructed above and below the cuff.

An experiment was attempted to connect the input cannula to a Statham pressure transducer, but because the silicon tubing was so soft, it offered minimal resistance to changes in pressure. If intestinal tone is to be assessed, in order to determine if the output cannula is plugged (which would decrease collection rate and cause distension of the segment), a more rigid material should be used for the intestinal cannulae.

Intestinal perfusates were collected by gravity, dripping directly into plastic disposable containers. For better accuracy, a few collection attempts were made using a fraction collector. In order to use the fraction collector, the output cannulae had to be connected to a smaller diameter tubing (PE-60). The connection to the smaller diameter tubing introduced too many complications to the design of the experiment (increased dead space of tubing, increased incidence of back pressure and plugging), and therefore use of the fraction collector was discontinued.

Approximately 1 out of every 15 cannulated segments either became blocked or contaminated with blood, within the first 20 minutes of perfusion, the so-called "flushing phase." A blocked segment was first indicated by a reduced or zero collection rate. When this was observed, if the segment was already inside the abdominal cavity, the abdomen was reopened, and the suspected blocked segment examined. If the segment was plugged, it would appear inflated to a varying degree depending on the severity of the plug, and on how long the segment had been plugged. If it appeared to be a minor block (still collecting some fluid, minimal distension), the segment was gently compressed with a moist gauze near the end of the output cannula. Sometimes this manoeuver would force the clogging material into or further down the output cannula, where it could then be carried away by the stream of BES which could now flow freely. If this procedure failed, the flow rate was tripled, in hopes that the increased flow rate would increase the driving pressure sufficiently to overcome the block. This procedure was only done when the segment was visible. If the increased flow rate did not remove the plug, then the segment would very quickly become super-inflated. This increased stress on the intestinal wall could result in changes of the permeability characteristics of the segment (Holzheimer and Winne, 1989), thus influencing the permeability results. If it was apparent that the block was not removed within a few seconds, the flow pump was immediately turned off. If the blockage remained, the output cannula was removed and rinsed clean. Before re-inserting the output cannula, the flow pump was turned back on. If any large mucus globs were near the incision, they were gently removed

with a moist cotton-tipped wooden applicator. Once the BES was observed to flow freely from the hole of the incision, the cannula was re-inserted and secured in place. Changing the output cannula should only be done as a last resort, as it creates further trauma to the tissue, and often results in blood in the output cannula. This latter case can occur when there has been excessive trauma to the tissue (as during surgery), or spontaneously in what appeared to be a perfectly cannulated segment. Only perfusates that were blood-free were used for analysis. Therefore if the stream of BES moving out of the output cannula had blood in it (detected by visual observation), the cannula was replaced and the segment recannulated as described above. However, recannulating the segment increases the tissue trauma and may exacerbate the bleeding. If on the third attempt, the output cannula still had blood in its perfusates, the flow pump to that segment was turned off, and no samples from that segment were used for analysis.

Preparation of ^{14}C-PEG4000

The ^{14}C-PEG4000 was obtained in powder form from New England Nuclear (NEN, Dupont), 1.00 mCi/g. Four mL of BES was added to the PEG to obtain a stock solution of 0.0125 mCi/mL. Ninety-six μL of this solution was then added to the 130 mL of the BES to obtain a final activity of 0.01 μCi/mL.

Preparation of ^{51}Cr-EDTA

The ^{51}Cr-EDTA was also obtained from NEN, as a 1.0 mCi solution. This stock solution was diluted in Lactate Ringer's, in order to obtain five or six 1.0 mL samples of 160 μCi of ^{51}Cr-EDTA.

Details of 5-HT and 5-HIAA Assays

At the appropriate time post-irradiation, ferrets were anesthetized with sodium pentobarbital (0.4 mg/ 100 g body weight). Tissue samples were quickly harvested and the animal sacrificed with overdose of sodium pentobarbital. Tissue samples were weighed, minced and placed in cold culture tubes. One mL of acidified butanol was added to each tube, and the samples homogenized on ice. Samples were then centrifuged for 10 minutes at 3000 rpm. The top layer was quickly transferred to another set of glass tubes (the bottom layer was discarded). One mL of heptane and 1.2 mL of 0.1 N HCl was added to each tube, and briefly vortexed. Samples were again centrifuged at 3000 rpm for 10 minutes to separate organic layer (containing 5-HT) from acid layer (containing 5-HIAA).

5-HT Reaction:

1. Add 200 μL diluent (blank), standard, sample
2. Add 200 μL o-phthaldialdehyde in methanol (50%) (opt/met)
3. Add 1.5 mL of concentrated HCl
4. Vortex briefly
5. Place in preheated 75 °C water bath for 30 minutes (cap with marbles)
6. Cool to room temperature
7. Read at 360/470 nm (excitation/emission) in Spectrophotofluorometer

5-HIAA Reaction:

1. Add 400 μL diluent (blank), standard, sample

Add the following, in the order given, vortexing between each addition

2. 50 μL 1% cysteine
3. 1.0 mL of concentrated HCl
4. 50 μL opt/met
5. 50 μL sodium metaperiodate
6. Place in preheated 75 °C water bath for 20 minutes (cap with marbles)
6. Cool to room temperature
7. Read at 360/470 nm (excitation/emission) in Spectrophotofluorometer

Appendix II

Sample Calculations

Calculations for Blood Gas Analysis

If,

pH = 7.386 at 37-38 °C
tCO_2 = 27.2

then factor = 0.6171 (from Blood pH Table, see following pages)

pCO_2 = tCO_2 ÷ factor
pCO_2 = 27.3 ÷ 0.6171
pCO_2 = 44.24 mmHg

dissolved CO_2 = 44.24 x 0.0301 = 1.33

HCO_3^- = tCO_2 - dissolved CO_2
= 27.3 - 1.33
= 25.97

Calculation of 51Cr-EDTA Clearance

From Experiment Feb. 11/91, Control Irradiated + Saline-Injected, Ileum Samples

Perfusion Sample	^{51}Cr in Perfusates (cpm/mL)	^{51}Cr in Plasma (cpm/mL)
P2	180	------
P3	205	30000
	mean= 192	

$$^{51}\text{Cr-EDTA Clearance} = \frac{^{51}\text{Cr in Perfusates x Perfusion Rate}}{^{51}\text{Cr in Plasma x Tissue Dry Weight}}$$

$$^{51}\text{Cr-EDTA Clearance} = \frac{192 \text{ cpm/mL x } 0.5 \text{ mL/min}}{30000 \text{ cpm/mL x } 0.31 \text{ g}}$$

^{51}Cr-EDTA Clearance = 0.01 mL/min/gDW = 0.1 mL/10 min/gDW

BLOOD

To Figure pCO_2 Divide MM. CO_2 by Factor of Corresponding Given pH.

pH	FACTOR	pH	FACTOR	pH	FACTOR	pH	FACTOR
6.25	.0726	6.51	.1075	6.77	.1709	7.03	.2863
6.26	.0736	6.52	.1093	6.78	.1742	7.04	.2923
6.27	.0746	6.53	.1111	6.79	.1775	7.05	.2984
6.28	.0757	6.54	.1130	6.80	.1810	7.06	.3046
6.29	.0767	6.55	.1149	6.81	.1845	7.07	.3110
6.30	.0778	6.56	.1169	6.82	.1881	7.08	.3175
6.31	.0789	6.57	.1189	6.83	.1917	7.09	.3243
6.32	.0801	6.58	.1210	6.84	.1955	7.10	.3311
6.33	.0812	6.59	.1231	6.85	.1994	7.11	.3380
6.34	.0824	6.60	.1253	6.86	.2033	7.12	.3452
6.35	.0836	6.61	.1275	6.87	.2073	7.13	.3526
6.36	.0849	6.62	.1298	6.88	.2115	7.14	.3601
6.37	.0861	6.63	.1321	6.89	.2157	7.15	.3678
6.38	.0874	6.64	.1345	6.90	.2200	7.16	.3761
6.39	.0888	6.65	.1369	6.91	.2245	7.17	.3838
6.40	.0901	6.66	.1394	6.92	.2290	7.18	.3920
6.41	.0916	6.67	.1419	6.93	.2336	7.19	.4002
6.42	.0930	6.68	.1445	6.94	.2383	7.20	.4091
6.43	.0945	6.69	.1472	6.95	.2432	7.21	.4181
6.44	.0960	6.70	.1499	6.96	.2481	7.22	.4268
6.45	.0975	6.71	.1527	6.97	.2532	7.23	.4361
6.46	.0991	6.72	.1556	6.98	.2584	7.24	.4456
6.47	.1007	6.73	.1585	6.99	.2637	7.25	.4554
6.48	.1023	6.74	.1615	7.00	.2692	7.26	.4651
6.49	.1040	6.75	.1646	7.01	.2748	7.27	.4753
6.50	.1057	6.76	.1677	7.02	.2805	7.28	.4858

Formula: $pH = 6.1 + \log \frac{CO_2 - .0301 pCO_2}{.0301\ pCO_2}$

$$[\text{Antilog } (pH - 6.1)]\ (.0301\ pCO_2) = CO_2 - .0301\ pCO_2$$

$$.0301\ pCO_2\ [\text{Antilog } (pH - 6.1) + 1] = CO_2 \text{ ----} pCO_2 = \frac{CO_2}{\text{Factor}}$$

pH	FACTOR	pH	FACTOR	pH	FACTOR	pH	FACTOR
7.29	.4963	7.52	.8217	7.75	1.375	7.98	2.313
7.30	.5071	7.53	.8404	7.76	1.4060	7.99	2.366
7.31	.5181	7.54	.8591	7.77	1.4381	8.00	2.421
7.32	.5301	7.55	.8783	7.78	1.4707	8.01	2.477
7.33	.5412	7.56	.8982	7.79	1.5044	8.02	2.534
7.34	.5531	7.57	.9184	7.80	1.539	8.03	2.592
7.35	.5651	7.58	.9391	7.81	1.5741	8.04	2.652
7.36	.5781	7.59	.9602	7.82	1.6097	8.05	2.713
7.37	.5908	7.60	.9819	7.83	1.6465	8.06	2.775
7.38	.6039	7.61	1.0041	7.84	1.684	8.07	2.839
7.39	.6171	7.62	1.0270	7.85	1.723	8.08	2.905
7.40	.6306	7.63	1.0499	7.86	1.7621	8.09	2.9715
7.41	.6447	7.64	1.0740	7.87	1.8024		
7.42	.6590	7.65	1.0980	7.88	1.8439		
7.43	.6736	7.66	1.1230	7.89	1.8861		
7.44	.6890	7.67	1.1483	7.90	1.9297		
7.45	.7040	7.68	1.1745	7.91	1.974		
7.46	.7197	7.69	1.201	7.92	2.019		
7.47	.7356	7.70	1.226	7.93	2.0652		
7.48	.7522	7.71	1.2564	7.94	2.112		
7.49	.7690	7.72	1.2849	7.95	2.161		
7.50	.7862	7.73	1.3142	7.96	2.2105		
7.51	.8036	7.74	1.3440	7.97	2.261		

Appendix III

Detailed Results

Figure 27

^{51}Cr-EDTA clearance in the jejunum (top) and ileum (bottom) at 20 minute intervals of the 60 minute experimental perfusion time. Values are mean ± SE, n values for control, 2, 24, and 48 hours post-irradiation (PIRR) are in order for jejunum: 5,5,6,5; for ileum: 6,6,6,6. † indicates significant difference from ileum at the same PIRR time point. ★ indicates significant difference from all other PIRR groups within the same tissue. • indicates significant difference from control and 24 hour PIRR groups within the same tissue.

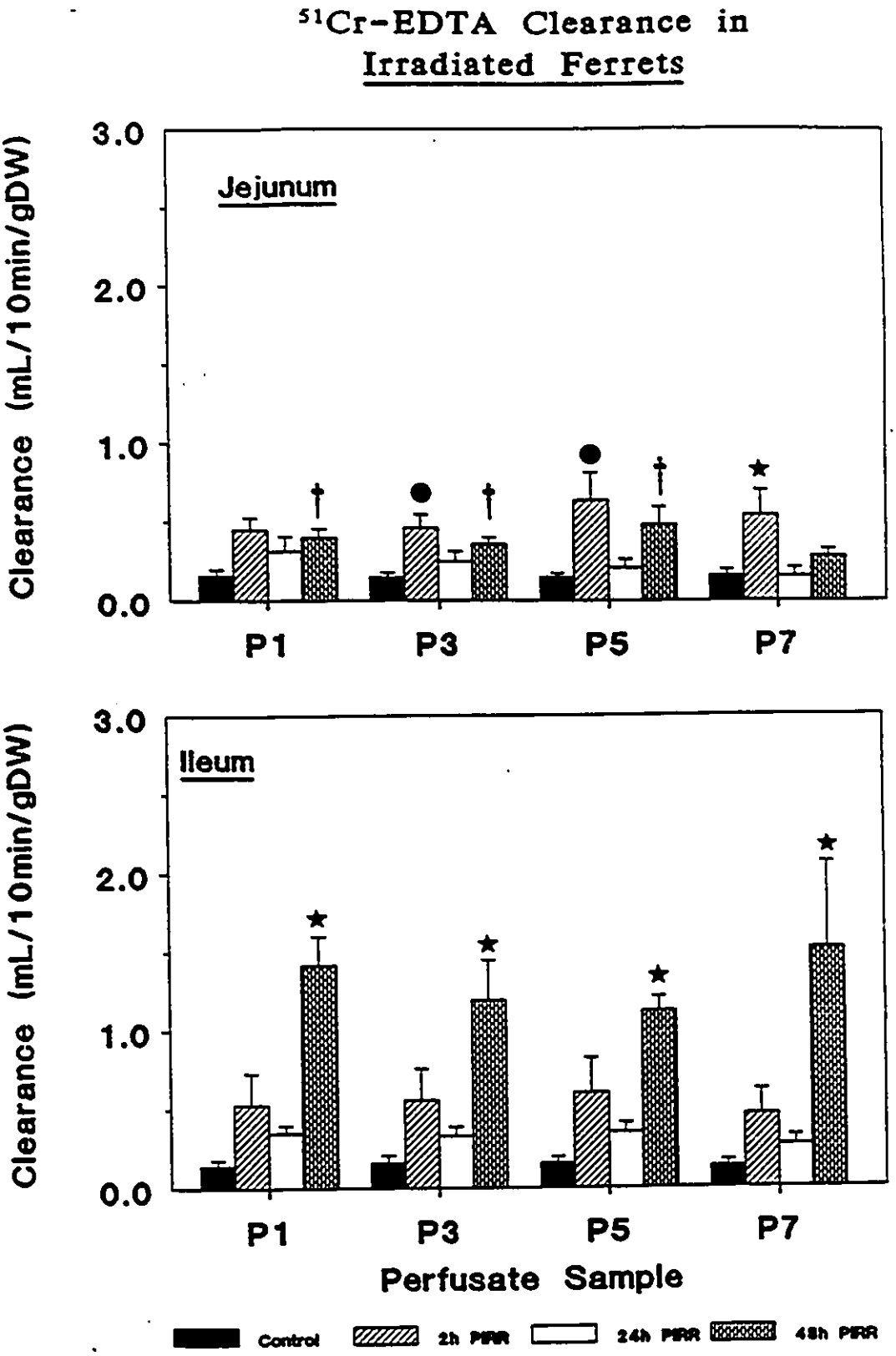
^{51}Cr-EDTA Clearance in
Irradiated Ferrets
Jejunum
Ileum
Clearance (mL/10min/gDW)
3.0
2.0
1.0
0.0
P1
P3
P5
P7
Perfusate Sample
Control
2h PIRR
24h PIRR
48h PIRR

Figure 28

Net fluid flux (J) in the jejunum (top) and ileum (bottom) for the four post-irradiation (PIRR) groups. Positive J values indicate net fluid secretion, negative values indicate net absorption of fluid. Values are expressed as mean ± SE, n values for jejunum are 5,5,6,5 and for ileum 5,6,6,5 for the different PIRR groups, respectively control, 2h, 24h, 48h PIRR. † indicates significant difference from the same post-irradiation group in the ileum.

Net Fluid Flux in Irradiated Ferrets